

OCRWM	DESIGN CALCULATION OR ANALYSIS COVER SHEET						1. QA: QA 2. Page 1	
3. System Engineered Barrier System				4. Document Identifier CAL-EBS-MD-000030				
5. Title Analysis of Mechanisms for Early Waste Package / Drip Shield Failure								
6. Group Regulatory Integration / Engineered Systems								
7. Document Status Designation <input checked="" type="checkbox"/> Preliminary <input type="checkbox"/> Final <input type="checkbox"/> Cancelled								
8. Notes/Comments This is a minor revision to address changes required for Regulatory Integration. The calculation was not re-run. All changes from the previous revision (Rev 00B) have been tracked with change bars.								
Attachments							Total Number of Pages	
I - Mathcad Spreadsheets							32	
II - Listing of Files on CD-ROM							4	
III - CD-ROM of Mathcad file and compressed SAPHIRE files							CD-ROM	
RECORD OF REVISIONS								
9. No.	10. Reason For Revision	11. Total # of Pgs.	12. Last Pg. #	13. Originator (Print/Sign/Date)	14. Checker (Print/Sign/Date)	15. QER (Print/Sign/Date)	16. Approved/Accepted (Print/Sign)	17. Date
00B	Revision to address technical editor and DOE comments and to update weld flow analysis	108	I-32	D. A. Brownson	J. K. Knudsen	J. E. Gebhart	D. A. Thomas	
00C	Revision to address regulatory integration comments.	144	II-4	C. Kimura SIGNATURE ON FILE 8/27/04	T. Koppental SIGNATURE ON FILE 8-27-04	C. Warren SIGNATURE ON FILE 8/27/04	N. Brown SIGNATURE ON FILE 8/27/04	

INTENTIONALLY LEFT BLANK

CONTENTS

	Page
1. PURPOSE	9
2. QUALITY ASSURANCE	9
3. USE OF SOFTWARE.....	10
4. INPUTS	10
4.1 DATA AND PARAMETERS	10
4.1.1 Waste Package and Drip Shield Design Parameters	10
4.1.2 Human Error Probabilities.....	11
4.1.3 Alloy 22 Weld Flaw Characteristics	13
4.1.4 Anomaly Distribution Curve for Hard-Alpha Inclusion in Titanium Alloy ..	16
4.2 CRITERIA	18
5. ASSUMPTIONS	19
5.1 ASSUMPTIONS RELATED TO FLAWS IN ALLOY 22 WELDS	19
5.1.1 Flaw Detection by Ultrasonic Testing.....	19
5.1.2 Representation of Ultrasonic Test Probability of Nondetection Curve	20
5.1.3 Extension of Outer Lid Weld Flaw Distribution Characteristics	21
5.2 ASSUMPTIONS RELATED TO FLAWS IN ALLOY 22 BASE METAL.....	22
5.2.1 Repair of Alloy 22 Base Metal.....	22
5.2.2 Ratio of Weld Flaws to Base Metal Flaws.....	23
5.3 ASSUMPTIONS RELATED TO IMPROPER WELD MATERIAL OR BASE METAL.....	23
5.3.1 Approximation of Probability of Using Improper Weld Material	23
5.3.2 Field Measurements of Material Compositions	24
5.3.3 Probability of Using Improper Base Metal	24
5.4 ASSUMPTIONS RELATED TO IMPROPER WASTE PACKAGE HEAT TREATMENT	25
5.4.1 Heat Treatment Process and Procedural Controls.....	25
5.4.2 Event Sequence Resulting in Improper Heat Treatment	26
5.4.3 Probability of a Significant Process Malfunction.....	27
5.5 ASSUMPTIONS RELATED TO IMPROPER LASER PEENING	28
5.5.1 Laser Peening Process and Procedural Controls	28
5.5.2 Automatic Generation of an Event Log	28
5.5.3 Approximation of Probability of a Significant Process Malfunction.....	28
5.6 ASSUMPTIONS RELATED TO WASTE PACKAGE CONTAMINATION.....	29
5.6.1 Naked-Eye Inspection of Waste Package for Contamination	29
5.6.2 Postexamination Contamination of the Waste Package.....	30
5.6.3 Possibility of Waste Package Contamination During Cleaning.....	30
5.7 ASSUMPTIONS RELATED TO IMPROPER WASTE PACKAGE HANDLING ..	31
5.7.1 Naked-Eye Inspection of Waste Package for Damage.....	31

CONTENTS (Continued)

	Page
5.7.2 Waste Package Damage Due to Mishandling After Reception But Before Final Inspection	31
5.7.3 Waste Package Damage Due to Mishandling During Final Inspection	32
5.7.4 Approximation of Damage Due to Mishandling	32
5.8 ASSUMPTIONS RELATED TO FLAWS IN TITANIUM WELDS	33
5.8.1 Flaw Density and Size Distributions in Titanium Welds	33
5.8.2 Ultrasonic Testing of Titanium Welds	33
5.9 ASSUMPTIONS RELATED TO FLAWS IN BASE METAL TITANIUM	34
5.9.1 Hard-Alpha Inclusions in Titanium Used for the Drip Shield	34
5.9.2 Frequency of Occurrence of High-Density Inclusions in Base Metal Titanium	34
5.10 ASSUMPTIONS RELATED TO DRIP SHIELD CONTAMINATION	35
5.10.1 Drip Shield Inspection	35
5.10.2 Drip Shield Secondary Inspection	35
5.10.3 Decontamination Process of Drip Shield	35
5.11 ASSUMPTIONS RELATED TO IMPROPER DRIP SHIELD HANDLING	36
5.11.1 Drip Shield Damage Inspections	36
5.11.2 Drip Shield Mishandling Opportunities	36
5.11.3 Additional Drip Shield Mishandling Opportunities	37
5.11.4 Drip Shield Improper Handling Damage Probability	37
5.12 ASSUMPTIONS RELATED TO DRIP SHIELD EMPLACEMENT ERROR	37
5.12.1 Drip Shield Emplacement Error Detection	37
6. ANALYSIS	38
6.1 REVIEW OF DEFECT-RELATED FAILURES OF CONTAINERS IN VARIOUS INDUSTRIES	38
6.1.1 Boilers and Pressure Vessels	38
6.1.2 Nuclear Fuel Rods	40
6.1.3 Underground Storage Tanks	41
6.1.4 Radioactive Cesium Capsules	42
6.1.5 Dry Storage Casks for Spent Nuclear Fuel	43
6.1.6 Summary	44
6.2 MECHANISMS FOR EARLY WASTE PACKAGE FAILURE	46
6.2.1 Weld Flaws	47
6.2.2 Base Metal Flaws	68
6.2.3 Improper Weld Material or Base Metal	71
6.2.4 Improper Heat Treatment	72
6.2.5 Improper Laser Peening	76
6.2.6 Contamination	82
6.2.7 Improper Handling	85
6.2.8 Administrative Error Leading to Unanticipated Conditions	88
6.3 MECHANISMS FOR EARLY DRIP SHIELD FAILURE	88
6.3.1 Weld Flaws	89

CONTENTS (Continued)

	Page
6.3.2 Base Metal Flaws	89
6.3.3 Improper Weld Material or Base Metal	91
6.3.4 Improper Heat Treatment	91
6.3.5 Contamination	92
6.3.6 Improper Handling	92
6.3.7 Drip Shield Emplacement Error	93
6.4 CONSEQUENCES OF THE OCCURRENCE OF DEFECTS ON WASTE PACKAGE OR DRIP SHIELD.....	94
6.4.1 Consequences of Weld Flaws or Base Metal Flaws.....	95
6.4.2 Consequences of Improper Weld Material or Base Metal	95
6.4.3 Consequences of Improper Heat Treatment.....	95
6.4.4 Consequences of Improper Laser Peening	96
6.4.5 Consequences of Contamination	96
6.4.6 Consequences of Damage by Mishandling	96
6.4.7 Consequences of Drip Shield Emplacement Error.....	96
6.4.8 Summary and Discussion	96
6.5 FEATURES, EVENTS, AND PROCESSES INCLUDED IN MODEL	99
7. CONCLUSIONS	100
8. INPUTS AND REFERENCES.....	103
8.1 DOCUMENTS CITED.....	103
8.2 CODES, STANDARDS, REGULATIONS, AND PROCEDURES.....	108
8.3 SOURCE DATA, LISTED BY DATA TRACKING NUMBER	108
8.4 SOFTWARE CODES.....	108

FIGURES

	Page
1. Schematic Representation of the Cross Section of the Alloy 22 Weld	14
2. Illustration of Closure Welds for the VSC-24 Dry Storage Cask	44
3. Cumulative Distribution Function for Flaw Size Before Ultrasonic Inspection in Outer Lid Weld	52
4. Cumulative Distribution Function for Flaw Density Parameter before Ultrasonic Inspection	54
5. Schematic Representation of Flaw Orientation on Specimen Ring	56
6. Comparison of Several Ultrasonic Probability-of-Nondetection Curves Identified in the Literature	60
7. Cumulative Distribution Function for Flaw Size After Ultrasonic Inspection and Repair in Outer Lid Weld	62
8. Cumulative Distribution Function for Flaw Density Parameter After Ultrasonic Inspection and Repair in Outer Lid Weld	63
9. Event Tree for Improper Heat Treatment of the Waste Package Shell	77
10. Event Tree for Improper Heat Treatment of the Waste Package Top Lid	78
11. Event Tree for Improper Laser Peening of the Outer Lid Weld of the Waste Package	81
12. Event Tree for Contamination of the Waste Package	85
13. Event Tree for Damage to the Waste Package by Mishandling	87
14. Anomaly Distribution Curve for Inclusions in the Drip Shield	91
15. Event Tree for Drip Shield Emplacement Error	94

TABLES

	Page
1. Materials Used for the Waste Package and the Drip Shield.....	10
2. Waste Package Design Parameters Used in the Analysis	11
3. Drip Shield Design Parameters Used in the Analysis	11
4. Estimates of Human Error Probabilities.....	12
5. Estimates of Error Factors for Human Error Probabilities.....	13
6. Weld Dimensions	14
7. Dimensions of the Ultrasonic Indications	15
8. Set of Data Points for Hard-Alpha Inclusion Anomaly Distribution Curve	17
9. Summary of VSC-24 Weld Cracking Events.....	43
10. Summary of Defect-Related Failures in Various Welded Metallic Containers	45
11. Parameters Needed for Calculating Weld Flaw Characteristics	65
12. Summary Table for Evaluating Flaw Characteristics.....	65
13. Main Characteristics of Flaws in Welds of Waste Package.....	66
14. Description of Events for Improper Heat Treatment of the Waste Package	74
15. Description of Events for Improper Laser Peening of the Waste Package Outer Lid Weld	80
16. Description of Events for Contamination of the Waste Package	84
17. Description of Events for Damage of the Waste Package by Mishandling	86
18. Probability of Having 0.5-mm or 1-mm Inclusions in the Drip Shield.....	90
19. Description of Events for Drip Shield Emplacement Error	93
20. Features, Events, and Processes Included (Screened In) in TSPA-LA and Addressed in this Report	100
21. Features, Events, and Processes Excluded (Screened Out) in this Report	100
22. Defect Types to Consider in Assessing Waste Package and Drip Shield Performance.....	102
23. CD-ROM Directory Listing	103

ACRONYMS AND ABBREVIATIONS

BWR	boiling water reactor
CDF	cumulative distribution function
FAA	U.S. Federal Aviation Administration
HEP	human error probability
HRA	human reliability analysis
NRC	U.S. Nuclear Regulatory Commission
PDF	probability density function
PND	probability of nondetection
PWR	pressurized water reactor
QA	Quality Assurance
UT	ultrasonic testing

1. PURPOSE

The purpose of this analysis is to evaluate the types of defects or imperfections that could occur in a waste package or a drip shield and potentially lead to its early failure, and to estimate a probability of occurrence for each. An early failure is defined as the through-wall penetration of a waste package or drip shield due to manufacturing or handling-induced defects, at a time earlier than would be predicted by mechanistic degradation models for a defect-free waste package or drip shield.

The scope of this analysis is limited to the manufacturing or handling-induced defects that might lead to the early failure of the waste package or drip shield. Also, for the waste package only the outer (Alloy 22) barrier is investigated. No credit is taken for the structural (stainless steel) shell of the waste package; therefore, it is not analyzed.

As a preliminary remark, it is important to note that even if a waste package is affected by a type of defect that may lead to its early failure, it does not mean that this waste package is due to fail at emplacement in the repository. Failure of the waste package will only occur after degradation processes take place, which may happen hundreds of years after emplacement. Also, even if a waste package was to fail early because of a defect, its radionuclide inventory may not necessarily be available for transport. This is because most through-wall penetrations, especially cracks from stress corrosion cracking, are usually of limited length and tight.

The intended use of this analysis is to provide information and inputs to performance assessment. These information and inputs will be used to evaluate the waste package and drip shield lifetime.

This calculation receives no direct input from other analysis reports or model reports or their associated data tracking numbers (DTNs). It provides direct inputs to *WAPDEG Analysis of Waste Package and Drip Shield Degradation* (ANL-EBS-PA-000001), *Engineered Barrier System Features, Events, and Processes* (ANL-WIS-PA-000002), and *Screening Analysis for Criticality Features, Events, and Processes for License Application* (ANL-EBS-NU-000008).

2. QUALITY ASSURANCE

This analysis is developed in accordance with *Technical Work Plan for: Regulatory Integration Modeling and Analysis of the Waste Form and Waste Package* (BSC 2004a). Also, the analysis is subject to the requirement of *Quality Assurance Requirements and Description* (DOE 2004) as determined in Section 8 of *Technical Work Plan for: Regulatory Integration Modeling and Analysis of the Waste Form and Waste Package* (BSC 2004a).

The development of this analysis is governed by AP-3.12Q, *Design Calculations and Analyses*.

The control of the electronic management of information was evaluated in accordance with AP-SV.1Q, *Control of the Electronic Management of Information*, as specified in *Technical Work Plan for: Regulatory Integration Modeling and Analysis of the Waste Form and Waste Package* (BSC 2004a, Section 8). The resulting methods used are given in the same reference.

3. USE OF SOFTWARE

The computer code SAPHIRE Version 7.18 (SAPHIRE V7.18, STN: 10325-7.18-00) was used to develop and quantify several event trees in the analysis. SAPHIRE is a qualified software code that was obtained from Software Configuration Management. It is appropriate for use in the present analysis and is used only within its range of validation in accordance with AP-SI.1Q, *Software Management*. SAPHIRE was installed on a Dell Dimension XPS T800i running Microsoft Windows 2000 Professional (central processing unit 151674). The inputs and output files are given in Attachment II.

Mathcad 2001i Professional, a commercial off-the-shelf software program, was also used in the preparation of this analysis. Mathcad was installed on a Dell Dimension XPS T800i running Microsoft Windows 2000 Professional (central processing unit 151674). The Mathcad calculations performed in the analysis are documented in Attachment I. This attachment lists all the inputs and formulas used as well as the corresponding outputs so that the work can be reproduced and checked independently without recourse to the originator of the analysis. Thus, the use of this software is considered exempt from the requirements of AP-SI.1Q, *Software Management*.

Finally, the input and output files given in Attachment II were compressed using Winzip 8.1. Because Winzip 8.1 is an office automation system, it is exempt from the requirements of AP-SI.1Q, *Software Management*.

4. INPUTS

4.1 DATA AND PARAMETERS

4.1.1 Waste Package and Drip Shield Design Parameters

The following parameters are appropriate for use in this analysis because they are from controlled documents and reflect the current design of the waste package and the drip shield. The materials comprising the waste package and drip shield are summarized in Table 1.

Table 1. Materials Used for the Waste Package and the Drip Shield

Item Description	Material Used
Inner vessel of the waste package (structural support)	Stainless steel (SA-240-S31600) ^a
Outer barrier of the waste package (corrosion resistance)	Alloy 22 (SB-575-N06022) ^a
Shield plates of the drip shield	Titanium Grade 7 (SB-265-R52400) ^b
Structural support of the drip shield	Titanium Grade 24 (SB-265-R56405) ^b

Source: ^a BSC 2003a, Table 2

^b BSC 2003b, Table 5

Dimensions of components of the 21-PWR (pressurized water reactor) waste package with absorber plates were taken from *Repository Design Project, RDP/PA IED Typical Waste Package Components Assembly 1 of 9* (BSC 2003c) and are summarized in Table 2. The 21-PWR waste package with absorber plates is a type of waste package designed to receive the

spent nuclear fuel from pressurized water reactors. The parameters pertaining to this kind of waste package were selected because the most common waste packages used in the repository will be of this type (BSC 2003a, Table 11).

A comparison of the parameters used in this calculation for the 21-PWR waste packages with those of the 44-PWR waste packages (the second most common waste package) and recent changes to both designs indicate that this calculation is adequate to address the current 21-PWR and 44-PWR waste packages.

Table 2. Waste Package Design Parameters Used in the Analysis

Parameter Description	Parameter Value
Thickness of outer barrier	20 mm ^a
Inner diameter of outer barrier	1524 mm ^b
Length of waste package	5165 mm ^a
Thickness of outer lid weld	25 mm ^b
Thickness of middle lid weld	10 mm ^b
Thickness of outer barrier bottom lid weld	25 mm ^b
Diameter of outer lid	1541 mm ^b
Diameter of middle lid	1527 mm ^b

Source: ^a BSC 2003c, Table 1

^b BSC 2003c, Directory (references BSC 2001a for this information)

The parameters used in the analysis related to the drip shield are summarized in Table 3.

Table 3. Drip Shield Design Parameters Used in the Analysis

Parameter Description	Parameter Value
Thickness of drip shield (plates)	15 mm ^a
Mass of drip shield	5000 kg ^b
Total mass of Titanium Grade 7 welds	110 kg ^b
Density of Titanium Grade 7	4.51 g/cm ³ ^c

Source: ^a BSC 2003b, Table 1

^b BSC 2003b, Table 5

^c ASM International 1990a, p. 620)

4.1.2 Human Error Probabilities

Estimates of human error probabilities (HEPs) provided by Swain and Guttman (1983) were used in this analysis. These probability estimates are accepted data. This is based on the fact that these data are recommended for use by *PRA Procedures Guide, A Guide to the Performance of Probabilistic Risk Assessments for Nuclear Power Plants* (NRC 1983, Sections 4.1 and 4.5.7) in order to evaluate the probability of occurrence of human errors in the conduct of probabilistic risk assessments for nuclear power plants.

The data used are summarized in Table 4. Based on information by Swain and Guttman (1983, pp. 2-18 and 2-19), the estimated HEPs are considered to follow a lognormal distribution. The nominal probability represents the median, and the 5th (respectively 95th) percentile is calculated by dividing (respectively multiplying) the median by an error factor, also shown in Table 4.

Table 4. Estimates of Human Error Probabilities

Item #	Description	Nominal Probability	Error Factor	Source: Swain & Guttman 1983
1	Failure to carry out a plant policy	0.01	5	Item 1 of Table 20-6
2	Failure to use written operations procedure under normal operating conditions	0.01	3	Item 3 of Table 20-6
3	Failure to use written test or calibration procedure	0.05	5	Item 6 of Table 20-6
4	Error of commission in reading and recording quantitative information from unannounced digital readout (less than 4 digits)	0.001	3	Item 2 of Table 20-10
5	Error of commission in check-reading ^a analog meter with difficult-to-see limit marks, such as scribe lines	0.002	3	Item 3 of Table 20-11
6	Selection of wrong control on a panel from an array of similar-appearing controls identified by labels only	0.003	3	Item 2 of Table 20-12
7	Improperly mate a connector (this includes failures to seat connectors completely and failure to test locking features of connectors for engagement)	0.003	3	Item 13 of Table 20-12
8	Checker failure to detect error made by others during routine tasks	0.1	5	Item 1 of Table 20-22
9	Operator failure to respond to an annunciator	0.0001	10	Item 1 of Table 20-23

Source: Swain and Guttman 1983

NOTE: ^a Check-reading means reference to a display merely to see if the indication is within allowable limits; no quantitative reading is taken.

The fact that the HEP values given in Table 4 correspond to nominal probabilities should be emphasized. No performance shaping factors are employed except in very particular cases for which their use is reasonable and realistic. In general, performance shaping factors are utilized to alter the nominal HEP in order to account for the effects of equipment design, operator skills, psychological and physiological stresses, etc. Because the procedures and equipment that will be employed to perform the fabrication and handling of the waste package and the drip shield have not yet been written or precisely identified, use of performance shaping factors would be premature at this stage. Only in very particular cases, for which the use of a nominal HEP would not adequately reflect the environmental conditions under which the operator is to operate, have the HEP been altered to represent more accurate operating conditions (see Sections 6.2.4 and 6.2.5).

In addition to the estimates given previously, Swain and Guttman (1983) provide general guidelines to assigning error factors to nominal HEPs, depending on the value of the probability and other factors such as stress level. This guideline was used in this analysis when no specific error factor was already assigned to the estimated probability. The values used are given in Table 5.

Table 5. Estimates of Error Factors for Human Error Probabilities

Item #	Description	Error Factor	Source: Swain & Guttman (1983)
1	Task consists of performance of step-by-step procedure conducted under routine circumstances; stress level is optimal. The estimated nominal probability is lower than 0.001.	10	Item 1 of Table 20-20
2	Task consists of relatively dynamic interplay between operator and system indications, under routine conditions; stress level is optimal. The estimated nominal probability is greater than 0.001.	5	Item 5 of Table 20-20

Source: Swain and Guttman 1983

As mentioned by Swain and Guttman (1983, pp. 1 and 2), the HEPs given previously are not only applicable to human reliability in nuclear power plants but also may be used for other large process plants such as chemical plants, oil refineries, etc. These types of industries can be characterized by highly controlled environment and are governed by strict quality standards and controls. This characterizes also the fabrication and handling operations of the waste package and the drip shield. Based on this information, the HEPs and error factors given previously appear to be appropriate for use in this analysis.

A review and comparison of *Handbook of Human Reliability Analysis with Emphasis on Nuclear Power Plant Applications Final Report* (Swain and Guttman 1983) and *Technical Basis and Implementation Guidelines for a Technique for Human Event Analysis (ATHEANA)* (NRC 2000) was performed. *Technical Basis and Implementation Guidelines for a Technique for Human Event Analysis (ATHEANA)* (NRC 2000) is a description of a specific step-by-step sequential application of the Human Reliability Analysis (HRA) methodology. Some background information and discussion of errors of commission and omission are included, but no new or updated HEPs are included.

4.1.3 Alloy 22 Weld Flaw Characteristics

Sixteen weld rings of Alloy 22 have recently been fabricated and examined using various nondestructive examination techniques, followed by a metallographic examination (BSC 2003d). Information gathered from these experiments has been used to develop a flaw density and size distribution applicable to the closure welds of the waste package. The parameters used are summarized in the following subsections.

4.1.3.1 Weld Ring Dimensions

Weld ring dimensions are summarized in Table 6 with visualization and reference points of the weld given in Figure 1. Dimensions are given in the unit provided in the corresponding source of information.

Table 6. Weld Dimensions

Parameter Description (see Figure 1)	Parameter Value	Source: BSC (2003d)
Radius of the half-circle A_1OA_2	0.125 in	Figure 2
Distance OC	0.97 in ^a	Figure 2
Distance BC	0.43 in ^b	Figure 2
Angle $B_3A_1B_1$	3 degrees	Figure 2
Angle $C_5B_3C_3$	25 degrees	Figure 3
Angle $B_2A_2B_4$	6 degrees	Figure 2
Angle $C_4B_4C_6$	29 degrees	Figure 3
Diameter of the ring from centerline of the weld	60.765 in ^c	Figure 2

NOTES: ^a Value calculated from dimensions given in BSC 2003d, Figure 2. Note that this value, which characterizes weld thickness, has been rounded to 25 mm in all further calculations.

^b Rounded average value from dimensions given in BSC 2003d, Figure 2.

^c Average value from dimensions given in BSC 2003d, Figure 2.

The parameters given previously are appropriate for use in this analysis because they conform to the current design of the Alloy 22 closure welds of the waste package.

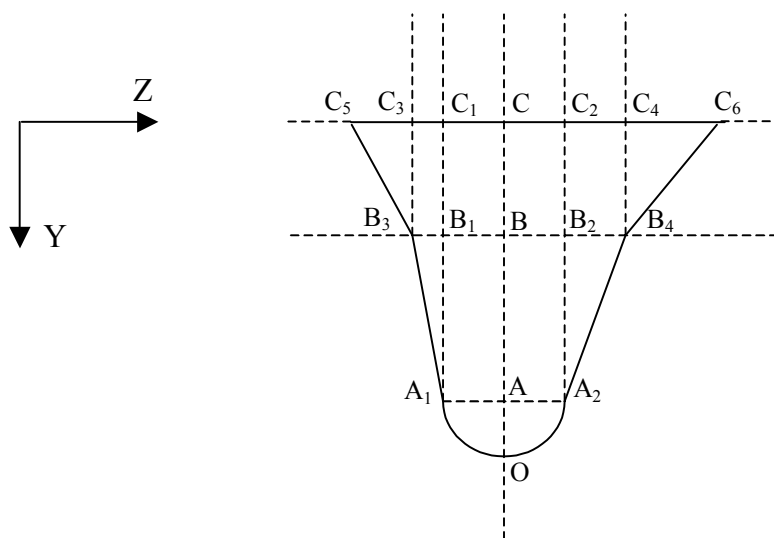


Figure 1. Schematic Representation of the Cross Section of the Alloy 22 Weld

4.1.3.2 Parameters for Ultrasonic Inspection and Flaw Characteristics

Several nondestructive examination techniques were used to detect weld flaws in the specimen rings. Surface examinations included liquid penetrant and eddy current inspections. Volumetric examinations included radiographic and ultrasonic testing (UT). The surface indications, which consisted of nonwelding related indications such as tooling marks, were irrelevant (BSC 2003d) and are discarded from further consideration in this analysis. As far as volumetric inspection is concerned, it should be noted that the radiographic testing was mainly used for a secondary check of the UT inspections. Therefore, only the volumetric indications of the UT are further considered.

RDP/PA IED Typical Waste Package Components Assembly (6) (BSC 2003d) indicates that the UT inspection threshold employed in the examination of the 16 weld rings that were fabricated

was 1 mm, which calls for detection of all flaws of size larger than 1 mm. This was confirmed by the metallographic inspections performed on the specimen rings: the weld imperfections discovered through this process were the same weld imperfections discovered during the UT inspections for all weld imperfections greater than 1 mm (BSC 2003d). The other imperfections were gas pores and the majority of them were less than 0.003 inch (around 0.08 mm) in diameter.

Based on the information provided in *RDP/PA IED Typical Waste Package Components Assembly (6)* (BSC 2003d, Table 27), UT inspections revealed seven flaws that were later confirmed by metallography. Two of the weld flaws listed in Table 27 of *RDP/PA IED Typical Waste Package Components Assembly (6)* (BSC 2003d) could not be verified by metallography (Rings K2 and S1F) and therefore were not included in this evaluation. The weld flaw dimensions in the X, Y, and Z directions, as evaluated by the UT inspections, are given in Table 7. Note that metallographic examinations confirmed the UT dimensions or showed that they slightly overestimated the actual flaw dimensions (BSC 2003d). The parameters given in Table 7 were determined from DTN: MO030214WPWF01.000.

Table 7. Dimensions of the Ultrasonic Indications

UT Flaw Number	X Direction		Y Direction		Z Direction	
	Flaw Onset	Flaw End	Flaw Onset	Flaw End	Flaw Onset	Flaw End
Ring K – UT-2 ^a	54 1/2 in	54 5/8 in	3/8 in	7/16 in	1/2 in	9/16 in
Ring K – UT-3 ^a	55 3/4 in	56 3/8 in	3/8 in	7/16 in	1/2 in	9/16 in
Ring R – UT-1 ^b	19 1/8 in	19 7/8 in	11/16 in	13/16 in	9/16 in	5/8 in
Ring R – UT-2 ^b	47 1/4 in	48 5/8 in	7/16 in	9/16 in	1/2 in	9/16 in
Ring R – UT-3 ^b	20 7/8 in	21 1/4 in	11/16 in	13/16 in	9/16 in	5/8 in
Ring W – UT-1 ^c	3 1/8 in	3 5/8 in	3/8 in	9/16 in	9/16 in	11/16 in
Ring X – UT-1 ^d	4 5/16 in	4 11/16 in	3/16 in	3/4 in	11/16 in	11/16 in

Source: ^a DTN: MO030214WPWF01.000, p. 133

^b DTN: MO030214WPWF01.000, p. 807

^c DTN: MO030214WPWF01.000, p. 1171

^d DTN: MO030214WPWF01.000, p. 1246

Based on *RDP/PA IED Typical Waste Package Components Assembly (6)* (BSC 2003d), the X direction gives the azimuthal location of the flaws in the direction of the weld (starting from some fixed point on the ring); the Y direction shows the position of the flaw in the through-wall extent of the weld; and the Z direction shows the radial position of the flaw in the weld. The Y and Z directions are shown on Figure 1. The X direction is shown on Figure 5, given in Section 6.2.1.1.4.

The flaws in Ring K are the result of a poor weld preparation (BSC 2003d) that was performed under conditions that are not representative of the highly controlled environment in which future manufacturing of the waste packages will take place. Nevertheless, following a conservative approach these flaws have been kept in this analysis. The other flaws reported in Table 7 are lack-of-fusion type defects (BSC 2003d).

The parameters given previously are appropriate for use in this analysis because they yield characteristics of flaws of Alloy 22 welds, whose design conforms to that of the closure weld of the waste package.

4.1.4 Anomaly Distribution Curve for Hard-Alpha Inclusion in Titanium Alloy

Information from the U.S. Federal Aviation Administration (FAA), published in an advisory circular related to the distribution of hard-alpha inclusions in titanium engine rotors, was used in this analysis. *Damage Tolerance for High Energy Turbine Engine Rotors* (FAA 2001) contains several anomaly distribution curves associated with hard-alpha inclusions (also called Type I defects) (i.e., the number of hard-alpha inclusions per million pounds of titanium as a function of their size). These anomaly distribution curves are accepted data. The rationale for this is that these curves are accepted by the FAA to show compliance with requirements of Federal Aviation Regulations (14 CFR 33.14). 14 CFR 33.14 contains requirements applicable to the design and life management of high energy rotating parts of aircraft gas turbine engines (FAA 2001, Section 1).

Briefly stated, the distributions were developed by modeling a complex series of interrelated steps that simulated the entire component manufacturing process from billet conversion to final machining as rotor components of aircraft engines. The final distributions were validated based on field experience. They are applicable to titanium rotor components manufactured after 1995 using the triple vacuum arc remelt process or the cold hearth melt plus vacuum arc remelt process (FAA 2001, p. S3-7).

Different distributions were developed reflecting different levels of sensitivity for the UT inspections performed at the billet stage and at the forging stage (FAA 2001, Appendix 3). Following a conservative approach, the anomaly distribution with the less sensitive UT inspections was selected for use in the present analysis. It corresponds to a UT inspection calibrated with #5 flat bottom hole at the billet stage and a UT inspection calibrated with #3 flat bottom hole at the forging stage. The flat bottom hole calibration standard consists of a block of material containing holes of varying diameters. The diameters of the holes are specified in multiples of 1/64 inch.

In the advisory circular, the anomaly distribution curve is provided on a log-log graph (FAA 2001, p. A3-2). From the log-log graph, a set of data points large enough to capture the main features of the curve was selected for use in this analysis and is given in Table 8.

According to *Damage Tolerance for High Energy Turbine Engine Rotors* (FAA 2001, p. A1-1), the anomalies are considered spherically shaped and uniformly distributed throughout the part. Also, the same reference states that when anomaly sizes are required outside the range of data provided, the curve shown on the log-log graph should be linearly extrapolated.

Table 8. Set of Data Points for Hard-Alpha Inclusion Anomaly Distribution Curve

Defect Inspection Area (square mils)	Exceedance ^a (per million pounds)	Defect Inspection Area (square mils)	Exceedance ^a (per million pounds)
100	6.6	2000	0.21
200	3.6	3000	0.084
300	2.6	4000	0.051
400	2.0	5000	0.037
500	1.7	6000	0.028
600	1.3	7000	0.022
700	1.1	8000	0.020
800	0.90	9000	0.017
900	0.75	10,000	0.016
1000	0.65	20,000	0.010

NOTE: ^a Number of inclusions of this size or larger.

Source: FAA 2001, p. A3-2

The data shown in Table 8 are appropriate for use in this analysis for the following reasons:

- Hard-alpha imperfections are a dominant source of internal defects for titanium metal base. Hua et al. (2002, p. 7) suggest that this kind of defect may have been responsible for an abnormally high corrosion rate that was observed on several annealed Titanium Grade 7 specimens exposed to a corrosive environment in a set of experimental tests. Hard-alpha defects are formed from very high nitrogen or oxygen concentrations in the bulk alloy and cannot be readily eliminated by a homogenizing heat treatment of primary mill processing (Hua et al. 2002, p. 7). These defects tend to string out during forging and rolling. Because they are hard they tend to break up during hot rolling and may form very small internal voids (Graham 2002). That is why they are accounted for among the potential defects that could lead to the early failure of the drip shield.
- It is recognized that the anomaly distribution curve used in this analysis was intended for machined titanium-alloy rotors used in aircraft engines. This is a different type of titanium than the commercially pure (Grade 7) titanium to be used for the drip shield. Also, drip shield plates are obviously not similar to engine rotors. Nevertheless, hard-alpha defects are inherited from material processing, and from this point of view, titanium-alloy and commercially pure titanium have a very similar process route (Graham 2002). Moreover, titanium plates have a less complex shape than engine rotors, which should make the UT inspection and consequently the detection of hard-alpha defects much easier. For these reasons, it is considered that use of the previous data is appropriate in this analysis as it will provide a conservative estimate of the number of hard-alpha defects expected in the base metal of the drip shield, as a function of their size. It should nevertheless be kept in mind that the data used are only applicable to triple vacuum arc remelt or cold hearth melt plus vacuum arc remelt processed titanium. Also, these data apply to titanium that gets two UT's (at the billet stage, with #5 flat bottom hole, and at the forging stage, with # 3 flat bottom hole).

4.2 CRITERIA

NRC requirements that pertain to the conduct of performance assessments are applicable to this evaluation. Section 63.102(j) of 10 CFR Part 63 states that:

The features, events and processes considered in the performance assessment should represent a wide range of both beneficial and potentially adverse effects on performance [...]. Those features, events, and processes expected to materially affect compliance with Sec. 113(b) or be potentially adverse to performance are included, while events (event classes or scenario classes) that are very unlikely (less than one chance in 10,000 over 10,000 years) can be excluded from the analysis.”

The current design basis waste package inventory anticipates 11,184 waste packages to be emplaced in the repository (number based on the sum of the nominal numbers of each type of waste package shown in Table 11 of *Repository Design Project, RDP/PA IED Typical Waste Package Components Assembly (2)* (BSC 2003a). Therefore, the previous requirement would indicate that any feature, event, or process that has a probability of occurrence of less than $10^{-4}/11,184 = 8.9 \times 10^{-9}$ per waste package over 10,000 years can be excluded from the performance assessment. Since this analysis results in early failure of waste packages and drip shields with a mean value on the order of 3×10^{-5} per waste package, this FEP is included in the TSPA-LA analysis.

Yucca Mountain Review Plan, Final Report (NRC 2003) contains Acceptance Criteria (AC) intended to establish the basis for the review of the material contained in the License Application. As this model report serves, in part, as the basis for the License Application, it is important that the information contained herein conform to those same Acceptance Criteria. This calculation addresses the degradation of two engineered barriers. Brief summary descriptions of these components are provided in Sections 1 and 4.1.1. Based on the engineered barrier role of the waste package and drip shield, the processes involved with its degradation, and the potential impact of its degradation, the Acceptance Criteria that are applicable to this calculation are delineated below.

YMRP Acceptance Criteria 2.2.1.1.3—System Description and Demonstration of Multiple Barriers

AC 1 – Identification of Barriers is Adequate

Barriers relied upon to achieve compliance with 10 CFR 63.113(b), as demonstrated in the total system performance assessment, are adequately identified and clearly linked to their capability.

AC 2 – Description of Barrier Capability Is Acceptable

The capability of the identified barriers to prevent or substantially reduce the movement of water or radionuclides from the Yucca Mountain repository to the accessible environment or prevent the release or substantially reduce the release rate of radionuclides from the waste is adequately identified and described:

(1) The information on the time period over which each barrier performs its intended function, including any changes during the compliance period, is provided;

(2) The uncertainty associated with barrier capabilities is adequately described;

(3) The described capabilities are consistent with the results from the total system performance assessment;

(4) The described capabilities are consistent with the definition of a barrier at 10 CFR 63.2

AC 3 – Technical Basis for Barrier Capability is Adequately Presented.

The technical bases are consistent with the technical basis for the performance assessment. The technical basis for assertions of barrier capability is commensurate with the importance of each barrier's capability and the associated uncertainties.

YMRP Acceptance Criterion 2.2.1.3.1.3, AC 3 (4) (NRC 2003) expects that the DOE use “appropriate methods for nondestructive examination of fabricated engineered barriers to assess the type, size, and location of fabrication defects that might lead to premature failure as a result of rapidly initiated engineered barriers degradation.” The criterion further states that the DOE specify and justify “the allowable distribution of fabrication defects in the engineered barriers and [assess] the effects that cannot be detected on the performance of the engineered barriers.” The analyses contained in this report consider the potential existence of such defects, the probability of their occurrence, and their potential impact.

5. ASSUMPTIONS

Many of the following assumptions are related to operations, processes and procedures governing the fabrication, closure, inspection and transportation of the waste packages and drip shields. No uncertainty or confidence level can be assigned at this time for the validity of these assumptions.

5.1 ASSUMPTIONS RELATED TO FLAWS IN ALLOY 22 WELDS

5.1.1 Flaw Detection by Ultrasonic Testing

Assumption: It is assumed that all flaws greater than 1 mm (UT detection threshold) have been detected during the UT inspection of the specimen rings: these are the indications reported in Section 4.1.3.2. It is also assumed that these indications are sufficient to characterize the significant flaws expected in the Alloy 22 outer closure welds of the waste package. By significant flaws it is meant those flaws that may jeopardize the performance (time to breach) of the waste package in the repository.

Rationale: The rationale for the first part of the assumption is as follows:

Metallographic inspections were performed on the specimen rings and the weld imperfections discovered through this process were the same weld imperfections discovered during the UT inspections for all weld imperfections greater than 1 mm (see Section 4.1.3.2). Of course, it was not possible to perform metallographic examination on the entire specimen rings since it is a very time-consuming process; instead, metallographic inspections (up to six per ring) were performed at randomly selected locations in the areas where no flaw had been detected through UT inspection. None of these metallographic inspections revealed a flaw of size larger than the UT detection threshold of 1 mm. This strongly suggests that the majority, if not all, of the flaws greater than 1 mm were detected.

The rationale for the second part of the assumption follows:

The imperfections uncovered through metallographic examinations, that were not detected through UT inspections, were gas pores, and the majority of them were less than 0.003 inch (around 0.08 mm) in diameter. Gas pores are spherical in shape and have no orientation. Therefore, they are not part of those flaws that are radially oriented. Gas pores are treated the same as spherical porosity in *Stress Corrosion Cracking of the Drip Shield, the Waste Package Outer Barrier, and the Stainless Steel Structural Material* (BSC 2003e, Section 6.2.2.1). In other words, they will not induce propagation of cracks via stress corrosion cracking. Thus, they are not likely to jeopardize the performance of the waste package and can be discarded from further consideration.

Use in the Calculation: This assumption is used in Section 6.2.1.1.

5.1.2 Representation of Ultrasonic Test Probability of Nondetection Curve

Assumption: It is assumed that the UT probability of nondetection (PND) curve of the flaws in the waste package closure weld (i.e., the curve that gives the PND of a flaw as a function of its size) can conservatively be represented by using Equation 21 with the following parameters: $\varepsilon = 0.005$, $\nu = 3$, and $s_0 = 2.5$ mm.

Rationale: This assumption is needed because the UT PND curve related to the UT inspection of the specimen rings was not developed. This makes it necessary to assume the shape of the curve and the associated parameter values. The rationale for this assumption is as follows. Equation 21 is based on results of previous UT reliability studies summarized by Bush (1983, pp. 13A.5.6 and 13A.5.7). The suggested parameter values are $\varepsilon = 0.005$, $\nu = 3$, and $s_0 = 5$ mm. However, these studies were performed in the late 1970s, and do not reflect the UT inspection capability attainable with current technology. More recent studies, such as that reported by Heasler and Doctor (1996), show significantly improved reliability. Also, the UT inspections performed on the specimen rings showed that flaws as small as 1 mm in size could effectively be detected (see Section 4.1.3.2). This is an important result since the welds on the specimen rings are very similar to the closure welds of the waste package. Based on this information, the parameter values suggested by Bush (1983) appear to be very conservative. Nevertheless, they have been kept for this analysis, except for the value of s_0 , which has been reduced to 2.5 mm. This has been done to have a more realistic representation of the UT PND curve and, in light of previous information, is still deemed conservative. Also, note that this value is appropriate to account for

those small flaws that will be detected, but left in the weld, because these flaws will not jeopardize the waste package performance.

Use in the Calculation: This assumption is used in Section 6.2.1.2.

5.1.3 Extension of Outer Lid Weld Flaw Distribution Characteristics

Assumption: The characteristics of the distributions of flaw size in the Y direction, flaw density, flaw depth, and flaw orientation investigated in Sections 6.2.1.1 and 6.2.1.2 were developed for the outer lid weld of the waste package. It is assumed that these characteristics also apply to the middle lid weld and seam welds of the waste package (see Section 6.2.1.3 for the definition of the seam welds).

Rationale: This assumption is needed because no flaw information concerning welds other than the outer lid weld is available. The rationale for this assumption is as follows:

- *Flaw size in the Y direction:* The evaluations performed in Section 6.2.1.1.1 show that Equation 6 is compatible with the size given by the UT indications in the Y direction. Equation 6 is based on an exponential distribution that was adjusted to fit the flaw sizes within the thickness t of the weld considered. There is no reason to believe that the flaws in the other welds of the outer barrier of the waste package would be of a different nature than those detected through UT indications. Based on this reasoning, it can be expected that the differences in size in the through-wall direction (Y direction) will be mainly governed by the cap imposed by the weld thickness. Equation 6 was devised to take into account this weld thickness effect. It is worth noting that a basic comparison with another possible form of the equation that could account for the weld thickness effect was also performed (see Section 6.2.1.1.1 and Attachment I). Equation 6 was shown to provide more conservative results. Based on this information, Equation 6 appears to provide a reasonable way to adjust the flaw size distribution in the Y direction to different weld thicknesses of the waste package outer barrier.
- *Flaw density:* The flaw density parameter (which corresponds to a mean number of flaws per meter of weld) evaluated in Section 6.2.1.1.2 pertains to a 25-mm thick weld. The middle lid weld and the seam welds are respectively 10 mm and 20 mm thick (see Section 6.2.1.3 for explanations). Since the density of flaws in the welds can be expected to be proportional to the mass of weld used, there should be fewer flaws per meter of weld in the middle lid weld and the seam welds than in the outer lid weld. Therefore, applying the flaw density pertaining to the outer lid weld to the other welds is conservative.
- *Flaw depth:* The investigation performed in Section 6.2.1.1.3 shows that the depth of the flaws detected through UT indications is uniformly distributed throughout the weld thickness. There is no reason to believe that the flaws expected to occur in the welds of the outer barrier of the waste package will be of a different nature than those that were detected through UT indications. Therefore, it is reasonable to consider that these flaws will be uniformly distributed throughout the through-wall extent of the welds.

- *Flaw orientation:* The investigation performed in Section 6.2.1.1.4 shows that the orientation of the majority of flaws follows the direction of the weld. This is due to the fact that the significant weld imperfections correspond for the most part to lack-of-fusions flaws. The investigation performed in Section 6.2.1.1.4 also accounts for a flaw making a 27-degree angle with the direction of the weld. This flaw was kept in the analysis though it resulted from a poor weld preparation that is not representative of the highly controlled conditions under which operations will be performed on the waste package (see Section 6.2.1.1.4). This makes the evaluation of the orientation of the flaw conservative. There is no reason to believe that the significant flaws in the other welds of the outer barrier of the waste package would be of a different nature than those detected through UT indications. Therefore, considering that the results obtained for the outer lid weld also apply to the other welds of the outer barrier of the waste package is reasonable.

Use in the Calculation: This assumption is used in Section 6.2.1.3.

5.2 ASSUMPTIONS RELATED TO FLAWS IN ALLOY 22 BASE METAL

5.2.1 Repair of Alloy 22 Base Metal

Assumption: It is assumed that repair of Alloy 22 base metal will occur on each waste package and affect approximately 100 cm² of base metal. It is also assumed that introduction of flaws in the base metal during repair will result from the failure of the welder to use the written procedure governing the repairs to base metal, followed by the failure of the checker to detect the errors made by the welder.

Rationale: The first part of this assumption is needed because, in absence of data, it is impossible to estimate an upper value for the frequency of improper base metal repair in the waste package. The rationale for the assumption is that assuming a base metal repair for each waste package is very conservative. Note that the number chosen for the affected area, 100 cm² (equivalent to a square with a side of 10 cm), is somewhat arbitrary. The difficulty here is that it is necessary to know the extent to which base metal repairs will be performed, but there is no available data. Nevertheless, it is known that rejectable defects detected during the UT inspection of the waste package may be repaired by welding, provided prior approval is granted by U.S. Department of Energy, and that defective material that cannot be satisfactorily repaired will be rejected and replaced (Plinski 2001, Section 6.5). Based on this information, it makes sense to consider that only a small portion of the waste package material might be subjected to repair and that beyond a certain extent, the material will be rejected. In that light, a 100-cm² area seems realistic. Notice that the arbitrariness of that number is tempered by the conservatism in considering that every single waste package will require base metal repair.

The rationale for the second part of the assumption is that the fabrication of the waste package will be performed following a strict quality assurance (QA) program (Plinski 2001, Section 6). Consequently, the basic scenario by which flaws could be introduced in the base metal appears to be adequate.

Use in the Calculation: This assumption is used in Section 6.2.2.

5.2.2 Ratio of Weld Flaws to Base Metal Flaws

Assumption: It is assumed that the ratio of weld flaws to base metal flaws resulting from repairs in the Alloy 22 barrier of the waste package is eight to one.

Rationale: This assumption is needed because there is no data available on the density of flaws in Alloy 22 base metal. The rationale for this assumption is that it is a conservative ratio, based on findings by Schuster et al. (2000, p. 2.3), resulting from the UT examination of an unused reactor pressure vessel. Schuster et al. (2000, pp. 4.2 and 4.3) propose several possible explanations for the flaws detected in base metal: laminations, imperfections at the clad-to-base metal interface of the vessel, and repairs to base metal. Here, it is conservatively considered that all the base metal flaws are a consequence of repairs. The ratio (Schuster et al. 2000, p. 23) was determined for a stainless steel container, but because of its conservative application in this assumption, it is also considered acceptable for the Alloy 22 barrier of the waste package.

Use in the Calculation: This assumption is used in Section 6.2.2.

5.3 ASSUMPTIONS RELATED TO IMPROPER WELD MATERIAL OR BASE METAL

The following assumptions were used in Section 6.2.3 to estimate the probability that improper weld or base metal material is inadvertently used in the manufacturing of the outer barrier of the waste package. Improper weld or base metal material, if not detected, may result in the emplacement of an out-of-specification waste package in the repository. Because the approach of Section 6.2.3 was also employed for evaluating the probability of using improper weld or base metal material in the drip shield, these assumptions also apply to Section 6.3.3.

5.3.1 Approximation of Probability of Using Improper Weld Material

Assumption: It is assumed that the probability of using improper weld material in the fabrication of the outer barrier of the waste package can be approximated by a lognormal distribution whose 5th and 95th percentile are respectively 1.5×10^{-5} and 8.2×10^{-5} .

Rationale: This assumption is needed because no data has yet been accrued on the use of improper weld material in the fabrication of a waste package.

The rationale for this assumption is based on the only well-documented occurrence of weld populations that were affected by improper weld material. In the preparation of a response to NRC Bulletin 78-12 (NRC 1978), which was prompted by the discovery that the weld chemistry of a portion of the Crystal River 3 surveillance-block weld did not meet the specification requirements, Babcock & Wilcox investigated their records to determine the extent to which out-of-specification weld wire may have been used in the fabrication of reactor vessels (Babcock and Wilcox 1979). Out of 1,706,556 pounds of weld wire (Babcock & Wilcox 1979, p. I-6) that was used to make 43 reactor vessels for the American market (Babcock & Wilcox 1979, Table 1 of Part II), it was estimated that 65 to 350 pounds of weld wire was out-of-specification (Babcock & Wilcox 1979, pp. 2 and I-4). No other instances of improper weld material were reported in other vendors' responses to NRC Bulletin 78-12 (NRC 1978). There have been around 120 reactors operated in the United States (rounded-down number, based on ANS 1999, pp. 52 to

55), so these 43 reactors account for less than 36 percent (43/120) of the vessels fabricated for use in the United States. Conservatively round up this number to 40 percent. Therefore, the total mass of weld material used to fabricate these vessels has been at least 4,266,390 pounds (1,706,556/0.4). Thus, the probability of using improper welding material ranges from 1.5×10^{-5} (65/4,266,390) to 8.2×10^{-5} (350/4,266,390).

The information provided in *Records Investigation Report Related to Off-Chemistry Welds in Material Surveillance Specimens and Response to IE Bulletins 78-12 and 78-12A – Supplement* (Babcock and Wilcox 1979) is not sufficient in itself to draw conclusions on the shape of the distribution for the probability of using improper welding material. Nevertheless, the lower and upper values estimated previously are assumed here to represent the 5th and 95th percentile of a lognormal distribution. The reason for choosing the 5th and the 95th percentiles is that it is common practice when evaluating lower and upper bounds: for example, this is the percentiles recommended by Swain and Guttman (1983, p. 2-19) in evaluating uncertainty of HEPs. As for the lognormal distribution, it has mainly been chosen for tractability reasons in the calculation of uncertainty bounds: this is based on the fact that the product of independent lognormal distributions (extensively used in this analysis) is also lognormal (Swain and Guttman 1983, pp. A-2 and A-4).

Use in the Calculation: This assumption is used in Section 6.2.3.

5.3.2 Field Measurements of Material Compositions

Assumption: It is assumed that quick field measurements of material compositions, using equipment such as a portable X-ray spectroscopy device, will be performed by a technician before welding material is used on the waste package.

Rationale: The rationale for this assumption is that the technology for these types of measurements is currently available (ASM International 1990b, pp. 1030 to 1032) and used in a variety of similar commercial applications.

Use in the Calculation: This assumption is used in Section 6.2.3.

5.3.3 Probability of Using Improper Base Metal

Assumption: It is assumed that the probability of using improper base metal in the fabrication of the outer barrier of the waste package is the same as the probability of using improper weld material (calculated in Assumption 5.3.1).

Rationale: The rationale for this assumption is that the processes that would lead to the use of improper base metal (e.g., procurement, selection, or shipment of the incorrect material) are of the same nature as those that would lead to the use of improper weld material. Therefore, it is reasonable to consider that these probabilities are equal. As discussed in Section 6.1.6, no instances of improper base material use have been identified.

Use in the Calculation: This assumption is used in Section 6.2.3.

5.4 ASSUMPTIONS RELATED TO IMPROPER WASTE PACKAGE HEAT TREATMENT

The following assumptions were used in Section 6.2.4 to estimate the probability that a waste package is improperly heat treated and that this improper heat treatment remains undetected. Because the approach of Section 6.2.4 was also employed for evaluating the probability of improper heat treatment of the drip shield, these assumptions also apply to Section 6.3.4.

5.4.1 Heat Treatment Process and Procedural Controls

Because the procedures and equipment for heat treating the waste package have not yet been written, it is necessary to make a set of assumptions on the process to be implemented and on the controls that will be put in place to detect any potential improper heat treatment of the waste package.

Rationale: The rationale for this set of assumptions is that, in absence of written procedures, they describe a realistic process for implementing and controlling the heat treatment of the waste package based on current industry heat treatment techniques. In particular, the main assumption is that the process will be computerized. This is based on information from *Heat Treating Progress, I* (ASM International 2001, p. 103), which describes computer control of heat treating operations as common practice. Compared to manually controlled heat treatment, computerization provides for higher precision of measurement and control, increased speed of measurement and response to process changes, and better accuracy in record keeping and reporting. The set of additional assumptions related to the implementation and control of the heat treatment process is as follows:

- It is assumed that the operator will have to select between several predefined heat treatment programs, each corresponding to a different kind of waste package. Also, it is considered that the heat treatment program will cover the heating phase as well as the quenching phase. Considering that the heat treatment program is predefined means that the temperature to reach inside the furnace, for the ramp-up and hold phases as well as the time required for quenching the waste package, is already known and executed by the program.
- It is assumed that the waste package temperature will be measured by thermocouples installed on the waste package before each heat treatment.
- It is assumed that the proper installation of the waste package thermocouples will be verified through an over-the-shoulder inspection performed by a checker.
- It is assumed that some fixed instrumentation will be used for measuring and controlling the parameters governing the heat treatment process such as temperature of the furnace, flow rate of the fluid used for quenching, time spent by the waste package in ramp-up, hold, and quench phase, etc. Because this type of instrumentation and control does not need to be reinstalled each time a waste package is processed, it is further assumed that it will be sufficiently redundant and diversified, such that any significant process malfunction would be detected and signaled to the operator by alarm.

- It is assumed that the thermocouples installed on the waste package will not be used to control the heat treatment program but only to measure the temperature of the waste package at specific locations and trigger an alarm if the measured temperatures deviate from the allowable range. The reason for this restriction in the role of the waste package thermocouples is that they need to be reinstalled for each waste package. As a consequence, they are more prone to improper installation and subsequent malfunction, than the fixed instrumentation of the furnace and the quenching equipment, instrumentation, which is considered more reliable since it can be more easily made redundant and diversified.
- It is assumed that a log of the control parameters and the events recorded during the heat treatment process will automatically be generated by the computerized heat treatment system. It is further assumed that this log will be reviewed through a QA check performed by an individual other than the operator.

Use in the Calculation: This assumption is used in Section 6.2.4.

5.4.2 Event Sequence Resulting in Improper Heat Treatment

Rationale: Additional assumptions are required to develop the event sequences that would lead to an undetected improper heat treatment of the waste package. The rationale for these complementary assumptions is that they are based on a conservative approach.

- It is assumed that for a waste package to be properly heat treated, it is necessary that the operator selects the correct heat treatment program. An incorrect heat treatment program selection will result in a waste package temperature drift outside of the allowable range for adequate heat treatment of the waste package. Notice that this drift in temperature will normally be captured by the thermocouples installed on the waste package and will prompt an alarm from the computerized heat treatment control system.
- It is assumed that if an incorrect heat treatment program is selected, the waste package thermocouples will not capture the temperature drift outside of the allowable range if their installation was improperly performed (for instance, the thermocouples might be incorrectly affixed to the waste package or installed in incorrect locations leading to different temperature measurements than those that a proper installation would yield). Conversely, notice that a correct selection of the heat treatment program combined with an incorrect installation of the thermocouples will not lead to an improper heat treatment of the waste package. This is due to the fact that the waste package thermocouples are utilized to measure the temperature, not to control the process (see Assumption 5.4.1). Therefore, this scenario cannot lead to an undetected improper heat treatment of the waste package.
- It is assumed that operator failure to respond to an alarm prompted by the computerized heat treatment control system, signaling a process malfunction, will result in an improper heat treatment of the waste package. If, during the review of the log generated by the computerized heat treatment system, the checker fails to detect that the operator did not respond to the alarm the improper heat treatment of the waste package will

remain unnoticed. Conversely, it is assumed that detection of the alarm by the operator or the checker cannot lead to an undetected improper heat treatment.

Use in the Calculation: This assumption is used in Section 6.2.4.

5.4.3 Probability of a Significant Process Malfunction

Assumption: It is assumed that the probability that a significant process malfunction occurs during the heat treatment of a waste package can be approximated by a lognormal distribution with a median of 0.005 and an error factor of 2.

Rationale: This assumption is needed because there is no operating experience on malfunctions that may affect the heat treatment of the waste package (i.e., no data is available). The rationale for the malfunction probability given previously is that it is conservative. More details are given in the following paragraphs.

The lognormal distribution was chosen for tractability reasons in the calculation of uncertainty bounds: this is based on the fact that the product of lognormal distributions (extensively used in this analysis) is also lognormal (Swain and Guttman 1983, pp. A-2 and A-4). A median of 0.005 and an error factor of 2 were chosen as conservative estimates for the probability of a process malfunction. This information can equivalently be expressed in terms of probability range with the 95th percentile for the distribution at $0.005 \times 2 = 0.01$ and the 5th percentile at $0.005/2 = 2.5 \times 10^{-3}$. On average, with the 95th percentile a process malfunction can be expected to occur every $1/0.01 = 100$ heat-treated waste packages and with the 5th percentile every $1/2.5 \times 10^{-3} = 400$ heat-treated waste packages. This range reflects a high frequency of malfunction occurrence. In reality, the heat treatment process can be expected to be much more reliable and it is not desirable to have a process jeopardize a valuable piece of equipment such as the waste package as often as predicted by the previous estimates.

The fact that these values are conservative is also confirmed by a very simple preliminary reliability assessment (since the designs of the furnace and the quenching system have not been decided yet, it is too early to make a precise evaluation of the system reliability). A critical parameter of the heat treatment process is the temperature in the furnace, which, for illustration purpose, is considered here to be regulated by heaters and the associated instrumentation for control. Based on information from Eide and Calley (1993, Table 2), the failure rate of an electrical heater is approximately $5.0 \times 10^{-6}/\text{h}$. Also, the failure rate for an element of instrumentation is $1.0 \times 10^{-6}/\text{h}$ and that for a transmitter is $3.0 \times 10^{-6}/\text{h}$. These components constitute a base unit for maintaining the furnace at its proper temperature. Assuming that the heater is expected to operate for 10 hours per each processed waste package (which is a reasonable to conservative number), a point estimate for the probability of failure of the heater with its associated instrumentation is $10 \times (5 + 1 + 3) \times 10^{-6} = 9 \times 10^{-5}$. Thus, it can be expected that proper operation of several heaters will be required for the correct heat treatment of the waste package. Also, it is reasonable to consider that the critical components will be redundant and diversified to lower their dependency to failure by common cause. Based on that information and the previous estimate, it can be expected that the heat treatment process will have a probability of malfunction in the 10^{-4} order of magnitude per heat-treated waste package (i.e., below the probability range considered in this assumption).

Use in the Calculation: This assumption is used in Section 6.2.4.

5.5 ASSUMPTIONS RELATED TO IMPROPER LASER PEENING

The following assumptions were used in Section 6.2.5 to estimate the probability that the closure welds of a given waste package is improperly laser-peened, preventing an adequate stress mitigation, and that this improper laser peening remains undetected.

5.5.1 Laser Peening Process and Procedural Controls

Assumption: It is assumed that the laser peening system will be fully computerized and that process malfunctions will be signaled to the operator via alarms.

Rationale: The rationale for this assumption is based on information provided by Sano et al. (2000), which describes a laser peening system that was successfully used for an industrial application, namely the stress mitigation of the core shroud of a nuclear reactor. The system included automated beam alignment/tracking function, remote handling equipment, an online monitor, and a system control unit (Sano et al. 2000, p. 2). Also, the system was computerized to allow continuous monitoring of the laser irradiation (Sano et al. 2000, p. 6). This example shows that a fully computerized laser peening system can be used for an industrial application. It is expected that a computerized system will be used for the laser peening of the waste packages, since more than 10,000 waste packages are expected to be processed, which calls for automation.

Use in the Calculation: This assumption is used in Section 6.2.5.

5.5.2 Automatic Generation of an Event Log

Assumption: It is assumed that a log of the control parameters and the events recorded during the laser peening process will automatically be generated by the computerized laser peening system. It is further assumed that this log will be reviewed through a QA check performed by an individual other than the operator. Lastly, it is conservatively assumed that the operator failure to respond to an alarm prompted by the computerized laser peening control system, signaling a process malfunction, will result in an improper laser peening.

Rationale: The rationale for this set of assumptions is that a computerized control system enables better reporting of the control parameters and better tracking of deviation from these parameters than a manually controlled system. Also, QA checks performed by independent checkers are common practice in the nuclear industry.

Use in the Calculation: This assumption is used in Section 6.2.5.

5.5.3 Approximation of Probability of a Significant Process Malfunction

Assumption: It is assumed that the probability that a significant process malfunction occurs during the laser peening of a waste package can be approximated by a lognormal distribution of median 0.005 and error factor of 2.

Rationale: This assumption is similar to Assumption 5.4.3 and its rationale is basically the same. Only the highlights are given here. This assumption is needed because no operating experience has been accrued on laser peening of the waste packages (i.e., no data exist). The lognormal distribution has been chosen for tractability reasons in the calculation of uncertainty bounds. The value of the parameters is such that the probability range is conservative: on average, a significant malfunction of the process is expected to occur for every 100 to 400 waste packages treated, which is a high frequency of occurrence for malfunctions jeopardizing a piece of equipment as valuable as the waste package.

Use in the Calculation: This assumption is used in Section 6.2.5.

5.6 ASSUMPTIONS RELATED TO WASTE PACKAGE CONTAMINATION

The following assumptions were used in Section 6.2.6 to estimate the probability that a waste package gets its surface contaminated by some corrosion-enhancing material and that this contamination remains undetected. Note that radiological contamination is not considered here.

5.6.1 Naked-Eye Inspection of Waste Package for Contamination

Assumption: It is assumed that a naked-eye inspection of the waste package will take place at reception to the surface facilities of the repository and that this inspection will detect all visible traces of contamination on the waste package (i.e., presence of foreign material on the waste package). It is also assumed that a remote inspection of the waste package (via camera) will take place just before the waste package is emplaced on the pallet in order to detect any visible trace of contamination. Lastly, it is assumed that these two inspections will be independent from each other.

This assumption is needed because the procedures governing the control of operations on the waste package have not been written yet.

Rationale: The rationale for the assumption is that performing an inspection when receiving a highly controlled piece of equipment such as the waste package, and another one before the equipment is going to be put in service, is to be expected since it is common practice to perform similar tasks in the nuclear industry on sensitive material. Also, it should be noted that when received at the facility the waste package can be easily and thoroughly inspected since it has not yet been loaded with nuclear waste and therefore is not radioactive. The final inspection is supposed to be performed right before emplacement on the pallet because it enables a complete inspection of the waste package and at the same time ensures that this inspection performed late in the process will catch potential contaminations that might have occurred earlier. Also, the final inspection is supposed to be performed remotely via a camera in order to account for protection of the operator against radiation. Independence of the two inspections is warranted by the fact that these inspections will take place at different locations, at different time, and using different means (naked-eye inspection versus remote inspection). Furthermore, these inspections will most likely be performed by different individuals.

Use in the Calculation: This assumption is used in Section 6.2.6.

5.6.2 Postexamination Contamination of the Waste Package

Assumption: It is assumed that after the final waste package inspection (just before it is emplaced on the pallet) the probability that the waste package is subjected to further contamination without that being detected is negligible.

Rationale: The rationale for this assumption is as follows: After the final waste package inspection, the most likely activity that could leave a foreign material on the waste package (i.e., causing its contamination) is through its handling. However, the waste package is subject to only one direct handling, namely its tilting onto the pallet. After that, it is the pallet which is directly handled, not the waste package (which merely sits on the pallet). Therefore, only the tilting operation is of concern here. At this time, the waste package will be loaded with radioactive waste. Consequently, for radioprotection purposes, the waste package tilting operation can be expected to be subjected to more scrutiny than the handling operations preceding the loading of the waste package with waste. In that light, it is unlikely that a contamination of the waste package would go unnoticed. Also, during its transport to the underground repository the waste package will be protected from exposure to exterior sources of contamination by the shielding from the waste package transporter. Then, the gantry will protect the waste package until it is emplaced in the drift.

Use in the Calculation: This assumption is used in Section 6.2.6.

5.6.3 Possibility of Waste Package Contamination During Cleaning

Rationale: Because contamination of the waste package could occur during one of its cleanings, and since no procedures governing the cleaning process have yet been written, it is necessary to make a set of assumptions on the circumstances that could cause such contamination. The rationale for these assumptions is that they describe realistic conditions for a contamination scenario.

- It is assumed that the Alloy 22 barrier will be subjected to a total of eight cleanings, namely: after each of five welds (two longitudinal and one circumferential for welding the outer barrier, one for welding the support ring, one for welding the bottom lid), after heat treatment, before shipping, and at reception at the surface facility of the repository.
- It is assumed that there are different operators for each cleaning occurrence and that each cleaning is independent of the other cleanings.
- It is assumed that contamination of the waste package through its cleaning may result only from the use of an improper cleaning agent. In other words, an incorrect cleaning process such as forgetting or incorrectly performing a step with proper cleaning agents cannot leave a residue that can have adverse effects on the metal.
- It is assumed that the maintenance policies governing the facilities where the waste package will be fabricated and handled will require that the cleaning agents used for the waste package be stored in a separate stockage area so as to avoid confusion with other cleaning products. A consequence of this assumption is that selection of an improper

cleaning agent by the technician in charge of waste package cleaning means that the maintenance policies are not properly carried out.

- It is assumed that a QA check will review the cleaning process after the cleaning has occurred. This is a check of the process, not the actual surface of the metal as the presence of contaminants from cleaning is considered not to be visible to the naked eye.

Use in the Calculation: This assumption is used in Section 6.2.6.

5.7 ASSUMPTIONS RELATED TO IMPROPER WASTE PACKAGE HANDLING

The following assumptions were used in Section 6.2.7 to estimate the probability that a waste package is damaged by mishandling and that the damage remains undetected.

5.7.1 Naked-Eye Inspection of Waste Package for Damage

Assumption: It is assumed that the inspections considered in Assumption 5.6.1 will also serve to detect traces of damage to the waste package. Recall that two inspections of the waste package are supposed to take place in the surface facilities of the repository: a naked-eye inspection when the waste package is received and a remote inspection (via camera) just before the waste package is emplaced on the pallet. Also, as in Assumption 5.6.1, it is assumed that the two inspections will be independent from each other and that the inspection at waste package reception will detect all visible traces of mishandling.

Rationale: The rationale for this assumption is the same as that given in Assumption 5.6.1.

Use in the Calculation: This assumption is used in Section 6.2.7.

5.7.2 Waste Package Damage Due to Mishandling After Reception But Before Final Inspection

Assumption: It is assumed that between the inspection at waste package reception and the final inspection, the waste package might be mishandled and damaged on four occasions: when installed on the turntable to receive its collars, when tilted in an upward position, when installed in the staging area, and when removed from the staging area and placed onto the waste package pallet.

Rationale: The rationale for this assumption is that these operations are the only ones during which the waste package is not expected to be protected from external shocks by some shielding equipment. When stored in the storage area or transported to the loading cell or the welding cell the waste package will be surrounded by protective equipment. Mishandlings that could occur when loading the fuel assemblies in the waste package are not considered because they will affect the waste package basket or at most the inner surface of the stainless steel cylinder, which is not of concern for the performance of the Alloy 22 barrier.

Use in the Calculation: This assumption is used in Section 6.2.7.

5.7.3 Waste Package Damage Due to Mishandling During Final Inspection

Assumption: It is assumed that after the final waste package inspection (just before it is emplaced on the pallet), the probability that the waste package is subjected to further damage by mishandling, without that being detected, is negligible.

Rationale: The rationale for this assumption is as follows. After the final waste package inspection, the most likely mishandling that could affect the waste package is its tilting onto the pallet. After that it is the pallet which is directly handled, not the waste package (which merely sits on the pallet). Therefore, only the tilting operation is of concern here. At this time the waste package will be loaded with radioactive waste. Consequently, for radioprotection purposes, the waste package tilting operation can be expected to be subjected to more scrutiny than the handling operations preceding the loading of the waste package with waste. In that light, it is very unlikely that damage of the waste package would go unnoticed. Also, during its transport to the underground repository the waste package will be protected from external shocks by the shielding from the waste package transporter. Then, the gantry will protect the waste package until it is emplaced in the drift. It is not expected that micro-shocks induced by vibrations during transportation will be significant enough to cause denting or gouging of the Alloy 22 barrier.

Use in the Calculation: This assumption is used in Section 6.2.7.

5.7.4 Approximation of Damage Due to Mishandling

Assumption: It is assumed that the probability of damaging a waste package, due to an improper handling, can be approximated by a lognormal distribution with a mean of 4.8×10^{-5} (per waste package handling) and an error factor of 10.

Rationale: The rationale for this assumption is as follows. No operating experience has been accrued on the handling of the waste packages, therefore no data exist that would enable a direct evaluation of the probability of damaging a waste package by mishandling. Instead, information on reported instances of damages to nuclear fuel assemblies during their handling was used to estimate that probability. This was done because a significant amount of operating experience has been accrued in that area. Also, fuel assembly handling activities are performed in a nuclear environment representative of the highly controlled conditions under which handling of the waste package is expected to occur. Therefore, it is deemed appropriate to use this information for estimating the probability of damaging a waste package by mishandling.

Waste Package Misload Probability (BSC 2001b, Table 5) evaluates the probability of fuel assembly damage at 4.8×10^{-5} per moved fuel assembly. This point estimate is assigned to the mean of the distribution for the probability of damaging a waste package when handled. Also, Table 4 of *Waste Package Misload Probability* (BSC 2001b) states that the majority of fuel assembly damage events are due to human errors. Thus, based on the information given on HEPs in Section 4.1.2, it is appropriate to consider that the probability of mishandling a waste package has a lognormal distribution. Additionally, based on Table 5, an error factor of 10 is assigned to this probability. This value has accordingly been assigned to the probability of waste package mishandling.

Notice that in Section 6.1.2, a corroborative estimate of the probability of damaging a fuel assembly by mishandling is performed based on information found by Yang (1997, p. 10). A probability of 4.6×10^{-4} per discharged fuel assembly is found (see Section 6.1.2). This number is not directly comparable to the results of *Waste Package Misload Probability* (BSC 2001b), which provides a probability per moved fuel assembly that accounts for additional fuel assembly handlings such as those occasioned by shuffles in the core of the reactor. In addition, the study by BSC (BSC 2001b) uses a larger operating experience than the study by Yang (1997). With these caveats in mind, the two numbers do not appear to be incompatible.

Use in the Calculation: This assumption is used in Section 6.2.7.

5.8 ASSUMPTIONS RELATED TO FLAWS IN TITANIUM WELDS

The following assumptions were used in Section 6.3.1 to estimate the probability of having weld flaws that remain undetected in the drip shield.

5.8.1 Flaw Density and Size Distributions in Titanium Welds

Assumption: It is assumed that the flaw density and size distributions of flaws in titanium welds are the same as those of Alloy 22 weld flaws.

This assumption is needed because no detailed information about the distributions of these flaws in titanium welds was found in the literature.

Rationale: The rationale for this assumption is based on the fact that welding of titanium is no more difficult than for many stainless steels (Ikeda and Shoesmith 1997, p. i). Based on *Welding, Brazing, and Soldering* (ASM International 1993, p. 740), weldability of Alloy 22 and stainless steel are similar. Therefore, it can be expected that the density and size distributions of flaws in titanium welds will be comparable to those of Alloy 22 welds. Moreover, the same reference mentions that molten nickel alloy weld metal does not flow as easily as steel weld metal. This might introduce more flaws in Alloy 22 welds. Consequently, applying the flaw density and size distribution of Alloy 22 weld flaws to flaws in titanium welds is likely to be conservative.

Use in the Calculation: This assumption is used in Section 6.3.1.

5.8.2 Ultrasonic Testing of Titanium Welds

Assumption: It is assumed that the titanium welds of the drip shield will be inspected by UT.

Rationale: The rationale for this assumption is that the welds will be inspected in order to verify that no significant defect is present. Several inspection methods are possible (Plinski 2001, Section 6). A UT inspection is assumed here because it is an effective method to detect significant flaws.

Use in the Calculation: This assumption is used in Section 6.3.1.

5.9 ASSUMPTIONS RELATED TO FLAWS IN BASE METAL TITANIUM

The following assumptions were used in Section 6.3.2 to estimate the probability of having base metal flaws that remain undetected in the drip shield.

5.9.1 Hard-Alpha Inclusions in Titanium Used for the Drip Shield

Assumption: It is assumed that the titanium that will be used for fabricating the drip shield will have hard-alpha inclusion levels corresponding at most to the levels found in triple vacuum arc remelt processed titanium that has had two UT's, once at the billet stage, with #5 flat bottom hole, and once at the forging stage, with #3 flat bottom hole.

This assumption is required to ensure that the data of Section 4.1.4 are adequate for evaluating the flaw density and size distribution in the titanium base metal used for the manufacture of the drip shield.

Rationale: The rationale for this assumption is that the triple vacuum arc remelt fabrication process and UT inspection sensitivity mentioned previously were used in the 1980s to produce alloy titanium rotors used for aircraft engines (Shamblen and Woodfield 2002). It is reasonable to expect that when the drip shield is fabricated the technology employed to produce the base metal titanium will be more performant or at least equivalent. Therefore, the frequency of occurrence for hard-alpha inclusions given in Section 4.1.4 can be expected to represent conservative levels of hard-alpha defects in the base metal titanium that will be used for the drip shield.

Use in the Calculation: This assumption is used in Section 6.3.2.

5.9.2 Frequency of Occurrence of High-Density Inclusions in Base Metal Titanium

Assumption: It is assumed that the frequency of occurrence of high-density inclusions in base metal titanium used for the drip shield is the same as the frequency of occurrence of hard-alpha defects.

Rationale: The rationale for this assumption is provided by Shamblen and Woodfield (2002, p. 3), who provide a figure showing the evolution in flaw frequencies for hard-alpha defects and high-density inclusions in premium-quality titanium alloys during the 1990s. It appears that the frequency of high-density inclusions is less than that of hard-alpha defects. Because the scale in the y-axis on the figure is not precisely defined, it is not possible to make a more detailed comparison. Nevertheless, it is conservative to state that both frequencies of occurrence are equal. It should be noted that the study performed by Shamblen and Woodfield (2002) pertains to titanium alloys used in the aircraft industry. Nevertheless, it is also considered applicable to Titanium Grade 7 and 24 that will be used for the drip shield. The reason for this is that high-density inclusions correspond to tungsten carbides that are introduced in the base metal by melting recycled scrap (Graham 2002); therefore, these inclusions occur in titanium alloys in the same manner as in commercially pure titanium.

Use in the Calculation: This assumption is used in Section 6.3.2.

5.10 ASSUMPTIONS RELATED TO DRIP SHIELD CONTAMINATION

The following assumptions were used in Section 6.3.5 to estimate the probability that a drip shield surface becomes contaminated by some corrosion-enhancing material and that this contamination remains undetected.

5.10.1 Drip Shield Inspection

Assumption: It is assumed that an inspection of the drip shield will take place at reception to the surface facilities of the repository and that this inspection will detect all visible traces of contamination on the drip shield (i.e., presence of foreign material on the drip shield). It is also assumed that an inspection of the drip shield will take place just before it is transported to the underground repository.

This assumption is needed because the procedures governing the control of operations on the drip shield have not yet been written.

Rationale: The rationale for this assumption is the same as that given in Assumption 5.6.1 and will not be repeated here. The only notable difference is that because the drip shield is not radioactive, the second inspection does not need to be performed remotely.

Use in the Calculation: This assumption is used in Section 6.3.5.

5.10.2 Drip Shield Secondary Inspection

Assumption: It is assumed that after the second inspection of the drip shield, the probability that the drip shield is subjected to further contamination is negligible.

Rationale: The rationale for this assumption is as follows. After the second inspection, the drip shield leaves the surface facilities and is transported to the subsurface areas. Contrary to the waste package, which will be protected from exterior contamination by the shielding compartment of the transporter, the drip shield is more likely to be exposed to contamination, like dirt for example. Nevertheless, these exterior sources of contamination will probably not be adverse to the long-term performance of the drip shield. Contamination that may have more severe consequences can be expected to occur during the handling of the drip shield, which occur mainly in the surface facilities. Once the transporter has docked in the subsurface facilities, the drip shield will be subjected to one more handling only: namely, its emplacement in the drift. It can be expected that extra precautions will be taken to ensure that the drip shield is not contaminated during this final handling because such contamination could also affect the waste packages located in the drift.

Use in the Calculation: This assumption is used in Section 6.3.5.

5.10.3 Decontamination Process of Drip Shield

Assumption: Assumption 5.6.3 is considered applicable for evaluating the contamination of the drip shield through its cleanings. It should be noted that in that assumption eight cleanings were considered for the waste package. The same number is kept for the drip shield. This is done for the sake of simplicity. As the procedures governing the fabrication of the waste package or the

drip shield have not yet been written, there is some subjectivity in determining how many cleanings should be considered.

Rationale: It can be expected that the technician in charge of the cleanings for weld preparation will group welds with a similar function together. For example, the cleaning of the drip shield welds could be gathered as follows: welding of the upper plate with both side plates: two cleanings; welding of the support beams to the side plates: two cleanings; welding of the internal support plates and the bulkheads: two cleanings; welding of the drip shield connectors: two cleanings. This yields a total of eight cleanings. Other breakdowns are possible, but it is reasonable to consider that they would all fall around eight cleanings, which is used for the waste package.

Use in the Calculation: This assumption is used in Section 6.3.5.

5.11 ASSUMPTIONS RELATED TO IMPROPER DRIP SHIELD HANDLING

The following assumptions were used in Section 6.3.6 to estimate the probability that a drip shield is damaged by mishandling and that the damage remains undetected.

5.11.1 Drip Shield Damage Inspections

Assumption: It is assumed that the inspections considered in Assumption 5.10.1 would also serve to detect traces of damage to the drip shield due to improper handling. Recall that two inspections of the drip shield are supposed to take place: one when the drip shield is received in the surface facilities of the repository and one just before it is transported to the underground repository. Also, as in Assumption 5.10.1, it is assumed that the inspection at drip shield reception will detect all visible traces of mishandling of the drip shield.

Rationale: The rationale for this assumption is the same as that given in Assumption 5.10.1.

Use in the Calculation: This assumption is used in Section 6.3.6.

5.11.2 Drip Shield Mishandling Opportunities

Assumption: It is assumed that between the inspection at drip shield reception and the second inspection just before departing for the underground repository, the drip shield might be mishandled and damaged on four occasions.

This assumption is needed because the details on how the drip shield will be handled from its reception to its emplacement are not yet known. In fact, there are only two easily identifiable opportunities for mishandling the drip shield in the surface facilities: when installing the drip shield in the staging area, and when moving it from the staging area to the transporter.

Rationale: The rationale for assuming four mishandling occasions is that it is the same number as the mishandling opportunities for the waste package, estimated in Section 5.7.2. This results in simplified estimates in Section 6.3.5. Moreover, assuming four mishandling opportunities, instead of the two identified, is clearly conservative.

Use in the Calculation: This assumption is used in Section 6.3.6.

5.11.3 Additional Drip Shield Mishandling Opportunities

Assumption: It is assumed that after the second drip shield inspection (just before the drip shield leaves for the underground repository), the probability that the drip shield is subjected to further damage by mishandling without being detected is negligible.

Rationale: The rationale for this assumption is similar to the rationale of Assumption 5.10.2. In contrast to the waste package, the drip shield will not be protected by the shielding compartment of the transporter; therefore, the chances for damage to the drip shield are greater. As a side remark, note that these damages would most likely not result from mishandling, but rather from events such as rockfalls. However, it is very unlikely that these events could significantly damage the drip shield and remain unnoticed. Another opportunity for damage to the drip shield would be during its last handling, namely: its emplacement in the drift. It can be expected that extra precautions will be taken to ensure that the drip shield is not damaged during this final handling because mishandling could also affect the waste packages located in the drift. Therefore, even if a mishandling were to occur it is very unlikely that it would remain undetected.

Use in the Calculation: This assumption is used in Section 6.3.6.

5.11.4 Drip Shield Improper Handling Damage Probability

Assumption: It is assumed that the probability of damaging a drip shield, due to an improper handling, can be approximated by a lognormal distribution with a mean of 4.8×10^{-5} (per drip shield handling) and an error factor of 10.

Rationale: This assumption is the same as Assumption 5.7.4. It is needed because there is no operating experience on the handling of the drip shields, so no direct evaluation of the probability of damaging a drip shield by mishandling is possible. Information pertaining to the handling of fuel assemblies was used instead because it is representative of the probability of mishandling sensitive material in the nuclear industry. The other justifications for this assumption are the same as those given in Assumption 5.7.4.

Use in the Calculation: This assumption is used in Section 6.3.6.

5.12 ASSUMPTIONS RELATED TO DRIP SHIELD EMPLACEMENT ERROR

The following assumption about verification of correct drip shield emplacement is used in Section 6.3.7.

5.12.1 Drip Shield Emplacement Error Detection

Assumption: It is assumed that once a drip shield is emplaced a remote inspection is performed to detect if the newly emplaced drip shield is properly interlocked with the adjacent drip shield.

This assumption is needed because the procedures governing the installation of the drip shield in the repository have not yet been written.

Rationale: The rationale for this assumption is that it describes a verification step that conforms to work practices in the nuclear industry.

Use in the Calculation: This assumption is used in Section 6.3.7.

6. ANALYSIS

6.1 REVIEW OF DEFECT-RELATED FAILURES OF CONTAINERS IN VARIOUS INDUSTRIES

This section presents the results of a literature review performed to determine rates of manufacturing defect-related failure for various types of containers. In addition to providing examples of the rates at which defective containers occur, this information provides insight into the various types of defects that can occur and the mechanisms that cause defects to propagate to failure.

6.1.1 Boilers and Pressure Vessels

Waste packages are similar to pressure vessels in the sense that they are welded, metallic components of similar thickness that are typically fabricated in accordance with accepted standards and inspected prior to entering service. In addition, there are several sources of statistics on the numbers and types of failures that have occurred in large populations.

One study (Doubt 1984, p. 7) examined data on 229 failures of pressure vessels constructed to Class I requirements of design codes recognized in the United Kingdom. The failures had occurred in a population of 20,000 vessels (Smith and Warwick 1978). The vessels were all welded or forged unfired pressure vessels with wall thicknesses greater than 9.5 mm and working pressures in excess of 725 kPa. The vessels included in the study were less than 40 years old as of 1976 (Smith and Warwick 1978, p. 22). Doubt (1984, p. 7) identified 17 instances of external leakage or in-service rupture that were caused by preexisting defects in weld or base metal or by incorrect material. Failures that were due to thermal or mechanical fatigue, corrosion, internal leaks, and part-through cracks found by visual examination or nondestructive examination were excluded. This yielded an estimated failure rate due to manufacturing defects of 8.5×10^{-4} per vessel. Further examination of the data (Smith and Warwick 1978, pp. 37 to 52) indicated that four of the failures were attributed to use of incorrect material in the weld, one to improper heat treatment, one to improper joint design, and the remaining failures were due to weld flaws. In all of the cases involving weld flaws, the vessels were in service for several years prior to failure, which suggests that fatigue also contributed to the propagation of the flaws through the walls of the vessels. In some cases, failures that were attributed to fatigue, and thus not included in the calculation of the previous failure rate, involved propagation of preexisting defects. Overall, approximately 29 percent of the failures appear to have involved a preexisting defect of some kind. Finally, it should be noted that the original source of the failure data (Smith and Warwick 1978, p. 24) indicates that many of the defects occurred in areas where it was not the practice at the time of construction, even with Class I Standard vessels, for nondestructive examination to be performed. Because waste packages are not subject to cyclic stresses (which is necessary for fatigue) and will be nondestructively

examined, application of the historical failure data for pressure vessels to estimate an early failure rate for waste packages would be extremely conservative.

Another source of information on failures is available from the National Board of Boiler and Pressure Vessel Inspectors (NBBPVI 1999). The National Board of Boiler and Pressure Vessel Inspectors maintains records on all boilers and pressure vessels that carry a National Board-registered stamping. For the period of 1919 through 1997, a total of 27,618,733 registrations have been filed (NBBPVI 1999). For the period of 1992 to 1997, incident reports indicate the number of failures that have occurred as a result of various causes. For the category of "Faulty Design or Fabrication," the average incident rate is 83 per year. Assuming that this rate is constant over the 79 years in which vessels were registered, a point estimate probability of 2.4×10^{-4} per vessel for failure due to fabrication or design defects can be calculated. Unfortunately, the National Board of Boiler and Pressure Vessel Inspectors information does not contain information on the cause of failure, and thus, its utility for this analysis is limited.

Data from the previous sources, and from similar databases in Germany, have been used in various studies to calculate the annual probability of vessel failure for use in risk assessments. The expected value for disruptive failure rates ranges from 2×10^{-6} to 4×10^{-5} per vessel-year, and the upper limit of the 99 percent confidence interval ranges from 5×10^{-6} to 8×10^{-5} per vessel-year (Tschoepe et al. 1994, pp. 2-9 to 2-11). In general, these rates were not based on actual failures that had occurred but on reports on the size of the weld defects observed during inspection and the perceived consequences had the vessel been returned to service without repair of the defect. Because these rates involve significant interpretation as to the effect of weld flaws on component life under specific operating conditions, they cannot be directly used to determine a waste package early failure rate.

Finally, two instances were also found in the literature where cracking of stainless steel cladding on the interior surface of reactor coolant system components occurred as a result of defects that occurred during fabrication or transport. In one case, during a visual examination following a hot functional test that was conducted in March 1975, Indian Point-3 personnel noted rust-colored deposits in the primary-water boxes of all four steam generators (S.M. Stoller and Company 1976, p. 44). A detailed chemical and metallurgical analysis of cladding samples was performed and three distinct types of cracking were identified: (1) longitudinal interbead cracks in the upper parts of the heads that propagated along grain boundaries, (2) transverse cracks adjacent to repair welds, and (3) extensive cracking in the lower half of the heads. Studies of the cladding samples identified stress corrosion and dilution of the clad deposit with base metal as possible causes for the imperfections. The supposition of stress corrosion was supported by the fact that the channel heads were accidentally exposed to seawater during shipment.

In a second instance, microfissures were found in the cladding of two straight and two elbow sections of reactor coolant system piping during construction of Oconee 1 (Babcock & Wilcox 1970a; Babcock & Wilcox 1970b). The fissures were found during a routine dye-penetrant exam while they were being reworked to accommodate the installation of Westinghouse reactor coolant pumps. They would likely not have been found before operation if the original Bingham pumps were installed. The cracks in the straight sections were caused by use of an improperly manufactured batch of flux in welding these sections. The cracking that occurred on the two elbow sections was attributed to the improper use of acidic cleaning agents. The Indian Point-3

and Oconee-1 cases were the only examples of contamination-related failures found in the nuclear-industry literature, and no efforts to determine their frequency of occurrence have been made.

While this review has provided general information on the reliability of large, welded, pressure retaining components, the failure rate data cannot be directly applied to waste packages due to significant differences in operational conditions and degree of inspection performed prior to service. However, this review has identified several types of manufacturing defects that may be applicable to waste packages:

- Weld flaws
- Base metal flaws
- Use of improper material in welds
- Improper heat treatment of welded or cold-worked areas
- Improper weld flux material
- Poor joint design
- Contaminants.

The applicability of these types of defects to waste packages and their potential consequences to postclosure performance are discussed in Section 6.2.

6.1.2 Nuclear Fuel Rods

Nuclear fuel rods are conceptually similar to waste packages in the sense that they are manufactured in large numbers, are subjected to rigorous quality controls and inspections, and have radionuclide containment as one of their primary functions. As such, it is useful to review the reliability of these components and the rate at which manufacturing-induced defects occur. However, they are also simple, single-barrier components with a very small wall thickness compared to waste packages and are subjected to significantly different operating conditions over a much shorter period of operation. Thus, the failure rate information presented here cannot be directly used to estimate a waste package early failure rate.

Because a significant amount of scrutiny by utilities, vendors, and the NRC follows any report of failure in nuclear fuel, there is a large database on the number and causes of fuel-rod failures. The fuel-rod failure rate for both PWR and boiling water reactor (BWR) fuel through 1985 ranged from 2×10^{-4} to 7×10^{-4} per rod (EPRI 1997, p. 4-1). As a result of vendor efforts to develop improved fuel designs to address some of the causes of failure, the current range of failure rates is from 6×10^{-5} to 3×10^{-4} per rod (EPRI 1997, p. 4-2). The failures of fuel rods have been caused by a variety of mechanisms (Yang 1997, p. 10; Framatome Cogema Fuels 1996, pp. 4-2 to 4-7), among which two are applicable to waste packages. These are handling damage and manufacturing defects. Handling damage represents a small amount of the fuel failures. It can occur during fabrication if loaded fuel rods are subjected to excessive flexing that causes defects, which lead to in-core failure or as a result of drops or other handling accidents which could occur at the utility. During the period from 1989 through 1995, there were a total of 10 handling-damage failures in a population of 21,810 PWR discharged assemblies (Yang 1997, p. 10), yielding a rate of 4.6×10^{-4} per discharged assembly. In each case, only a few rods in each assembly were actually damaged.

Manufacturing defects also represent a small fraction of fuel failures. Types of manufacturing defects associated with the cladding include contamination by solvents; oils or filings; flawed or missing seal welds; flawed, missing or mislocated endcap welds; base metal flaws (stringers, inclusions); and out-of-specification weld material (Framatome Cogema Fuels 1996, Section 5). General Electric reports only 47 manufacturing-defect-related failures in 4,734,412 rods fabricated between 1974 and 1993 (Potts and Proebstle 1994, p. 92), which yields a rate of 9.9×10^{-6} per rod. As of October 1990, Advanced Nuclear Fuels had experienced seven BWR fuel rod failures and nine PWR fuel rod failures related to manufacturing defects out of 570,200 BWR fuel rods and 1,391,740 PWR fuel rods placed into service (Tschoepe et al. 1994, p. 2-4). The resulting rates are 1.2×10^{-5} , 6.5×10^{-6} , 8.2×10^{-6} for BWRs, PWRs, and combined failures, respectively. In addition to the previously mentioned defects, one occurrence of a rod that failed in service due to a missing seal weld was reported in *Fuel Integrity* (Framatome Cogema Fuels 1996, p. 5-1). The rod had not passed the inspection process but had been inadvertently left with the accepted rods. Because this was an isolated event, it can be expected that the corresponding occurrence rate would be much lower than the reported global failure rate, excluding debris and fretting, of $1/200,000 = 5 \times 10^{-6}$ per rod (Framatome Cogema Fuels 1996, p. 3-1).

While this review has provided general information on the reliability of fuel rods, the failure rate data cannot be directly applied to waste packages due to significant differences in construction and operational conditions. However, general types of manufacturing defects were identified in the review that may be applicable to waste packages:

- Weld flaws
- Base metal flaws
- Mislocated welds
- Contamination
- Missing welds
- Improper weld material
- Handling damage.

The applicability of these types of defects to waste packages, and their potential consequences to postclosure performance, are discussed in Section 6.2.

6.1.3 Underground Storage Tanks

A substantial amount of information is available on causes of early failure for underground-storage-tank systems. The most extensive data source, which was compiled by the U.S. Environmental Protection Agency, provides data on a large population of bare-steel, clad- or coated-steel, and fiberglass-reinforced-plastic tank systems through 1987 (EPA 1987a; EPA 1987b). While overfilling and leakage of attached piping are dominant contributors to leakage from underground storage tank systems, failure of the tank itself is also a significant contributor. The majority of the tanks in service during the period covered by the study were bare-steel tanks, and 95 percent of those failures were caused by corrosion (EPA 1987a, p. 7). One interesting observation was that many bare-steel tanks that have been unearthed were found to have corrosion holes that were plugged with corrosion product and showed no signs of leakage (EPA 1987a, p. 6).

The study also indicates that 5 to 7 percent of bare-steel tanks leaked when they were tested for the first time due to manufacturing or installation defects (EPA 1987a, p. 6). However, failures found during such a leak test would generally be repaired and the fraction of the total population failed by unidentified defects would be much lower. The study indicates that 4 percent of a population of 980 in situ tanks were found to be leaking and 0.9 percent of 24,452 leaking tanks were found to be leaking in within 0 to 5 years (early life of the underground storage tank) of being placed into service (EPA 1987a, p. 8). This suggests an upper bound of approximately 0.04 percent ($4\% \times 0.9\%$) of the fraction of the total population initially failed by an unidentified defect. Additional information provided by the Steel Tank Institute indicates that the fraction of the population failed by unidentified manufacturing defects is closer to 0.0003 percent (Grainawi 1999). Types of noncorrosion defects identified as causing failure include installation damage (EPA 1987a, p. 10) and failure of weld seams (EPA 1987b, p. 82).

While this review has provided general information on the fraction of the total population of underground storage tanks that fail due to any cause, rates of early failure by defects are generally obscured by the high rate of early corrosion failures. The information obtained is not directly applicable to waste packages because an underground storage tank made of bare steel is basically a single, less robust, noncorrosion-resistant barrier. However, it still indicates that even commercial-grade quality controls can produce components that have a relatively low rate of unidentified failures entering service. In addition, general types of manufacturing defects were identified in the review that may be applicable to waste packages:

- Weld flaws
- Handling or installation damage.

The applicability of these types of defects to waste packages, and their potential consequences to postclosure performance, are discussed in Section 6.2.

6.1.4 Radioactive Cesium Capsules

During the period between 1974 and 1983, 1,600 radioactive cesium capsules were fabricated at the U.S. Department of Energy's Hanford facility. These capsules were double-walled cylinders initially designed and tested to be stored in storage pools at Hanford that were later used by commercial companies as radiation sources (Tschoepe et al. 1994, p. 2-7). One of these capsules failed during 1988 as a result of its use in environmental conditions that were drastically different from those for which the capsules were designed and from the development test conditions. An investigation into this failure concluded that, despite other deficiencies that were found, the capsule would not have failed if it had operated in the environment for which it was designed. The remaining capsules were recalled to Hanford after this incident and there have been no other failures to date. Thus, the failure rate to date is 6.3×10^{-4} per capsule.

While this type of administrative or operational error does not represent an actual defect in the fabrication of the component, it, nonetheless, caused an early failure. The applicability of this type of defect to waste packages, and its potential consequences to postclosure performance, are discussed in Section 6.2.

6.1.5 Dry Storage Casks for Spent Nuclear Fuel

Dry storage casks that are sealed with a closure weld (as opposed to bolting) represent a close analog to waste packages. Examples include the Dry Shielded Canister that is part of TransNuclear's NUHOMS system and the VSC-24 dry storage cask fabricated by Sierra Nuclear Corporation (Hodges 1998). While there have been no recorded cases of closure welds failing after casks were placed into service, there have been four cases where cracks in closure welds have been identified during postweld inspection of the cask (Hodges 1998). All of these cases have been associated with the VSC-24 of which there were 19 in service through July 1998. Table 9 summarizes relevant information on each of the cracking events. Figure 2 provides an illustration of the VSC-24 closure welds. A VSC-24 Owners Group weld review team, composed of industry experts in metallurgy, welding, and nondestructive examination, evaluated each of the four weld-cracking events to identify the root causes.

The team concluded that the Palisades weld crack was caused by an existing condition in the rolling plane of the shell material that was opened up by the process of making the shield lid weld (Hodges 1998). Metallographic analysis revealed a crack that propagated along prior austenitic grain boundaries of a preexisting weld of unknown origin (the weld had not been documented during fabrication). This base metal defect may have resulted from improper repair or incomplete removal of temporary low quality welds used to facilitate the fabrication process (i.e., attachment of strong backs to assist in the rolling of plate material).

Table 9. Summary of VSC-24 Weld Cracking Events

Facility	Date	Detection	Location	Crack Description
Palisades	3/95	Helium leak test	Shield lid-to-shell weld	About 6 inches long by 1/8 inch deep that extended from about 1/8 inch above the shield lid-to-shell weld fusion line into the shell base metal
Point Beach	5/96	Dye-penetrant test	Structural lid-to-shell weld Structural lid-to-shield lid weld	Three cracks, each less than 1 inch long, located along the center of the root pass at locations where the fit-up gap between the lid and the backing ring was widest. In addition, cracking and weld porosity were found in the structural lid-to-shield lid seal weld (fillet weld associated with the vent port covers)
Arkansas Nuclear One	12/96	Helium leak test	Shield lid-to-shell weld	About 4 inches long located along the weld fusion line
Arkansas Nuclear One	3/97	Dye-penetrant test	Shield lid-to-shell weld	About 18 inches long located along the weld fusion line of the root pass

The causes of the weld cracks at Point Beach were found to be associated with weld flaws caused by poor welding technique and moisture contamination (Hodges 1998). The cracks on the root pass of the structural lid-to-shell weld were caused by wide fit-up gaps that were not properly filled by the welding technique. The cracking and weld porosity found in the structural lid-to-shield lid seal weld were found to be caused by moisture contamination of the weld. The moisture came from water forced out of the drain line during cask loading. The team concluded that none of the cracks at Point Beach were caused by the mechanism that produced the Palisades cracks.

The crack in the shield lid-to-shell weld for the first cask loaded at Arkansas Nuclear One was initially attributed to lamellar tearing based on visual observations of the crack by the welders before it was repaired (Hodges 1998). However, it was later shown that this crack was similar in appearance to the second crack that was discovered, which was attributed to hydrogen-induced cracking. The hydrogen-induced cracking was attributed to (1) high hydrogen content of the weld wire, (2) susceptible microstructure of the steel welded, and (3) a highly restrained weld joint configuration leading to residual stresses at or near the yield level.

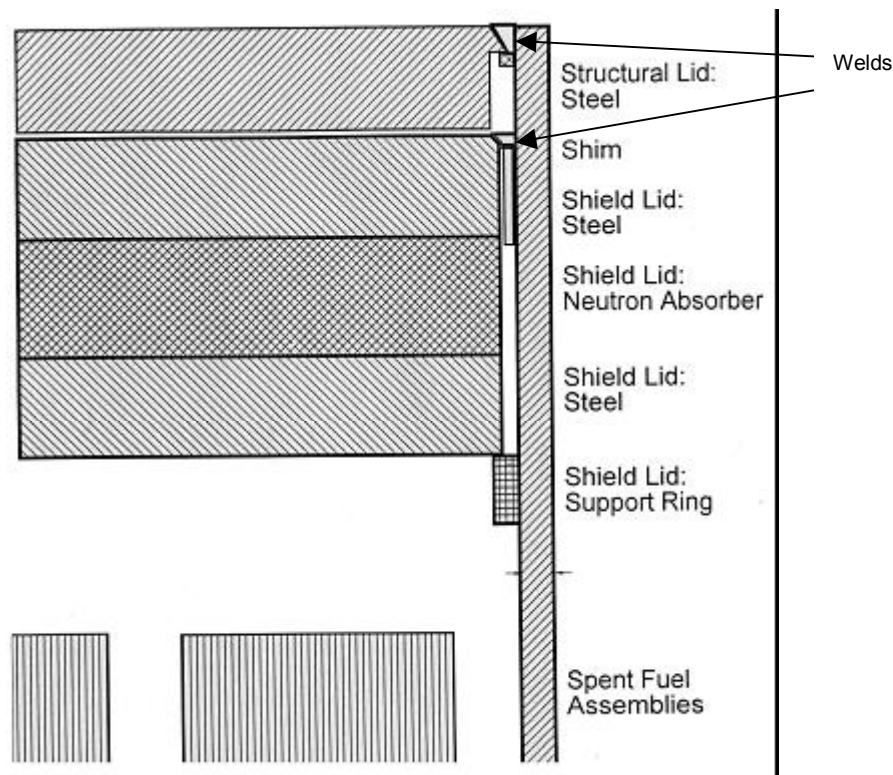


Figure 2. Illustration of Closure Welds for the VSC-24 Dry Storage Cask

General types of manufacturing defects were identified in the review that may be applicable to waste packages. These types of defects are:

- Weld flaws
- Base metal flaws
- Contamination.

The applicability of these types of defects to waste packages, and their potential consequences to postclosure performance, are discussed in Section 6.2.

6.1.6 Summary

Table 10 briefly summarizes the information obtained from the literature search on the rate and causes of manufacturing defects in welded metallic containers. Eleven generic types of defects were identified:

- Weld flaws
- Base metal flaws
- Improper weld material
- Improper heat treatment
- Improper weld-flux material
- Poor weld-joint design
- Contaminants
- Mislocated welds
- Missing welds
- Handling or installation damage
- Administrative or operational error.

Table 10. Summary of Defect-Related Failures in Various Welded Metallic Containers

Container Type	Information on Failure	Types of Defects Leading to Early Failure
Boilers and Pressure Vessels	17 out of 20,000 pressure vessels fabricated less than 40 years old as of 1976 failed due to manufacturing defects (dominant cause was fatigue growth of weld flaws). Stainless steel cladding on some reactor coolant system components for two nuclear units (different fabricators) cracked due to surface contamination remaining from transport or fabrication.	<ul style="list-style-type: none"> - Weld flaws - Base metal flaws - Improper weld material - Improper heat treatment - Improper weld flux - Poor weld-joint design - Contaminants
Nuclear Fuel Rods (PWR and BWR)	Undetected manufacturing defect-related failure rate approximately one rod per 100,000. Overall failure rates in the range of 2 to 7 rods per 10,000 before 1985, 0.6 to 3 rods per 10,000 from 1985 to 1997.	<ul style="list-style-type: none"> - Weld flaws - Base metal flaws - Mislocated welds - Contamination - Missing welds - Improper weld material - Handling damage
Underground Storage Tanks	Fraction of population initially failed due to manufacturing or handling defects in the range of 0.04% to 0.0003%.	<ul style="list-style-type: none"> - Handling or installation damage - Weld flaws
Radioactive Cesium Capsules	One failure out of 1,600 capsules.	<ul style="list-style-type: none"> - Administrative error resulting in unanticipated operating environment
Dry Storage Casks for Spent Nuclear Fuel	4 out of 19 Sierra Nuclear VSC-24 casks found to have cracked closure welds during postweld inspection (dye-penetrant and helium leak test only).	<ul style="list-style-type: none"> - Weld flaws - Base metal flaws - Contamination

A complementary type of defect is added to the previous list: out-of-specification (improper) base metal. This type of defect was not identified in the literature search: only instances of improper weld material were found. Nevertheless, for the sake of completeness, it is reasonable to consider the possibility that base metal, as well as weld material, might be out of specification.

Weld flaws (e.g., slag inclusions, porosity, lack of fusion, hydrogen-induced cracking) were a dominant contributor to early failure but usually required an external stimulus (e.g., cyclic fatigue) or environmental condition to cause the flaw to propagate to failure. In many cases, components with unidentified defects entered service not because the defect was missed by an inspection, but because no inspection for that type of defect was required at the time they were fabricated. For dry-storage casks, all of the defects were identified by postweld inspection prior

to commencement of the storage phase and thus do not represent early failure as it is defined for this analysis. The 12 types of defects (11 from the literature search, plus improper base metal) are reviewed for their applicability to waste packages in Section 6.2. Section 6.2.5 also discusses the probability of improper laser peening that could result in early stress corrosion cracking. The probability of occurrence and consequences for postclosure performance of the package are assessed for the applicable defects.

As indicated previously, many of the defects require an external stimulus or the component was not subjected to inspections that would have identified the defect. Furthermore, there is insufficient information available to defensibly relate the cumulative effect of the environment or stresses to which the component was subjected to that of the waste package (e.g., are the cumulative effects of the stresses and environmental conditions experienced by a pressure vessel in a 40 to 60 year life equivalent to 100, 1,000, or 10,000 years of waste package lifetime?). Accordingly, the information on the fraction of components that experienced defect-related failure during their intended lifetime is not directly applicable to waste packages. In addition, these population-based failure rates do not provide any insight into the time distribution of early failures. However, in some cases information on the occurrence rate of particular types of defects was obtained from the literature search. This information proved useful in the waste package defect probability and consequence portion of the analysis.

6.2 MECHANISMS FOR EARLY WASTE PACKAGE FAILURE

A list of 12 generic types of defects were identified in Section 6.1 as potential causes for early failure of metallic containers. Many of these types of defects could also be introduced to a waste package during fabrication, transport to the repository, storage, loading, or emplacement. However, the following generic defect types are not considered further (for the waste package or the drip shield):

- *Improper weld-flux material:* Waste package welds will employ a welding method (such as tungsten inert gas or metal inert gas) that does not use weld-flux material.
- *Poor joint design:* A significant development and testing effort will have gone into the design of the final closure joint. Lessons learned from the types of closure weld problems that have been experienced in the dry-storage cask systems (see Section 6.1.5) are expected to be incorporated in the design of closure welds for waste packages. Therefore, problems with the design of the weld joint for the waste packages are not expected. This does not exclude weld flaws or other types of weld related defects that could occur during the closure process.
- *Missing welds:* Data on the occurrence of this type of defect in fuel rods (presented in Section 6.1.2) indicated that it would occur at a rate much lower than 5×10^{-6} per rod. A missing weld on a waste package would be easier to identify than on a fuel rod and would have a noticeable effect on the configuration of the waste package (e.g., a missing closure weld could cause the lid to fall off when the waste package is tilted to a horizontal position). Therefore, it is expected that the occurrence rate of this defect for a waste package would be significantly less than the dominant failure mechanism of improper heat treatment.

- *Mislocated welds*: This defect is mainly applicable to very small, single pass welds (e.g., fuel rod end caps). For larger multipass welds, such as those on the waste package, any significant mislocation of the electrode would cause the weld arc not to strike. This would be immediately obvious to both the operator and the control system for the automated welder. This is much less likely than the dominant failure mechanism of improper heat treatment.

The remaining defects are evaluated in the following subsections.

6.2.1 Weld Flaws

Weld flaws are among the most extensively studied types of defects that can affect the performance of metallic components used in the nuclear industry. For example, results from Khaleel et al. (1999), which report flaw density and size distributions in nuclear piping welds, were extensively used to determine the main characteristics of the flaws to be expected in the closure welds of the waste package (CRWMS M&O 2000). The major drawback of this approach is that the inputs utilized from Khaleel et al. (1999) were primarily developed for stainless steel and not Alloy 22.

Work has been performed involving the welding of Alloy 22 specimen rings that duplicate as closely as possible the actual outer lid weld of a waste package (BSC 2003d). Although the design of the outer lid has since been modified since this work was performed, the modifications do not impact the validity of the results. Only the closure weld configuration was modeled in the test. The changes in design only effect the reinforcement around the weld configuration and the actual weld groove has not changed. Sixteen specimen rings were welded employing procedures, processes, and equipment similar to that expected to be used for the closure of the waste package. Nondestructive examination followed by metallographic examination made it possible to accumulate significant information on the weld flaws. Based on this information, summarized in Section 4.1.3, several distributions are developed in Section 6.2.1.1 to characterize the size of the flaws in the through-wall extent of the weld (Y direction on Figure 1), their density (mean number of flaws per meter of weld) and their depth (distance between the outer surface of the weld and the onset of the flaw in the Y direction). In addition, the orientation of the flaws in the plane of the specimen rings, with respect to the direction of the weld, is used to make an estimate on the probability that a flaw has an angle greater than 45 degrees.

UT inspections will be performed on the welds of the waste package in order to identify those flaws that may jeopardize its performance so that these flaws can be removed. The characteristics of the flaws that will remain in the welds, especially their size and density, are investigated in Section 6.2.1.2.

Section 6.2.1.3 gives a summary guideline for calculating the main characteristics of the flaws expected in the welds of the waste package. The main results for the outer lid weld, the middle lid weld, and the other welds of the outer barrier are given. Also, a comparison of the developed distributions is made with the results from Khaleel et al. (1999), which pertain to nuclear piping weld flaws and on which estimates performed for the Site Recommendation and the Supplemental Science and Performance Analysis were based.

The calculations in the following subsections were carried out using Mathcad. A paper copy is given in Attachment I. Note that the results of the calculations performed are shown with rounded values. A reader wanting to re-do the calculations should carry them out from the input values given in Section 4, and not use the intermediate values, unless otherwise stated.

6.2.1.1 Flaw Characteristics in Welds Before Inspection and Repair

6.2.1.1.1 Flaw Size Distribution in the Y Direction

The flaw size distribution in the Y direction (see Figure 1 for conventions on orientation) is estimated using the Bayesian approach with a noninformative prior. Information on the Bayesian approach in the evaluation of parameters is given in NUREG/CR-2300 (NRC 1983, Section 5.5.2). Briefly stated, the Bayesian estimation consists of updating the analyst's belief about the parameter (embodied in a prior distribution) with evidence from observation (quantified in a likelihood function) to obtain a posterior distribution.

The reason for using the Bayesian approach, rather than the classical (also named frequentist) approach, is that it utilizes a probability distribution on the parameter to be estimated in order to express confidence. As mentioned in NUREG/CR-2300 (NRC 1983, p. 12-16), this has been a common way of representing uncertainty since WASH-1400 (NRC 1975). Expressing uncertainty around a parameter in terms of a probability distribution is also adequate for subsequent performance assessments of the waste package.

The reason for using a noninformative prior distribution is that in generating the posterior estimate, this minimizes the relative importance of the prior distribution compared to the data (NRC 1983, p. 5-34). This is appropriate here because there is very little generic information on flaws in Alloy 22 welds.

An exponential distribution has been chosen to represent the size distribution of the weld flaws in the Y direction. The reason for this choice is that it is a widely used distribution, determined by a single parameter, which makes it very tractable. Notice that the exponential distribution is a particular case of the more general Weibull distribution, which has been employed to characterize flaw size distributions (Schuster et al. 1998, p. 8.2). Weibull distributions are determined with two parameters, one more than the exponential, which allows for more flexibility in the shape of the distribution. However, it will be shown in the following that an exponential distribution is sufficient to fit the UT indication dimensions in the Y direction accrued on the specimen ring welds. Therefore, for tractability reasons, it has been decided to use the exponential distribution to characterize the flaw size in the Y direction.

The cumulative exponential distribution for the flaw size s (in mm) in the Y direction of the weld has the form (Martz and Waller 1991, p. 330):

$$P_s(s) = 1 - e^{-\lambda_s \cdot s} \quad (\text{Eq. 1})$$

where λ_s is the parameter (in mm^{-1}) that is to be determined. It will be referred to as the flaw size parameter in the following. Note that s is always positive.

Based on Assumption 5.1.1, the information presented in Section 4.1.3.2 is appropriate to characterize the size distribution of the significant flaws in the welds.

In order to calculate the probability density function (PDF) related to the flaw size parameter, it is first necessary to determine which sampling scheme was employed to get the flaw size information. The information presented in Section 4.1.3.2 can be viewed as a fixed number of flaws n_f ($n_f = 7$) to which correspond random flaw sizes. A sampling scheme characterized by a fixed number of items (namely, the number of flaws) to which is associated a random variable (namely, the size of the flaws) is referred to as gamma sampling (Martz and Waller 1991, pp. 330 and 331). Based on the same reference, for this kind of sampling, a sufficient statistic for estimating λ_s is s_t , the sum of all flaw sizes, which has been evaluated at 31.75 mm.

According to Martz and Waller (1991, p. 336) the noninformative prior distribution for λ_s based on gamma sampling is proportional to $1/\lambda_s$. The resulting posterior PDF p_{λ_s} of the flaw size parameter λ_s is given as:

$$p_{\lambda_s}(\lambda_s) = \frac{s_t^{n_f}}{\Gamma(n_f)} \cdot \lambda_s^{n_f-1} \cdot e^{-\lambda_s \cdot s_t} \quad (\text{Eq. 2})$$

where Γ is the gamma function.

The posterior mean, λ_{sm} , the 5th percentile, $\lambda_{s0.05}$, and the 95th percentile, $\lambda_{s0.95}$, are respectively given by (Martz and Waller 1991, pp. 336 and 337):

$$\lambda_{sm} = \frac{n_f}{s_t} \quad (\text{Eq. 3})$$

$$\lambda_{s0.05} = \frac{\chi_{\gamma/2}^2(2 \cdot n_f)}{2 \cdot s_t} \quad (\text{Eq. 4})$$

$$\lambda_{s0.95} = \frac{\chi_{1-\gamma/2}^2(2 \cdot n_f)}{2 \cdot s_t} \quad (\text{Eq. 5})$$

where, given $\gamma = 0.1$, $\chi_{\gamma/2}^2(2 \cdot n_f)$ and $\chi_{1-\gamma/2}^2(2 \cdot n_f)$ respectively represent the 5th and 95th percentiles of the chi-square distribution with $2 \times n_f = 14$ degrees of freedom. This yields the following values: $\lambda_{sm} = 0.22/\text{mm}$, $\lambda_{s0.05} = 0.10/\text{mm}$, and $\lambda_{s0.95} = 0.37/\text{mm}$.

It is interesting to compare these results to the values that would be found using the classical (frequentist) approach. According to this approach, no probability distribution is attached to λ_s , the parameter of the exponential distribution defined in Equation 1. Instead, λ_s has a fixed but unknown value, which can be approximated by calculating the maximum likelihood estimator. Also, the classical approach makes it possible to determine the lower and the upper value of the 90 percent two-sided confidence interval for λ_s . Based on work by Martz and Waller (1991, pp. 336 and 337), these estimators are respectively equal to λ_{sm} , $\lambda_{s0.05}$, and $\lambda_{s0.95}$ calculated in

Equations 3 to 5. Therefore, the Bayesian approach concurs with the classical (frequentist) approach.

Based on previous parameters, the size distribution of the weld flaws in the Y direction follows an exponential distribution of parameter λ_s , with λ_s having a PDF given by Equation 2. Notice that Equation 2 is only applicable to the outer lid weld of the waste package and not to welds with other thicknesses such as the middle lid weld, which has a smaller thickness (10 mm instead of 25 mm, see Section 4.1.1). Because it is desirable to have a flaw size distribution that could be applicable for different weld thicknesses, it has been decided to use a modified version of the exponential distribution which includes an additional parameter, namely the thickness t of the weld. The cumulative flaw size distribution $P_{sg}(s, \lambda_s, t)$ for a flaw of s mm in the Y direction of a weld of thickness t mm with the flaw size parameter λ_s (in mm^{-1}) is taken to be:

$$P_{sg}(s, \lambda_s, t) = \frac{1 - e^{-\lambda_s \cdot s}}{1 - e^{-\lambda_s \cdot t}} \text{ with } 0 \leq s \leq t \quad (\text{Eq. 6})$$

As a reminder, in Equation 6 the variable of interest is the flaw size s , while λ_s and t are parameters. In order to be consistent with Mathcad notations used in Attachment I, λ_s and t are shown on the left side of the equation along with s .

It should be noted that the form of the equation proposed previously is not the only one possible. For example, an alternative choice would be to discard the denominator and introduce t inside the exponential term of the numerator. This case is examined in Attachment I and shown to be less conservative than Equation 6. Based on this comparison, only the modified exponential distribution given in Equation 6 is considered in the following.

It is worth noting that in the case of the specimen rings, most of the UT indications report flaws that are much smaller than the weld thickness. Therefore, Equation 6 is a modified flaw size distribution that is, numerically, only slightly different from the original exponential distribution.

To verify that it is not unreasonable that $P_{sg}(s, \lambda_s, t)$ adequately fits the data from the UT indications, a chi-square test is performed using λ_{sm} as the flaw size parameter and $t = 25$ mm. Several other types of goodness-of-fit tests exist such as the Kolmogorov-Smirnov test or the Anderson-Darling test. The chi-square test is often less powerful than those tests but is nevertheless chosen because it is a widely used statistic that applies to any distribution and is the most generally applicable test of fit (D'Agostino and Stephens 1986, p. 63).

The chi-square test requires the empirical data to be partitioned into several cells. The following statistic is then calculated (D'Agostino and Stephens 1986, p. 64):

$$X^2 = \sum_{i=1}^M \frac{(N_i - n \cdot p_i)^2}{n \cdot p_i} \quad (\text{Eq. 7})$$

where

- X^2 = chi-square statistic (also called Pearson statistic)
- M = number of cells into which the empirical data are partitioned
- p_i = probability that a random observation falls into cell i (i varies from 1 to M)
- n = total number of empirical data (for the flaw size data, $n = n_f$)
- N_i = number of empirical data that fall into cell i

Based on the recommendations of D'Agostino and Stephens (1986, pp. 70 and 71), the cells are chosen to be approximately equiprobable. Also, D'Agostino and Stephens (1986, p. 71) mention the following guidelines for choosing the value of M : M should be greater than or equal to 3, n greater than or equal to 10, and the ratio n^2/M greater than or equal to 10. Of course, because $n = n_f = 7$, it is not possible to respect one of the previous rules, but with choosing $M = 3$, the other rules (i.e., M greater than or equal to 3, and $n^2/M = 16.3$ greater than or equal to 10) are met. Therefore, the cells will be divided into $M = 3$ equiprobable cells.

To determine whether or not the flaw size data fit the distribution, the Pearson statistic X^2 is compared to $\chi_{0.95}^2(M-1-1)$, which represents the 95th percentile of the chi-square distribution with $M-1-1 = 1$ degree of freedom. The 95th percentile is chosen because it corresponds to a level of significance of the test of $1 - 0.95 = 0.05$, which is often used (D'Agostino and Stephens 1986, p. 70). The number of degrees of freedom is determined based on the fact that one parameter of the distribution, namely λ_{sm} , has been estimated using the empirical data. Because λ_{sm} is also the maximum likelihood estimator, it is appropriate to consider $M-1-1$ degrees of freedom (D'Agostino and Stephens 1986, pp. 67 and 68).

The cells are found to be approximately equiprobable by selecting the following ranges: 0 to 1.8 mm, 1.8 mm to 4.9 mm, and 4.9 mm to 25 mm. Calculation of the Pearson statistic yields around 2.0, which is lower than $\chi_{0.95}^2(1) = 3.8$. In other words, using $P_{sg}(s, \lambda_{sm}, t)$ to represent the weld flaw sizes in the Y direction is not contradicted by the data at the 0.05 significance level. Attachment I provides the detail of the calculation performed to obtain the previous results.

The PDF p_{sg} for the flaw size distribution based on Equation 6 is given by:

$$p_{sg}(s, \lambda_s, t) = \frac{\lambda_s \cdot e^{-\lambda_s \cdot s}}{1 - e^{-\lambda_s \cdot t}} \quad \text{with } 0 \leq s \leq t \quad (\text{Eq. 8})$$

As a reminder, in Equation 8 the variable of interest is the flaw size s , while λ_s and t are parameters.

As complementary information, the PDF p_{msg} accounting for all possible values of λ_s , weighted by their probability, is calculated. The PDF p_{msg} is a function of s , with parameter t , and is evaluated using the following equation:

$$p_{msg}(s, t) = \int_0^\infty \frac{\lambda_s \cdot e^{-\lambda_s \cdot s}}{1 - e^{-\lambda_s \cdot t}} \cdot p_{\lambda_s}(\lambda_s) d\lambda_s \quad (\text{Eq. 9})$$

The associated cumulative distribution function (CDF), P_{msg} , on the flaw size s (t being a parameter) is determined by:

$$P_{msg}(s, t) = \int_0^s p_{msg}(u, t) du \quad (\text{Eq. 10})$$

Figure 3 shows P_{msg} for the outer lid weld ($t = 25$ mm).

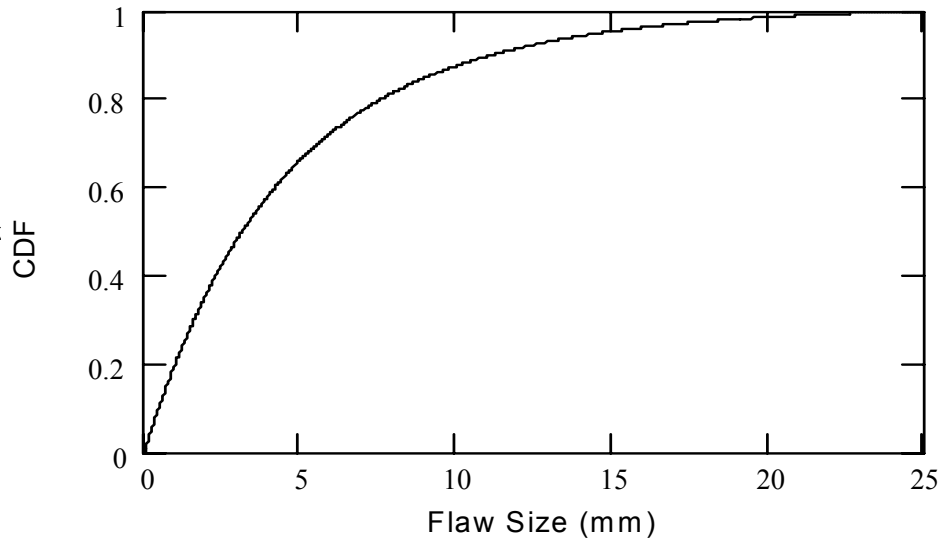


Figure 3. Cumulative Distribution Function for Flaw Size Before Ultrasonic Inspection in Outer Lid Weld

In conclusion, the size s (in mm) of the flaws in the Y direction of a weld of thickness t (in mm) can be evaluated using the cumulative distribution $P_{sg}(s, \lambda_s, t)$ given in Equation 6. The flaw size parameter λ_s has the PDF defined in Equation 2. It is worth noting here that the use of $P_{sg}(s, \lambda_s, t)$ has been justified only for the outer lid weld (i.e., for $t = 25$ mm). Applicability to other weld thicknesses will be addressed in Section 6.2.1.3.

6.2.1.1.2 Flaw Density

The flaw density is the mean number of flaws per meter of weld. The flaw density is investigated because it will help predict the number of flaws expected in the waste package. In searching for a distribution that can adequately describe the number of flaws (which takes discrete values), the Poisson distribution was chosen because it is a discrete distribution that is used for characterizing many processes. Given a length of weld L (in m) and a flaw density parameter λ_d , the Poisson distribution characterizing the probability on the number of flaws n has the form (Martz and Waller 1991, pp. 254 and 255):

$$P_n(n, \lambda_d, L) = e^{-\lambda_d \cdot L} \cdot \frac{(\lambda_d \cdot L)^n}{n!} \quad (\text{Eq. 11})$$

Note that the mean of this distribution is $\lambda_d \times L$ (Martz and Waller 1991, p. 17).

The length of weld in a waste package is known; therefore, the number of flaws to be expected will be governed by λ_d whose PDF is determined in the following. The Bayesian approach with a noninformative prior is used for the PDF determination for the same reasons as those presented in Section 6.2.1.1.1.

Based on Assumption 5.1.1, the information on UT indications presented in Section 4.1.3.2 is appropriate to characterize the flaw density of the significant flaws in the closure welds. In the total weld length of the 16 specimen rings, $n_f = 7$ flaws were detected. Here, n_f is random while the length of weld is fixed. This corresponds to Poisson sampling (Martz and Waller 1991, pp. 254 and 255). According to Martz and Waller (1991, p. 286), the noninformative prior distribution for λ_d based on Poisson sampling is proportional to $\lambda_d^{-1/2}$. The resulting posterior PDF p_{λ_d} of the flaw density parameter λ_d is given in the same reference as:

$$p_{\lambda_d}(\lambda_d) = \frac{L_t^{n_f+0.5}}{\Gamma(n_f+0.5)} \cdot \lambda_d^{n_f-0.5} \cdot e^{-\lambda_d \cdot L_t} \quad (\text{Eq. 12})$$

where L_t is the total weld length examined. Sixteen specimen rings have been welded and each of them has a diameter approximately equal to the diameter of the outer lid weld (the diameter of a specimen ring is 60.765 inches [see Section 4.1.3.1], or equivalently 1.543 m, while the diameter of the outer lid is 1.541 m [see Section 4.1.1]). This yields a weld length of around 4.85 m for a specimen ring, which is the value used in the rest of this analysis. The 16 rings account for a total weld length, $L_t = 77.60$ m.

The associated CDF P_{λ_d} is given in Equation 13 and is shown on Figure 4.

$$P_{\lambda_d}(\lambda_d) = \int_0^{\lambda_d} p_{\lambda_d}(u) du \quad (\text{Eq. 13})$$

The posterior mean, λ_{dm} , the 5th percentile, $\lambda_{d0.05}$, and the 95th percentile, $\lambda_{d0.95}$, are respectively given by (Martz and Waller 1991, pp. 286 and 287):

$$\lambda_{dm} = \frac{2 \cdot n_f + 1}{2 \cdot L_t} \quad (\text{Eq. 14})$$

$$\lambda_{d0.05} = \frac{\chi_{\gamma/2}^2 (2 \cdot n_f + 1)}{2 \cdot L_t} \quad (\text{Eq. 15})$$

$$\lambda_{d0.95} = \frac{\chi_{1-\gamma/2}^2 (2 \cdot n_f + 1)}{2 \cdot L_t} \quad (\text{Eq. 16})$$

where $\gamma = 0.1$. This yields the following values: $\lambda_{dm} = 0.097$ flaw per meter of weld, $\lambda_{d0.05} = 0.047$ flaw per meter of weld, and $\lambda_{d0.95} = 0.16$ flaw per meter of weld. As mentioned in Martz and Waller (1991, pp. 286 and 287), these estimates are close to the classical maximum likelihood estimator, the lower, and the upper value of the 90 percent confidence interval for λ_d .

This shows that the Bayesian approach used to estimate the flaw density parameter is in agreement with the classical (frequentist) approach.

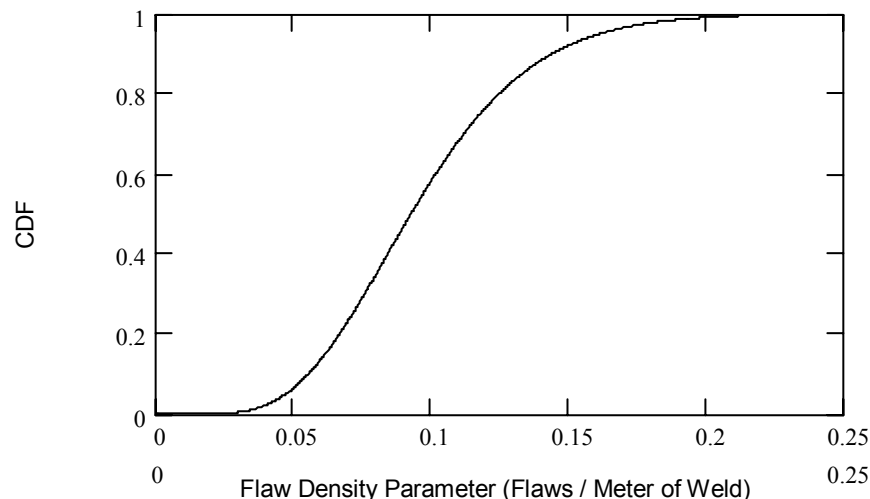


Figure 4. Cumulative Distribution Function for Flaw Density Parameter before Ultrasonic Inspection

Based on previous parameters, the distribution on the number of flaws in the weld follows a Poisson distribution $P_n(n, \lambda_d, L)$ (Equation 11) with λ_d having the PDF given in Equation 12.

To verify that $P_n(n, \lambda_d, L)$ adequately fits the data from the UT indications a chi-square test is performed using λ_{dm} as the flaw size parameter and $L = L_{wp}$, the length of weld in a specimen ring (4.85 m). The chi-square test is selected because it can be applied to test the goodness-of-fit of discrete distributions (D'Agostino and Stephens 1986, p. 63).

The symbols of Equation 7 are utilized to perform the goodness-of-fit test. The test is carried out using the number of flaws reported in each of the specimen rings, yielding a total of $n = 16$ observations. The test is done at the 0.05 significance level using $M = 4$ cells. The cells are determined by the number of flaws observed in the specimen rings as follows: 0 flaw, 1 flaw, 2 flaws, and 3 or more flaws. It should be noted that contrary to what was done in Section 6.2.1.1.1 for the flaw size in the Y direction, it is not possible to choose equiprobable cells (this is because the distribution tested is discrete). Nevertheless, the recommendations of D'Agostino and Stephens (1986, p. 71) on the selection of the cells are respected. These recommendations are to choose M greater than or equal to 3, n greater than or equal to 10, and n^2/M greater than or equal to 10. Additionally, it is recommended that when cells are not equiprobable, n should be greater than $2 \times M$ at the 0.05 significance level. Attachment I provides information used to calculate the Pearson statistic, which is found equal to 5.3.

The number of degrees of freedom to consider in the test is determined based on the fact that one parameter of the distribution, namely λ_{dm} , has been estimated using the empirical data. Because λ_{dm} is fairly close to the maximum likelihood estimator, it is appropriate to consider $M-1-1 = 2$ degrees of freedom (D'Agostino and Stephens 1986, pp. 67 and 68). This yields $\chi^2_{0.95}(2) = 6.0$, which is greater than the Pearson statistic. Therefore, using the Poisson distribution to predict the number of flaws in the specimen rings (and thus the waste package

outer lid weld since they have approximately the same length of weld) is not in contradiction with the data at the 0.05 significance level.

In conclusion, the probability on the number of flaws n in a length of weld L can be evaluated using the Poisson distribution $P_n(n, \lambda_d, L)$ given in Equation 11. The flaw density parameter λ_d has the PDF defined in Equation 12. It is worth noting that this probability distribution was evaluated for use on the outer lid weld of the waste package only. Applicability to other welds will be addressed in Section 6.2.1.3.

6.2.1.1.3 Flaw Depth

The flaw depth is the distance between the outer surface of the weld and the onset of the flaw in the Y direction (see Figure 1 for orientation of the Y direction).

A uniform distribution has been chosen to represent the flaw depth. The reason for this choice is that the UT indications shown in Table 7 seem to indicate that flaws are scattered over the entire extent of the Y direction.

To verify that the use of a uniform distribution is not unreasonable to represent flaw depths, a chi-square test is performed at the 0.05 significance level.

The symbols of Equation 7 are utilized to perform the goodness-of-fit test. The evaluation performed is based on Assumption 5.1.1. The onsets of the $n = 7$ UT indications in the Y direction are partitioned into $M = 3$ equiprobable cells: one ranging from 0 to 8.33 mm, one ranging from 8.33 mm to 16.67 mm, and the last ranging from 16.67 mm to 25 mm. Three cells have been chosen for the same reason as that given in Section 6.2.1.1.1. The resulting Pearson statistic is 2.0 (see Attachment I for the detail of the calculations).

The number of degrees of freedom is $M - 1 = 2$, based on D'Agostino and Stephens (1986, p. 64). Notice that no parameter needs to be estimated with the uniform distribution. That is why, contrary to what was done in the previous sections, there is no need to remove an extra degree of freedom. This yields $\chi^2_{0.95}(2) = 6.0$, which is greater than the Pearson statistic. Therefore, using a uniform distribution to estimate the flaw depth distribution is not in contradiction with the data.

In conclusion, the depth of the flaws in the outer lid weld of the waste package is considered to follow a uniform distribution. Applicability to other welds will be addressed in Section 6.2.1.3.

6.2.1.1.4 Flaw Orientation

The orientation of the flaws is investigated in the plane of the specimen rings. The objective is to investigate the angle θ that the flaws make with the direction of the weld (see Figure 5 for schematic representation). This is important in trying to determine an estimate of the flaws which are radially oriented (a broad definition of radially orientated flaws is those flaws that have an angle θ greater than 45 degrees).

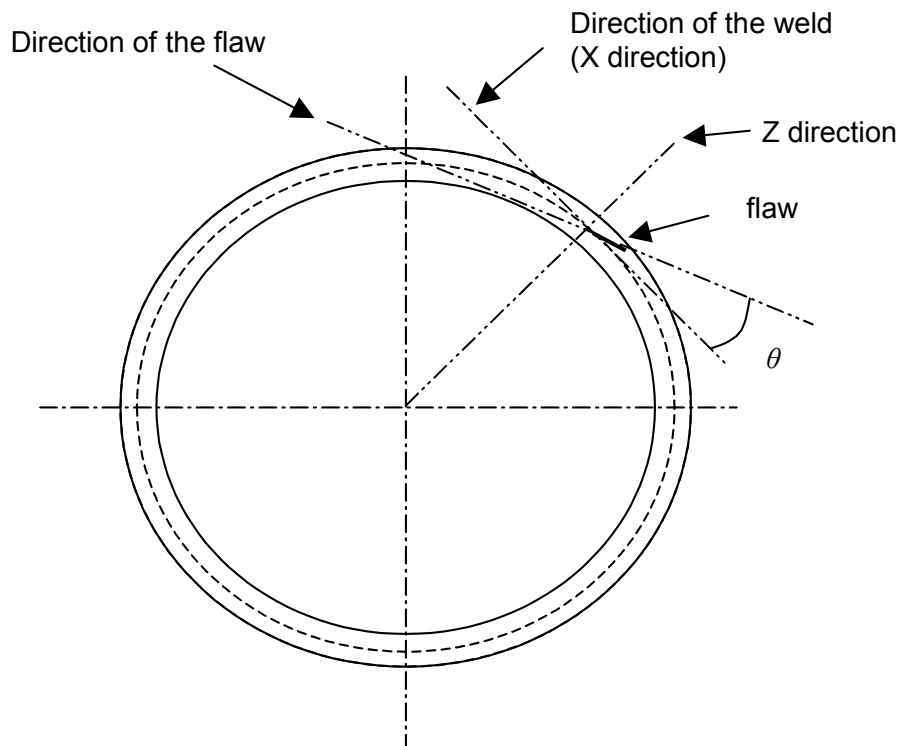


Figure 5. Schematic Representation of Flaw Orientation on Specimen Ring

The calculations which follow are based on Assumption 5.1.1. The extent of the UT indications in the radial direction (Z direction) and their length in the direction of the weld (X direction) are given in Section 4.1.3.2. Because the largest flaw in the X direction does not exceed 3.5 cm, which is very small compared to the radius of the specimen ring (around 77 cm, see Section 4.1.3.1), the effect of the curvature in the direction of the weld is negligible. Therefore, the angle θ of a flaw can be calculated by taking the arctangent of the ratio of its extent in the Z direction over its extent in the X direction. Notice that the inputs given in Section 4.1.3.2 make it possible to evaluate the absolute value of θ only, not its sign.

Orientation of defects in welds has been investigated by Shcherbinskii and Myakishev (1970). They report that the angle between a defect and the direction of the weld can be fit to a centered normal distribution with a standard deviation of around 5 degrees. Based on this information, the present analysis considers a centered normal distribution in trying to fit the data.

The fact that the distribution is chosen to be centered (i.e., with a mean of 0 degree) is natural since most of the defects observed are lack-of-fusion flaws, which typically are in the direction of the weld. The standard deviation of 5 degrees is discarded from further consideration since the available data report a flaw with an angle around 27 degrees, which suggests a larger standard deviation. It should be noted that the flaw with an angle around 27 degrees is not a lack-of-fusion defect but results from a poor weld preparation (flaw found on ring K: see Section 4.1.3.2 and angle values calculated in Attachment I). In a conservative approach, this flaw was kept in the analysis though it is not representative of the highly controlled conditions under which operations will be conducted on the waste package. The standard deviation σ of the

normal distribution is evaluated using the Bayesian approach with a noninformative prior. A noninformative prior is selected so as to put maximum emphasis on the information provided by the data.

Only the absolute values for θ are available, not their signs. Therefore, the distribution for θ is not normal by definition, since it is defined only by positive values. In fact, there are two possible initial angle values (one positive, one negative) that correspond to a single value of θ . Therefore, the actual PDF p_θ for θ is equal to twice the PDF of the centered normal distribution, with standard deviation σ . The PDF of a normal distribution is found in Martz and Waller (1991, p. 49), and the resulting PDF for θ is as follows.

$$p_\theta(\theta, \sigma) = 2 \cdot \frac{1}{\sigma \cdot \sqrt{2\pi}} \cdot \exp\left[-\frac{1}{2} \cdot \left(\frac{\theta}{\sigma}\right)^2\right] \text{ for } \theta \geq 0 \quad (\text{Eq. 17})$$

The corresponding CDF P_θ is:

$$P_\theta(\theta, \sigma) = 2 \cdot \int_0^\theta \frac{1}{\sigma \cdot \sqrt{2\pi}} \cdot \exp\left[-\frac{1}{2} \cdot \left(\frac{u}{\sigma}\right)^2\right] du \quad (\text{Eq. 18})$$

Based on Martz and Waller (1991, pp. 225 and 226), a noninformative prior for σ when considering the quasi-normal PDF $p_\theta(\theta, \sigma)$ is $1/\sigma$.

Applying Bayes' theorem leads to the following expression for the posterior PDF p_σ of σ (Martz and Waller 1991, pp. 174 and 175):

$$p_\sigma(\sigma) = \frac{\frac{L_\theta(\sigma)}{\sigma}}{\int_0^\infty \frac{L_\theta(\sigma)}{\sigma} d\sigma} \quad (\text{Eq. 19})$$

where $L_\theta(\sigma) = \prod_{i=1}^{n_f} p_\theta(\theta_i, \sigma)$ is the likelihood function related to the $n_f = 7$ observed angles θ_i .

Based on the posterior PDF, the mean value of σ_m is calculated to be around 13.9 degrees. The 5th and 95th percentiles are around 8.7 and 21.6 degrees, respectively. The maximum likelihood estimator, based on the formula given in Martz and Waller (1991, p. 225) is around 12.3 degrees, which is relatively close to σ_m .

To verify that it is not unreasonable that the flaw orientation information fits P_θ , a chi-square test is performed at the 0.05 significance level, using σ_m as the standard deviation.

The variables of Equation 7 are utilized to perform the goodness-of-fit test. There are $n = 7$ data points, and the fitted distribution has one of its parameters evaluated from the data. The same approach as that outlined in Section 6.2.1.1.1 (i.e., partition the flaw orientation dataset into

$M = 3$ approximately equiprobable cells and compare the Pearson statistic to the 95th percentile of the chi-square with 1 degree of freedom is performed).

The cells are found to be approximately equiprobable by selecting the following ranges: 0 to 5.6 degrees, 5.6 to 12.7 degrees, and more than 12.7 degrees. The Pearson statistic is located around 0.44, which is lower than $\chi^2_{0.95}(1) = 3.8$ (see Attachment I for the detail of the calculations). In other words, fitting the flaw orientation information to $P_\theta(\theta, \sigma_m)$ is not contradicted at the 0.05 significance level.

Based on previous developments, the expected fraction of flaws, F_θ , that have an angle θ greater than 45 degrees is calculated using the following formula:

$$F_\theta = \int_0^\infty [1 - P_\theta(45, \sigma)] \cdot p_\sigma(\sigma) d\sigma \quad (\text{Eq. 20})$$

This yields $F_\theta = 8 \times 10^{-3}$. Therefore, around 0.8 percent of the flaws will have an angle greater than 45 degrees.

In conclusion, investigation of flaw orientation has shown that almost all of the flaws are in the direction of the weld. The fraction of flaws that are radially oriented (i.e., making an angle of 45 degrees or more with respect to the direction of the weld) is 0.8 percent of the flaws. This result was obtained for the flaws in the outer lid weld of the waste package. Applicability to other welds will be addressed in Section 6.2.1.3.

6.2.1.2 Flaw Characteristics in Welds after Inspection and Repair

The flaw characteristics that were developed in Section 6.2.1.1 are representative of those to be expected in the noninspected outer lid weld of a waste package. A UT inspection will be performed to detect and repair the flaws that may adversely affect the waste package performance. The objective of this section is to assess the characteristics of the flaws remaining in the waste package.

6.2.1.2.1 Ultrasonic Inspection Characterization

This section investigates the UT PND of a flaw of size s in the Y direction. The corresponding PND curve was not developed during the UT inspection of the specimen rings. Nevertheless, information from the literature, available results from UT inspection capability on the specimen rings, and anticipation that not every detected flaw will need to be removed from the weld were combined to elaborate a conservative UT PND curve.

Bush (1983, pp. 13A.5.6 and 13A.5.7) summarizes the results of previous studies on UT reliability and provides parameter values for a PND curve defined as follows:

$$P_{ND1}(s, \varepsilon, s_0, \nu) = \varepsilon + \frac{1}{2} \cdot (1 - \varepsilon) \cdot \operatorname{erfc} \left[\nu \cdot \ln \left(\frac{s}{s_0} \right) \right] \quad (\text{Eq. 21})$$

where

- s = size of the flaw (in mm)
- ε = lower limit of P_{NDI} (from assumption 5.1.2 = 0.005)
- ν = shape factor (from assumption 5.1.2 = 3)
- s_0 = characteristic flaw size, in mm, for which around 50 percent of the flaws are detected (from assumption 5.1.2 = 2.5 mm)
- erfc = complementary error function

It should be noted that in Equation 21, s is the variable while ε , ν , and s_0 are parameters.

Focusing on detection of intergranular stress corrosion cracking in austenitic piping, Bush (1983, p. 13A.5.7) suggests using the following parameter values: $\varepsilon = 0.005$, $\nu = 3$, and $s_0 = 5$ mm. Notice that these results are based on experiments performed in the late 1970s, so they reflect detection capabilities that have been significantly surpassed. A way to account for finer detection capabilities is to reduce the value of s_0 , for example take s_0 at 2.5 mm (Bush 1983, p. 13A.5.7). This value is not reduced further in order to account for those small flaws that are detected but are left in the weld because the welds will not jeopardize the waste package performance.

A more recent study on UT detection of intergranular stress corrosion cracking in stainless steel, reported in Heasler and Doctor (1996), shows significantly improved reliability. This reference provides the parameters for a logistic function giving the probability of detection as a function of flaw size s for near-side access (i.e., the defect is located on the accessible side of the weld centerline). The PND curve based on Heasler and Doctor (1996, p. 5.1) has the form:

$$P_{ND2}(s) = 1 - \frac{1}{1 + \exp(-\beta_1 - \beta_2 \cdot s)} \quad (\text{Eq. 22})$$

where:

- s = flaw size in mm
- β_1 = -2.67, based on Heasler and Doctor (1996, p. 5.9)
- β_2 = 1.6709 /mm, based on Heasler and Doctor (1996, p. 5.9)

The resulting UT PND curves identified previously are summarized in Figure 6.

It should be noted that the references reviewed previously indicate that the PND for flaws of various sizes is dependent on a number of variables such as the type of material, operator skill, access to the weld, and type of defect. In that context, the UT inspections performed on the specimen rings provide useful information, since they were carried out on welds very similar to the closure weld of the waste package.

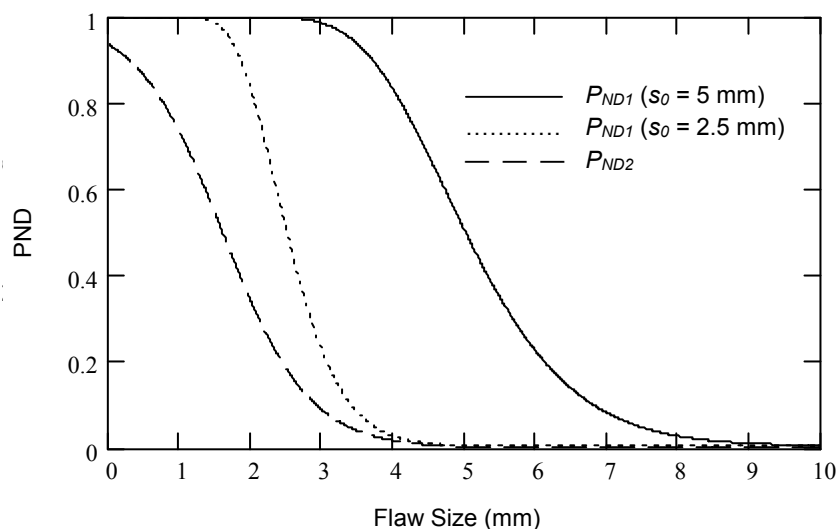


Figure 6. Comparison of Several Ultrasonic Probability-of-Nondetection Curves Identified in the Literature

As mentioned in Section 4.1.3.2, the UT inspection threshold employed in the examination of the specimen rings had a sensitivity of 1 mm, which calls for detection of flaws of this size or larger. This was confirmed by metallographic examination of the specimen rings: all the uncovered flaws that were larger than 1 mm had been detected through the previous UT inspections. Therefore, the UT PND curves shown in Figure 6 appear to display less detection capability than what is attainable on waste package closure welds using current industry equipment.

Lastly, the fact that a flaw is detected through UT inspection does not mean that it will be removed. The reason for this is that weld repairs are time- and resource-consuming and will therefore be implemented only when deemed necessary to ensure waste package performance. It can be expected that small flaws and flaws located deep in the weld will be left if it is shown that they will not cause early waste package breach. Also, gas porosities will not be removed since they have no orientation and therefore do not promote stress corrosion cracking.

Based on the elements of information given previously, a conservative assumption (Assumption 5.1.2) has been developed. It is assumed that an acceptable UT PND curve, applicable to the waste package closure weld, is given in Equation 21 with the following parameter values: $\varepsilon = 0.005$, $\nu = 3$, and $s_0 = 2.5$ mm. This UT PND curve is used in the following to develop the flaw density and size distributions of the flaws remaining in the weld after inspection and repair. Notice that this curve is shown on Figure 6 (it is the curve plotted with dots, designated by P_{ND1} with $s_0 = 2.5$ mm). With this curve the flaws smaller than 1 mm are not detected. Around 50 percent of the 2.5 mm flaws are detected.

A weld flaw detection criteria equal to or greater than 1.6 mm ($1/16^{\text{th}}$ of an inch) has been established for the fabrication of a prototype waste package (BSC 2003f, Requirements 7.1.B and 7.1.C). This detection criteria specifies that the UT inspection method employed must be able to detect all weld flaws equal to or greater than 1.6 mm ($PND=0.0$). This will result in smaller weld flaws being detected than is being modeled in this calculation since, as shown in Figure 6, the PND of a 1.6 mm flaw is approximately 1.0 (i.e., the model predicts that no weld flaws 1.6 mm or smaller would be detected).

6.2.1.2.2 Flaw Size Distribution in the Y direction

Equation 8 in Section 6.2.1.1.1 gives the PDF for the flaw size distribution of flaws of size s in the Y direction based on welds of thickness t , before UT inspection. It is a function of the random parameter λ_s whose PDF is given by Equation 2.

The UT inspection and subsequent weld repair are characterized by the UT PND P_{NDI} curve given in Equation 21 with the parameter values: $\varepsilon = 0.005$, $v = 3$, and $s_0 = 2.5$ mm.

Using the calculated value of λ_s , the fraction of flaws that remain in the closure weld after UT inspection and weld repair is calculated with the following equation:

$$F_{ND}(t, \lambda_s, \varepsilon, s_0, v) = \int_0^t p_{sg}(s, \lambda_s, t) \cdot P_{NDI}(s, \varepsilon, s_0, v) ds \quad (\text{Eq. 23})$$

The corresponding CDF for the flaw size of those flaws remaining in the closure weld after UT inspection and weld repair, P_{sgut} , is given by the following equation:

$$P_{sgut}(s, t, \lambda_s, \varepsilon, s_0, v) = \frac{\int_0^s p_{sg}(u, \lambda_s, t) \cdot P_{NDI}(u, \varepsilon, s_0, v) du}{F_{ND}(t, \lambda_s, \varepsilon, s_0, v)} \quad (\text{Eq. 24})$$

It should be noted that in Equation 24, s is the variable while t , λ_s , ε , s_0 , and v are parameters.

As complementary information, p_{msgut} , the PDF for the size of the remaining flaws accounting for all possible values of λ_s , weighted by their probability, can be calculated using the following equation:

$$p_{msgut}(s, t, \varepsilon, s_0, v) = \int_0^\infty \frac{p_{sg}(s, \lambda_s, t) \cdot P_{NDI}(s, \varepsilon, s_0, v)}{F_{ND}(t, \lambda_s, \varepsilon, s_0, v)} \cdot p_{\lambda_s}(\lambda_s) d\lambda_s \quad (\text{Eq. 25})$$

The corresponding CDF is:

$$P_{msgut}(s, t, \varepsilon, s_0, v) = \int_0^s p_{msgut}(u, t, \varepsilon, s_0, v) du \quad (\text{Eq. 26})$$

Figure 7 shows $P_{msgut}(s, t, \varepsilon, s_0, v)$ for $t = 25$ mm, which corresponds to the size distribution of the flaws remaining in the outer lid weld of the waste package after UT inspection and repair. Recall that this CDF accounts for all possible values of λ_s , weighted by their probability.

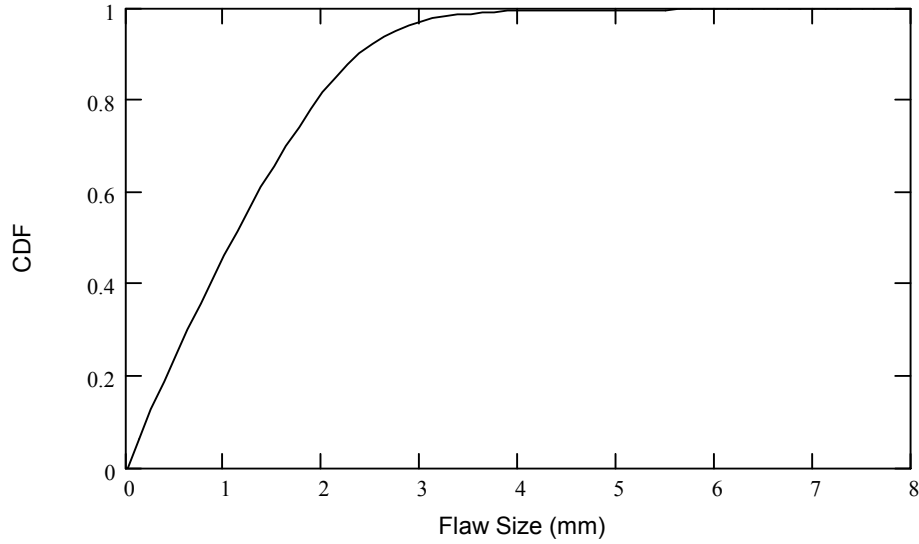


Figure 7. Cumulative Distribution Function for Flaw Size After Ultrasonic Inspection and Repair in Outer Lid Weld

The corresponding mean size, for the flaws remaining in the 25-mm thick closure weld, is given by:

$$s_{msgut}(t, \varepsilon, s_0, \nu) = \int_0^t p_{msgut}(u, t, \varepsilon, s_0, \nu) \cdot u \, du \quad (\text{Eq. 27})$$

This yields a value of 1.3 mm. As for the 5th and 95th percentiles, they are calculated by solving Equation 26 for values of P_{msgut} equal to 0.05 and 0.95, respectively. This yields 9.9×10^{-2} and 2.8 mm.

6.2.1.2.3 Flaw Density

Recall that before UT inspection, the mean number of flaws per meter of weld is given by the flaw density parameter λ_d , whose PDF is shown in Equation 12 of Section 6.2.1.1.2. After UT inspection and repair, the mean number of remaining flaws per meter of weld, λ_{dut} , will be equal to λ_d , adjusted by the fraction F_{ND} of flaws that will not be detected. This corresponds to the following equation:

$$\lambda_{dut}(\lambda_d, \lambda_s, t, \varepsilon, s_0, \nu) = \lambda_d \cdot F_{ND}(t, \lambda_s, \varepsilon, s_0, \nu) \quad (\text{Eq. 28})$$

where F_{ND} is evaluated with Equation 23.

It should be noted that in Equation 28, λ_{dut} is a function of two independent random parameters (λ_d and λ_s), and four fixed parameters (t , ε , s_0 , and ν).

As complementary information, the CDF of λ_{dut} , accounting for all possible values of λ_s and λ_d , weighted by their probability, is calculated using Latin Hypercube Sampling.

The principle of Latin Hypercube Sampling is provided in Modarres (1993, p. 244). For this case there are two random parameters: λ_d and λ_s . To start the process the range [0,1] is divided into n_s equal intervals. Within each of these intervals a random value u_i is chosen. Considering the CDF associated with λ_d , each u_i can be interpreted as the probability that λ_d will not exceed a certain value λ_{di} . Each λ_{di} is evaluated at each u_i , so that n_s values of λ_{di} are obtained. This same procedure is repeated with λ_s so as to obtain a sample of n_s values associated with λ_s . The two samples are then randomly combined according to Equation 28, in order to have a set of n_s random values, λ_{duti} , associated with λ_{dut} . This set is sorted out to obtain a sample CDF of λ_{dut} .

Figure 8 shows the result obtained from the Latin Hypercube Sampling performed on Equation 28 with $n_s = 2000$. A large value was chosen for n_s in order to ensure that the results of the sample CDF is close to the true CDF of λ_{dut} .

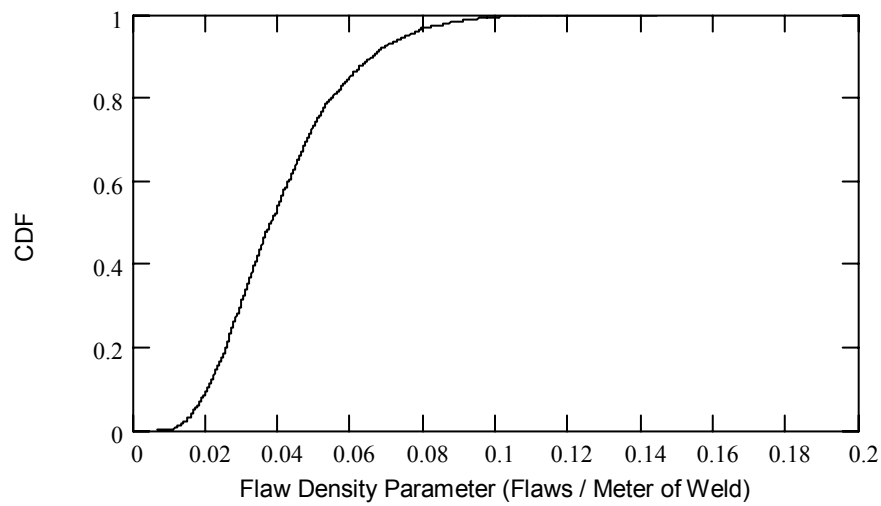


Figure 8. Cumulative Distribution Function for Flaw Density Parameter After Ultrasonic Inspection and Repair in Outer Lid Weld

The mean density parameter of the flaws remaining in the 25-mm thick closure weld after UT inspection and repair is evaluated based on the sample CDF using the following equation:

$$\lambda_{mdut} = \frac{1}{n_s} \cdot \sum_{i=1}^{n_s} \lambda_{duti} \quad (\text{Eq. 29})$$

where λ_{duti} is the i^{th} Latin Hypercube Sample value of λ_{dut} . This yields $\lambda_{mdut} = 4.1 \times 10^{-2}$ flaw /m of weld. The 5th and 95th percentiles are estimated by linear interpolation on the sorted set of sample values of λ_{dut} , around the 5th and 95th percentiles. This helps delimit a range for the flaw density parameter that encompasses 90 percent of the probability. The large value $n_s = 2000$ selected for Latin Hypercube Sampling ensures that the estimates for the 5th and 95th percentiles are close to the true value, but is too small to reach complete certainty on the first two significant figures. Therefore, only a range that encompasses the true 5th and 95th percentile is presented here. It is evaluated by rounding down the 5th percentile estimate, and rounding up the 95th percentile estimate. The resulting values are 1.6×10^{-2} flaws /m of weld and 7.6×10^{-2} flaws /m of weld, respectively. Note that because of the long time required for computation, it was not judged useful to make the calculation with a larger value of n_s . Besides, the value that was

selected proved sufficient to make an estimate of the mean with two significant figures. This is due to the fact that, by nature, Latin Hypercube Sampling provides estimates of the mean which are more stable than those related to lower and upper percentiles.

In conclusion, the probability on the number of flaws n remaining in a weld of length L (in m) after UT inspection and repair is calculated using the following Poisson distribution:

$$P_{nut}(n, \lambda_{dut}, L) = e^{-\lambda_{dut} \cdot L} \cdot \frac{(\lambda_{dut} \cdot L)^n}{n!} \quad (\text{Eq. 30})$$

where λ_{dut} is estimated based on Equation 28.

6.2.1.2.4 Flaw Depth and Flaw Orientation

The flaws that are detected during UT inspection will be evaluated in accordance with the ASME Code. It is planned that this inspection be performed in-situ as the weld is made. In the event that a flaw is identified, the flaw will be evaluated to determine if it fails to meet code requirements. If any flaw not meeting requirements is identified, the welding process will be interrupted and the flaw removed and that flaw site repair welded. The flaws that do not meet code requirements are most likely to jeopardize the long-term performance of the waste package and, therefore, is additional justification for their removal.

As a consequence, it is expected that any flaws that remain in the closure weld will be smaller than Code allowable. This and the test data indicating that none of the expected flaws are perpendicular (or greater than 5 degrees from the hoop stress) means that flaws remaining in any closure weld will be very small and unlikely to grow due to applied stresses.

The repair of weld flaws may affect the flaw depth distribution and flaw orientation results of Sections 6.2.1.1.3 and 6.2.1.1.4. This means that the flaw depth distribution will no longer be uniform. Nevertheless, following a conservative approach, the results of Sections 6.2.1.1.3 and 6.2.1.1.4 are still considered adequate to characterize the flaw depth distribution and the flaw orientation in the closure welds that have been inspected and repaired.

6.2.1.3 Summary of Results and Comparison with Results from Literature

In this section, the information needed to calculate the characteristics of the flaws expected in the waste package welds is summarized in Tables 11 and 12. The overall results are summarized in Table 13 (see Attachment I for the details of the calculations performed to obtain the results).

Table 11. Parameters Needed for Calculating Weld Flaw Characteristics

Type of Parameter	Symbol	Description	Numerical Value or Related Equation
Random variable	s	Flaw size in the Y direction (in mm)	See Table 12
	n	Number of flaws in the weld	See Table 12
Fixed parameter	t	Thickness of the weld (in mm)	10 mm for middle lid weld 20 mm for seam welds 25 mm for outer lid weld
	L	Length of the weld (rounded-up values, in m)	4.80 m for middle lid weld 4.85 m for outer lid weld 15 m for seam welds
	n_f	Number of UT indications in specimen rings	7
	s_t	Sum of UT indications sizes in the Y direction (in mm)	31.75 mm
	L_t	Total length of weld examined in specimen rings (in m)	77.60 m
	ε	Lower limit for UT PND	0.005
	s_0	Characteristic flaw size for UT PND (in mm)	2.5 mm
	ν	Shape factor for UT PND	3
	A	Cross sectional area of specimen ring weld ^a	239.88 mm ²
Random parameter	λ_s	Flaw size parameter in the Y direction (in mm ⁻¹)	PDF: see Equation 2
	λ_d	Flaw density parameter (flaws per meter of weld)	PDF: see Equation 12

NOTES: ^a Value given for convenience (not used in the equations referred to in Table 12). Value calculated in Attachment I.

Table 12. Summary Table for Evaluating Flaw Characteristics

Flaw Characteristic	Before UT Inspection	After UT Inspection and Weld Repair
Flaw size (s , in mm)	CDF P_{sg} given in Equation 6 Secondary equation: 2 Parameters: λ_s, t, n_f, s_t	CDF P_{sgut} given in Equation 24 Secondary equations: 2, 8, 21, 23 Parameters: $\lambda_s, t, n_f, s_t, \varepsilon, s_0, \nu$
Flaw number (n)	Poisson distribution: Equation 11 Secondary equation: 12 Parameters: λ_d, L, n_f, L_t	Poisson distribution: Equation 30 Secondary equations: 2, 8, 12, 21, 23, 28 Parameters: $\lambda_d, L, n_f, L_t, \lambda_s, t, \varepsilon, s_0, \nu, s_t$
Flaw orientation	0.8% of the flaws are radially oriented	0.8% of the flaws are radially oriented
Flaw depth	Uniform distribution on weld thickness	Uniform distribution on weld thickness

In addition to the outer lid weld of the waste package, which has been extensively studied previously, the parameters and the results pertaining to the middle lid weld and the seam welds of the waste package are provided. This was done based on Assumption 5.1.3. It should be noted that the seam welds are those welds that are required to fabricate the outer cylinder of the waste package with its associated bottom lid. The outer cylinder is composed of two plates rolled to form two half-cylinders (longitudinal welds), which are then welded to each other (circumferential weld). An additional weld is made to attach the bottom lid to the cylinder (Plinski 2001, pp. 14 and 15). The dimensions taken for the seam welds are as follows. The diameter of the bottom lid is taken to be the same as the outer lid diameter, and the length of the longitudinal welds is that of the waste package. This yields a total length of 15 m (see Attachment I for details of the calculation). The weld thickness is taken to be 20 mm, which is

the thickness of the outer cylinder wall (it should be noted that for the bottom lid weld, the thickness of the weld in reality is 25 mm; considering that it is only 20-mm thick is conservative). In Table 12, note that the expression “radially oriented” flaws for the flaws located in the seam welds should be interpreted as those flaws that deviate from an angle of more than 45 degrees from the direction of the weld.

Table 13 shows the mean, the 5th, and the 95th percentiles of the predicted flaw sizes, before UT inspection and after UT inspection and weld repair. These values are calculated based on the distribution of the flaw size, weighted with the probability values assumed by λ_s (see Equations 10 and 26).

Table 13 also shows the probability of having zero, one, and two or more flaws in the welds of the waste package before UT inspection and after UT inspection and weld repair. In each case, these probabilities have been calculated using the mean flaw density parameter. Notice that in contrast to what has been done for the flaw size, this calculation does not take into account the uncertainty of the flaw density parameter. This is because after UT inspection and weld repair, the calculation of the flaw density parameter is based on two random parameters, namely λ_d and λ_s , which makes the evaluations more complex. In this case, it is simpler to use the mean value of the flaw density parameter than trying to incorporate the uncertainty of this parameter in the calculation.

Table 13. Main Characteristics of Flaws in Welds of Waste Package

Flaw Size ^a (mm)	Before UT Inspection			After UT Inspection and Weld Repair		
	mean	5 th percentile	95 th percentile	mean	5 th percentile	95 th percentile
Outer lid weld	4.8	0.23	15.2	1.3	0.099	2.8
Middle lid weld	3.3	0.20	8.6	1.2	0.098	2.7
Seam welds ^b	4.6	0.23	13.8	1.2	0.099	2.8
Number of Flaws^c	0	1	2 or more	0	1	2 or more
Probability per outer lid weld	0.63	0.29	0.08	0.82	0.16	0.02
Probability per middle lid weld	0.63	0.29	0.08	0.80	0.18	0.02
Probability per seam weld ^c	0.23	0.34	0.43	0.54	0.33	0.13

NOTES: ^a Flaw sizes are given with two significant figures.

^b For information only – Do not use in calculations (see previous explanations).

^c Probability values on number of flaws are rounded so as to add up to 1.

It is important to note that the numbers reported in Table 13 for seam welds account only for UT inspection. This is extremely conservative since the fabrication welds of the waste package will undergo several types of inspections, including radiographic and liquid-penetrant testing (Plinski 2001, pp. 14 and 15), and therefore it is expected that any significant flaw will be detected and removed. Thus the seam weld flaw characteristics in Table 13 are given for information only and should not be used in further calculations.

Notice that the UT inspection followed by weld repair is an effective filter regarding the flaw size. This is because the UT inspection detects the larger flaws, which are then removed through weld repair. In other words, the UT inspection puts a cap on the maximum size of the flaws,

regardless of the thickness of the weld. It is worth noting that this cap is dependent on the shape of the UT PND curve. For example, using a different value than $s_0 = 2.5$ mm would yield a different cap. As previously mentioned in Section 6.2.1.2.1, the UT PND considered in this analysis is considered conservative.

Khaleel et al. (1999, Figure 7), reported results from simulations of flaws in welds that pertained to nuclear piping. The report modeled the flaw sizes in stainless steel welds (manufactured using the tungsten inert gas method) with a lognormal distribution, for which they give the median flaw size (in inches) and the shape parameter (no dimension) as a function of the weld thickness (in inches). Converting to the metric system, their equations become:

$$s_{50k} = 0.1169 \cdot 25.4 - 0.0445 \cdot t + 0.00797 \cdot \frac{t^2}{25.4} \quad (\text{Eq. 31})$$

$$\sigma_k = 0.09733 + 0.3425 \cdot \frac{t}{25.4} - 0.07268 \cdot \left(\frac{t}{25.4} \right)^2 \quad (\text{Eq. 32})$$

where s_{50k} , σ_k , and t are respectively the median flaw size (in mm), the shape parameter (no dimension), and the thickness of the weld (in mm). The PDF of the associated lognormal distribution is (Khaleel et al. 1999, p. 131):

$$p_{sk}(s) = \frac{1}{\sigma_k \cdot s \cdot \sqrt{2\pi}} \cdot \exp \left[-\frac{[\ln(s/s_{50k})]^2}{2 \cdot \sigma_k^2} \right] \quad (\text{Eq. 33})$$

where s is the size of the flaw in mm.

Also, based on Khaleel et al. (1999, p. 131), the mean flaw size s_{mk} (in mm) can be calculated as:

$$s_{mk} = s_{50k} \cdot \exp \left(\frac{\sigma_k^2}{2} \right) \quad (\text{Eq. 34})$$

The previous equations are used to calculate the mean, the 5th, and the 95th percentiles of the flaw size for a 25-mm thick weld. This yields 2.2 mm, 1.1 mm, and 3.8 mm, respectively (see Attachment I for details of the calculation).

It should be noted that these flaw sizes were developed with simulations that included the effects of inspection (Khaleel et al. 1999, p. 132). Therefore, they are to be compared to the post-UT inspection and weld repair results shown in Table 13. However, because the parameters used for modeling the inspections in the paper by Khaleel et al. (1999) are not known, it is difficult to make a meaningful comparison, especially regarding the 95th percentile since it reflects the size of the larger flaws (i.e., those flaws which are the most sensitive to the inspection parameters).

That is why, for a sensitivity case, it has been decided to investigate the effects that a UT inspection of the type used in this analysis would have on the flaws reported by Khaleel et al. (1999). The calculation, detailed in Attachment I, is similar to that shown in Section 6.2.1.2.2,

the only difference being the use of a lognormal distribution in lieu of an exponential. The new mean, 5th, and 95th percentiles are now: 1.8 mm, 1.1 mm, and 2.7 mm.

Notice that the 95th percentile of the flaw size is nearly identical to that shown in Table 13, which confirms the filtering effect of the UT inspection on the larger flaws. This also shows that the cap put by the UT inspection on the maximum flaw size is not dependent on the shape of the distribution used to characterize the flaw size but is rather governed by the UT PND curve (a different UT PND curve would provide a different cap).

The major difference between the flaw sizes reported by Khaleel et al. (1999) and the results shown in Table 13 is the size of the small flaws. The 5th percentile flaw size for the former is 1.1 mm, while it is 0.099 mm for the latter (see Table 13). The difference is due to the shapes of the lognormal and exponential distributions.

The flaw density is the other possible element of comparison between the literature and the results of this analysis. Khaleel et al. (1999, Table 6) report 0.0448 flaw per inch for a noninspected 1-inch thick weld. This corresponds to 1.8 flaws per meter of weld. This can be directly compared to the mean flaw density parameter of a 25-mm thick weld before UT inspection, calculated in Section 6.2.1.1.2, which is 0.097 flaw per meter of weld. The flaw density reported by Khaleel et al. (1999) is therefore about 18 times larger than the flaw density calculated in this analysis. This difference can be explained in part by the fact that the software code (RR-PRODIGAL), which was used to perform the weld flaw simulations of Khaleel et al. (1999), makes conservative estimates. This is mentioned by Simonen and Chapman (1999, p. 105) which report that the flaw frequencies predicted by RR-PRODIGAL were consistent with measured flaws found in actual piping and vessel welds, or were conservative by a factor as large as ten. Another reason to explain the large difference in flaw frequencies is that the welds compared are different: those simulated by Khaleel et al. (1999) were meant to model nuclear piping welds made of stainless steel, while the specimen rings studied in this analysis are made of Alloy 22 and meant for sealing waste packages. Thus, keeping in mind the conservatism of the RR-PRODIGAL simulation code and the inherent differences of the welds examined, the difference in the flaw frequencies is explicable and within reasonable limits.

6.2.2 Base Metal Flaws

In contrast to the wealth of information on the occurrence of weld flaws, information on the occurrence of flaws in base metal material is sparse. The occurrence frequency of base metal flaws has been estimated using results from various nondestructive examination techniques, including detailed UT examination of an unused reactor pressure vessel, validated by metallography (Schuster et al. 2000). While the primary emphasis of the study was on the density and depth distribution of weld flaws, flaw densities in the base metal regions outside of the heat-affected zone were also examined.

UT inspection showed that the density ratio of weld flaws to base metal flaws was 8 to 1 (Schuster et al. 2000, p. 2.3). The validation efforts (metallography) were unfortunately very limited, which led Schuster et al. (2000, pp. 4.2 and 4.3) to propose a list of potential explanations for the unvalidated base metal UT indications. Among those, only laminations and repairs to base metal may apply to the waste package (the other listed flaws were related to the

clad-to-base metal interface of the reactor vessel and are consequently not of interest here). Laminations are not a concern since they are in a plane parallel to the surface of the component and are therefore not expected to significantly jeopardize its integrity. This leaves repairs to base metal, which appeared to be associated with the larger flaws (Schuster et al. 2000, p. 5.2). It turned out later that these flaws were only clusters of small indications with little or no potential significance to structural integrity (Schuster et al. 2000, p. xiii). Nevertheless, based on previous information, repairs to base metal emerge as the dominant mechanism by which flaws with a significant through-wall extent could be introduced in the base metal. It is important to note that such flaws would result from an improper implementation of the procedure related to base metal repairs.

Several assumptions are required to evaluate the probability of the number of base metal flaws expected in the Alloy 22 barrier of the waste package. Because these assumptions are conservative, only a point estimate is calculated.

The frequency of occurrence for introducing base metal flaws is based on Assumption 5.2.1. This frequency of occurrence is considered to be initiated by an error of the welder performing a base metal repair (a base metal repair is conservatively assumed to be performed for each waste package). The failure of the welder to use the written procedure governing the repairs to base metal can be represented by the HEP for failing to follow a written procedure under normal operating conditions, and is estimated at 0.01 (median) with an error factor of 3 (Item 2 of Table 4). The failure of the checker to detect the errors made by the welder is estimated at 0.1 (median) with an error factor of 5, based on Item 8 of Table 4.

As mentioned in Section 4.1.2, the HEPs follow lognormal distributions. The relationship between the error factor EF and the shape parameter σ_k of a lognormal distribution (see Equation 33) is given by (Modarres 1993, p. 266):

$$\sigma_k = \frac{\ln(EF)}{1.645} \quad (\text{Eq. 35})$$

Therefore, using this result with Equation 34 makes it possible to express the mean m of a lognormal distribution as a function of its median m_{50} and its error factor EF as follows:

$$m = m_{50} \cdot \exp \left[\frac{1}{2} \cdot \left(\frac{\ln(EF)}{1.645} \right)^2 \right] \quad (\text{Eq. 36})$$

The product of independent lognormal distributions yields a lognormal distribution (Swain and Guttman 1983, pp. A-2 and A-4). The resulting median m_r and error factor EF_r can be calculated using the following equations (NRC 1983, pp. 12 to 33):

$$m_r = \prod_i m_i \quad (\text{Eq. 37})$$

$$EF_r = \exp \left[\sqrt{\sum_i (\ln(EF_i))^2} \right] \quad (\text{Eq. 38})$$

where m_i and EF_i are the individual medians and the error factors of the lognormal distributions.

Based on Equations 36 to 38, applied to the means and error factors of the HEPs given previously, the mean, F_{bm} , for the frequency of occurrence of base metal flaws due to repairs can be calculated as $F_{bm} = 2.0 \times 10^{-3}$ per waste package. Note that this concerns an area of 100 cm^2 , or equivalently, a volume V_{rbm} of repaired base metal equal to $2 \times 10^{-4} \text{ m}^3$, since the thickness of the Alloy 22 barrier is 20 mm (see Table 2).

The ratio of weld flaws to base metal flaws resulting from repairs in the Alloy 22 barrier of the waste package is 8 to 1, based on Assumption 5.2.2. It should be noted that this number is based on results of Schuster et al. (2000), which compared the densities of flaws in the welds and base metal of an unused reactor pressure vessel. Because this reactor vessel had been fabricated under standard quality procedures used for the manufacturing of nuclear equipment, it had been subjected to regular nondestructive examination tests for detecting and removing unacceptable flaws. As a consequence, the flaw densities found by Schuster et al. (2000) pertained to inspected material. Thus, the weld flaw density to consider here is the weld density after UT inspection.

Based on Section 6.2.1.2.3, the mean weld flaw density of an inspected 25-mm thick weld is 4.1×10^{-2} flaws/m of weld. In order to evaluate a flaw density applicable to base metal flaws, this number needs to be expressed in terms of a volumetric density. Based on the calculations performed in Attachment I and after applying the 1/8 correction factor mentioned previously, the flaw density pertaining to base metal, λ_{bm} , was obtained. λ_{bm} is found to be approximately 21 base metal flaws per cubic meter.

The previous information is used to obtain the CDF P_{nbm} on the numbers n of base metal flaws in the Alloy 22 barrier of a waste package. It is the sum of the probability that the base metal repair is correctly performed, evaluated at $1 - F_{bm}$ (yielding a waste package with zero base metal flaws), and the probability that n flaws are present, given that the base metal repair is defective. As in Section 6.2.1.2.3, a Poisson distribution is used to calculate the probability of the number of base metal flaws, given that the base metal repair is faulty. With a volume $V_{rbm} = 2 \times 10^{-4} \text{ m}^3$ of base metal, the expression for the CDF is:

$$P_{nbm}(n, \lambda_{bm}, V_{rbm}) = (1 - F_{bm}) + F_{bm} \cdot e^{-\lambda_{bm} \cdot V_{rbm}} \cdot \sum_{i=0}^n \frac{(\lambda_{bm} \cdot V_{rbm})^i}{i!} \quad (\text{Eq. 39})$$

The expected number of base metal flaws is $F_{bm} \times \lambda_{bm} \times V_{rbm} = 8.6 \times 10^{-6}$ per waste package. Because the parameter of the Poisson distribution is very small ($\lambda_{bm} \times V_{rbm}$ is around 0.004), the probability that a randomly selected waste package has at least one base metal flaw is also approximated by $F_{bm} \times \lambda_{bm} \times V_{rbm} = 8.6 \times 10^{-6}$.

After investigating the probability of the number of previous flaws, the size distribution of these potential flaws is examined. It is likely that the flaws present in improperly repaired base metal will not be detected through the UT inspections performed during the faulty repair. Also, a base metal repair consists of a patch of weld material aimed at replacing the initial defective base metal. Therefore, the size distribution of the flaws present in improperly repaired base metal can

be represented by the flaw size distribution developed in Section 6.2.1.1.1 (i.e., the weld flaw size distribution in noninspected weld). Note that the thickness t to consider is 20 mm, which is the thickness of the Alloy 22 barrier. The flaw sizes will be the same as those found in the seam welds of the waste package before UT inspection (see Table 13 for main flaw size characteristics).

6.2.3 Improper Weld Material or Base Metal

While the use of improper weld materials was responsible for early failures in several of the container types examined in Section 6.1, there is little information to support the development of its probability for a waste package. As for the use of improper base metal material, no instance was found in the literature search reported in Section 6.1.

The only well documented occurrence of the extent to which a weld population was affected by improper weld material is described in *Records Investigation Report Related to Off-Chemistry Welds in Material Surveillance Specimens and Response to IE Bulletins 78-12 and 78-12A – Supplement* (Babcock and Wilcox 1979). This inspection of all vendors' welding records was prompted by the discovery that the weld chemistry of a portion of the Crystal River 3 surveillance-block weld did not meet the specification requirements. Based on this information, Assumption 5.3.1 was developed and the frequency for use of improper welding material was evaluated as a lognormal distribution whose 5th and 95th percentiles are 1.5×10^{-5} and 8.2×10^{-5} , respectively.

Using the fact that the 5th percentile (respectively the 95th percentile) can be obtained by multiplying (respectively dividing) the median m_{50} by the error factor EF , the following formulas are written:

$$m_{50} = \sqrt{5^{th} \text{ percentile} \times 95^{th} \text{ percentile}} \quad (\text{Eq. 40})$$

$$EF = \sqrt{\frac{95^{th} \text{ percentile}}{5^{th} \text{ percentile}}} \quad (\text{Eq. 41})$$

This yields a median of 3.5×10^{-5} and an error factor of 2.3.

Records Investigation Report Related to Off-Chemistry Welds in Material Surveillance Specimens and Response to IE Bulletins 78-12 and 78-12A – Supplement (Babcock and Wilcox 1979) concluded that the evolution of shop practices as of 1979 had virtually eliminated the possibility that improper weld material would be used in the fabrication of a reactor vessel. New instrumentation, such as portable X-ray spectroscopy equipment, makes it possible to perform quick field measurements of material compositions (ASM International 1990b, pp. 1030 to 1032). It is assumed (Assumption 5.3.2) that such a verification will be performed. However, there is still the possibility that the technician in charge of this work fails to perform the operation correctly. This HEP can be approximated by the (lognormal) probability of improperly checking a digital display, which has a median of 0.001 and an error factor of 3 (Item 4 of Table 4).

The probability that an improper welding material is inadvertently used in the manufacturing of the Alloy 22 barrier of the waste package, and that this mistake is not detected, is the combination of the previous probability distributions. Using Equations 37 and 38, the resulting median and error factor are 3.5×10^{-8} per waste package and 4.0, respectively. The mean is 5.0×10^{-8} per waste package based on Equation 36.

Based on Assumption 5.3.3, the frequency for use of improper base metal in the fabrication of the outer barrier of the waste package is the same as the frequency of use of improper weld material. In other words, it follows a lognormal distribution whose 5th and 95th percentiles are 1.5×10^{-5} and 8.2×10^{-5} , respectively.

In addition, only certified material will be used for the fabrication of the waste package (Plinski 2001, Section 6.2.3). Therefore, it is expected that a check of base metal composition similar to that done for the weld will be performed. The failure to perform this operation correctly is quantified with the same HEP as that considered for the weld.

Consequently, the probability that an improper base metal is inadvertently used in the manufacturing of the Alloy 22 barrier of the waste package, and that this mistake is not detected, is the same as the probability of using an improper welding material. It follows a lognormal distribution with a median of 3.5×10^{-8} per waste package and an error factor of 4.0. The mean is 5.0×10^{-8} per waste package.

6.2.4 Improper Heat Treatment

The procedures and equipment that will be employed to perform the heat treatment during the fabrication of the waste package components have not yet been decided. Therefore, in order to evaluate the probability that the waste package components will be subjected to an improper heat treatment, without being detected prior to emplacement in the repository, it is necessary to make a set of assumptions on the general elements of the heat treatment process. These are Assumptions 5.4.1 and 5.4.2.

Based on Assumptions 5.4.1 and 5.4.2, events involved in the improper heat treatment of the waste package components are developed. These events are then combined into event sequences identifying the scenarios that could lead to waste package components improper heat treatment. This is done by developing an event tree. This event tree is then used to quantify the corresponding probability.

The elementary probabilities of the events involved in the improper heat treatment event tree are as follows:

- The operator failure to choose the correct heat treatment/quenching program is approximated by the selection of a wrong control on a panel from an array of similar-appearing controls identified by labels only (Item 6 of Table 4). The median of the corresponding HEP is 0.003 and the error factor is 3. Notice that this HEP is an error of commission, not an error of decision (i.e., the operator mistakenly pushes a wrong button that launches an improper heat treatment program). Since similar types of waste packages will most likely receive the same heat treatment, there will be a very limited

number of possible heat treatment programs to choose from. It is therefore not credible that the operator gets confused on the program to select for the type of waste package to be heat treated. In other words, the most plausible cause for mistake is an error of commission.

- The technician failure to properly install the waste package thermocouples is considered to be caused by the failure to use a written test or calibration procedure. The corresponding HEP is 0.05 (median) with an error factor of 5 (Item 3 of Table 4). Notice that installation of the thermocouples at correct locations is necessary to obtain meaningful temperature measurements. The most probable reason for failing to perform this task correctly is to overlook the corresponding written procedure. The HEP related to the failure to use a written test or calibration procedure was chosen in lieu of the HEP related to the failure to use written operations procedure under normal operating conditions (Item 2 of Table 4). This is because the former is more appropriate than the latter to account for the repetitive aspect of the task, which might lead the technician in charge of the thermocouple installation to ignore the procedure. Note that the corresponding HEP is greater (0.05 versus 0.01 for Item 2 in Table 4).
- The failure of the checker to detect an improper installation of the waste package thermocouples by the technician is approximated by an HEP of 0.1 (median) with an error factor of 5. This is based on Item 8 of Table 4, which evaluates the probability of failing to detect error made by others during routine tasks.
- During the QA check of the log generated by the computerized heat treatment system, the failure of the checker to detect that the operator chose a wrong heat treatment program is approximated by an HEP of 0.1 (median) with an error factor of 5, based on Item 8 of Table 4.
- The probability that a process malfunction will occur during the heat treatment of a waste package is approximated by a lognormal distribution with a median of 0.005 and an error factor of 2. This is based on Assumption 5.4.3.
- The probability that the operator fails to respond to an alarm (annunciator) signaling a process malfunction during the heat treatment of a waste package is approximated by an HEP of 0.0001 (median) and an error factor of 10. This is based on Item 9 of Table 4. Note that the main reason for such an error would be inattention.
- During the QA check of the log generated by the computerized heat treatment system, the failure of the checker to detect that the operator did not respond to an alarm generated by a process malfunction is approximated by an HEP of 0.02 (median) and an error factor of 5. The fact that an alarm was triggered during the heat treatment of the waste package will be written in the report generated by the computerized heat treatment system. It is expected that this alarm will catch the attention of the checker and prompt him/her to be more attentive of the operator response than he/she would be in the case of unannunciated anomalies such as improper thermocouple calibration, for instance. The corresponding HEP is based on Item 8 of Table 4, but because of the alarming factors,

the lower bound of the HEP is chosen instead of the point estimate value (which is 0.1). As for the error factor, it is based on Item 2 of Table 5.

The previous information is used to develop an event tree for the improper heat treatment during the fabrication of the waste package components. Although there are three components that are to be heat treated separately, namely the waste package outer lid, middle lid and outer barrier (including the outer barrier bottom lid), only two of these components are considered in this analysis (the waste package outer lid and the outer barrier). The waste package middle lid is not considered because it is not heat treated subsequent to the performance of its closure weld. Two separate event trees representing the heat treatment processes of these components have been developed. Although there is no significant difference between the two processes and the event trees are identical, they have different names to maintain independence between the two heat treatment processes.

The SAPHIRE software code is used to perform this task, and the resulting event trees are shown on Figures 9 and 10. The electronic files of the SAPHIRE project are contained in Attachment II. Table 14 shows the events, along with their mean probability. The means are calculated based on the median and the error factor, using Equation 36.

Table 14. Description of Events for Improper Heat Treatment of the Waste Package

Event Name	Event Description (Failure-Oriented)	Mean Probability	Correlation Class
INIT	Placeholder initiating event	1 ^a	N/A
HT_PRCDR_S HT_PRCDR_L	Operator fails to select correct heat treatment/quenching program	3.75×10^{-3}	HTSL
INSTLN_S INSTLN_L	Technician fails to properly install the waste package thermocouples	8.07×10^{-2}	INST
HT_CCR_S HT_CCR_L	Checker fails to detect that waste package thermocouples were improperly installed	1.61×10^{-1}	HTCK
HT_PCR_S HT_PCR_L	Checker fails to detect that operator chose incorrect heat treatment/quenching program	1.61×10^{-1}	HTCK
HT_PRCSS_S HT_PRCSS_L	Process malfunction occurs during the heat treatment of the waste package	5.46×10^{-3}	HTPC
HT_ANN_S HT_ANN_L	Operator fails to respond to alarm (annunciator) triggered by process malfunction	2.66×10^{-4}	HTAN
HT_ACR_S HT_ACR_L	Checker fails to detect that operator did not respond to alarm triggered by process malfunction	3.23×10^{-2}	HTAC

NOTE: ^aThis is a placeholder with a value of unity. It has no uncertainty.

It should be noted that the probabilities of nominally identical events have been correlated together. By nominally identical events, it is meant those events that are distinct but for which the states of knowledge that determine their distributions are identical. When performing the quantification of the event tree, and especially an uncertainty analysis, these events should be treated as completely dependent events (Apostolakis and Kaplan 1981, pp. 136 to 139). Table 14 indicates the correlation classes that were assigned in SAPHIRE to each event. Nominally dependent events share the same correlation class.

The sequences that lead to an improper heat treatment end state on Figures 9 and 10 are labeled “IPHT.”

A Monte Carlo sampling was performed with 90,000 realizations on the resultant events. The principle of the Monte Carlo sampling method is explained in Modarres (1993, pp. 243 and 244) and is not repeated here. Monte Carlo sampling is performed to propagate the variability of the events to obtain the characteristics of the resulting distribution. The seed value for the sampling (which is randomly chosen) was 59,027. The sample size was chosen large enough to get a good approximation on the main characteristics of the distribution.

The resulting mean, median, 5th percentile, and 95th percentile are 2.7×10^{-5} , 3.0×10^{-6} , 1.2×10^{-7} , and 1.1×10^{-4} per waste package, respectively.

It should be noted that the probability of improper heat treatment estimated here is independently corroborated by the pressure vessel failure statistics reported in Section 6.1.1. Those statistics indicated that one vessel in 20,000 experienced failure due to improper heat treatment. This yields a probability of 5×10^{-5} per vessel for this type of defect.

In the discussion that follows, which will be used in Section 6.4.8, it is shown that the probability that a waste package is improperly heat treated is independent of the fact that another waste package has already been improperly heat treated. In other words, the fact that a waste package receives an improper heat treatment does not increase the probability that the subsequent waste package to be processed also receives an improper heat treatment.

As shown on Figures 9 and 10, an improper heat treatment of a waste package may result from two types of failure scenarios.

The first type of scenario is the occurrence of a significant process malfunction. This will in turn trigger an alarm. Improper heat treatment will ensue if both the operator and the checker fail to respond to the alarm. There is no reason other than coincidence for the subsequent waste package to receive an improper heat treatment, unless the operator and the checker consider that the alarm triggered by the process malfunction is a false indication. This situation can be discarded from further consideration because it is incompatible with the highly controlled operating conditions under which heat treatment of the waste package will be performed. Indeed, the operator and the checker would have to justify why they considered the alarm to be a false indication, and subsequent verifications would prove them wrong. The fact that the corresponding waste packages were subjected to an improper heat treatment would thus be detected.

The second type of scenario is the failure of the operator to select the correct heat treatment program. As previously mentioned at the beginning of Section 6.2.4, this corresponds to an error of commission, rather than an error of selection (i.e., the operator knows which type of waste package is to be heat treated but mistakenly pushes the wrong button that launches an incorrect heat treatment program). By nature, this type of mistake is unlikely to be made again, except through coincidence, when the program for the subsequent waste package to be heat treated is launched.

Therefore, based on the previous information, occurrences of waste package improper heat treatment can be considered independent from each other.

6.2.5 Improper Laser Peening

No final decision has been reached on the stress mitigation technique to be used for the outer lid weld of the waste package. The laser peening method is considered in the following because it is deemed representative of the advanced technical process that will be employed.

The procedures and equipment that will be employed if the laser peening method is chosen for stress mitigation of the outer lid weld of the waste package have not yet been decided. Therefore, in order to evaluate the probability that the outer lid weld of a given waste package will be subjected to an improper laser peening, without being detected prior to emplacement in the repository, it is necessary to make a set of assumptions on the general elements of the laser peening process. These are Assumptions 5.5.1 and 5.5.2.

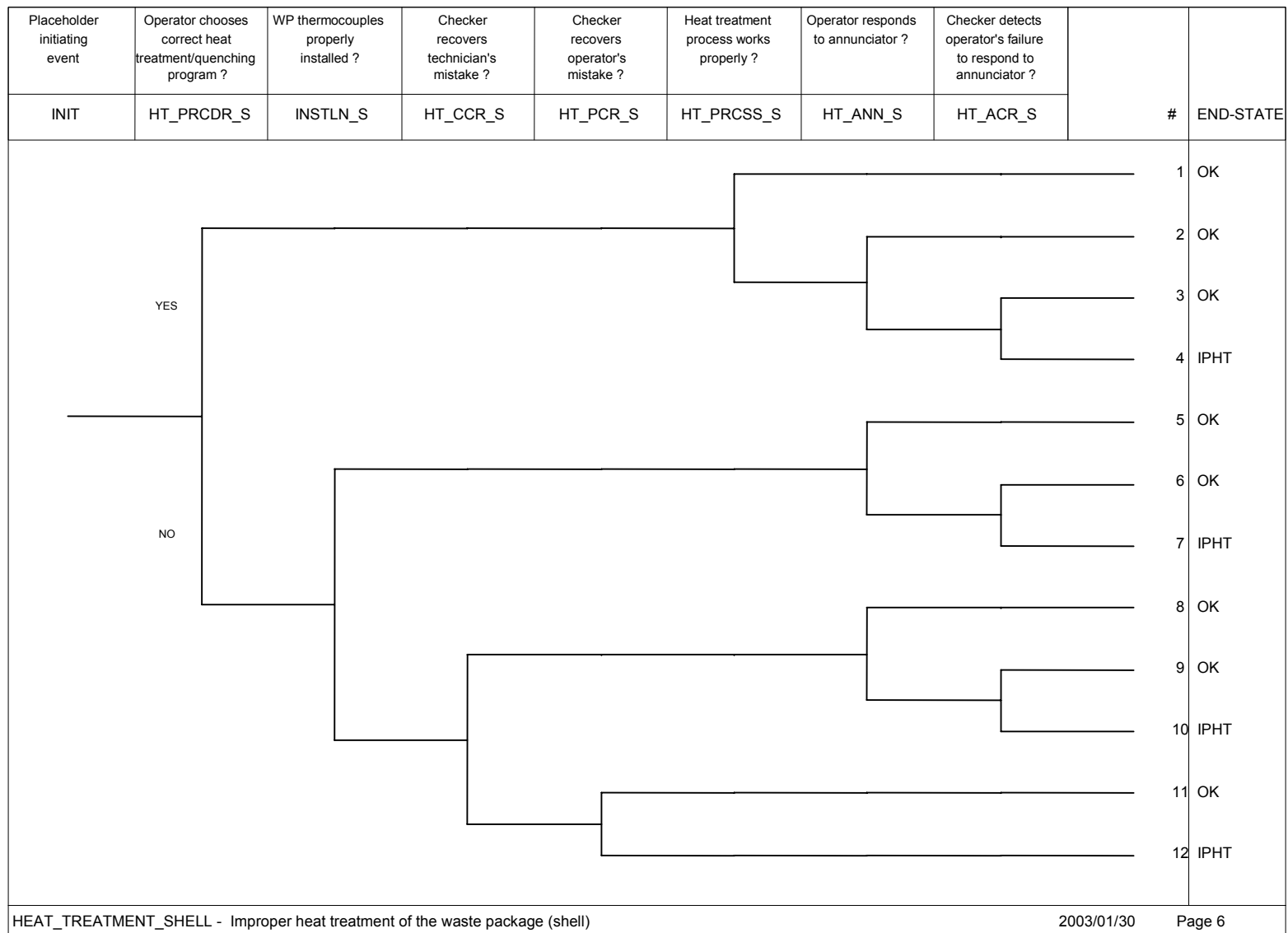


Figure 9. Event Tree for Improper Heat Treatment of the Waste Package Shell

Analysis of Mechanisms for Early Waste Package/Drip Shield Failure

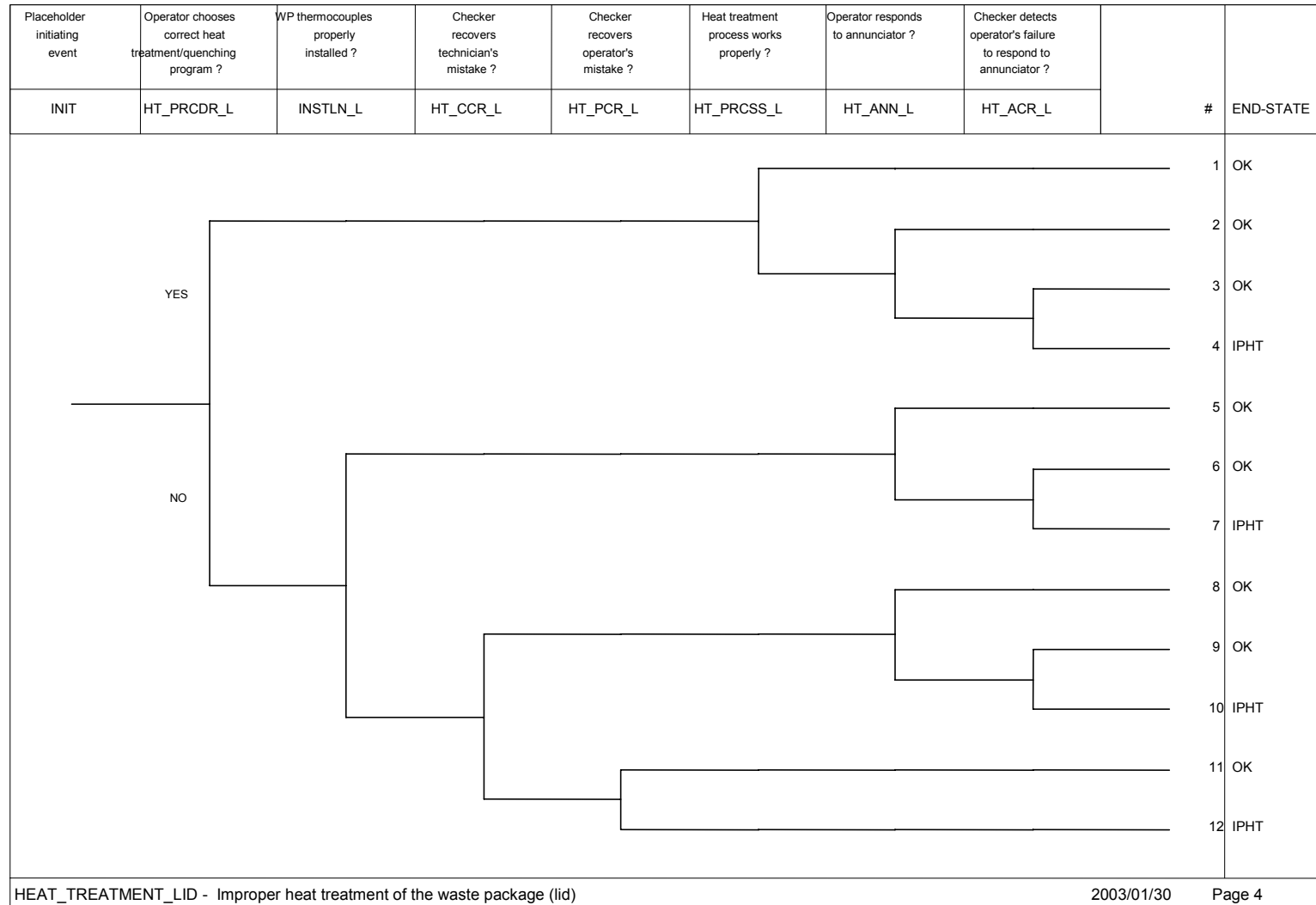


Figure 10. Event Tree for Improper Heat Treatment of the Waste Package Top Lid

Based on Assumptions 5.5.1 and 5.5.2, events involved in the improper laser peening of the waste package outer lid weld are developed. These events are then combined into event sequences identifying the scenarios that could lead to improper laser peening. This is done by developing an event tree. This event tree is then used to quantify the corresponding probability.

The elementary probabilities of the events involved in the improper laser peening event tree are as follows:

- The probability that a process malfunction will occur during the laser peening of the outer lid weld is approximated by a lognormal distribution with a median of 0.005 and an error factor of 2. This is based on Assumption 5.5.3.
- The probability that the operator fails to respond to an alarm (annunciator) signaling a process malfunction during the laser peening of the outer lid weld of a waste package is approximated by an HEP of 0.0001 (median) and an error factor of 10. This is based on Item 9 of Table 4.
- During the QA check of the log generated by the computerized laser peening system, the failure of the checker to detect that the operator did not respond to an alarm generated by a process malfunction is approximated by an HEP of 0.02 (median) and an error factor of 5. The fact that an alarm was triggered during the laser peening process will be written in the report generated by the computerized laser peening system. It is expected that this alarm will catch the attention of the checker and prompt him/her to be more attentive of the operator response than he/she would be in the case of unannunciated anomalies. The corresponding HEP is based on Item 8 of Table 4, but because of the alarming factors, the lower bound of the HEP is chosen instead of the point estimate value (which is 0.1). As for the error factor, it is based on Item 2 of Table 5.

The previous information is used to develop an event tree for the improper laser peening of the outer lid weld of the waste package. The software code SAPHIRE is used to perform this task, and the resulting event tree is shown on Figure 11. The electronic files of the SAPHIRE project are contained in Attachment II. Table 15 shows the events along with their mean probability. Note that the means are calculated based on the median and the error factor using Equation 36. Also, notice that none of the events are correlated together because each of them represents a different type of failures (see Section 6.2.4 for more information on correlation of events). Nevertheless, correlation classes are assigned to the events shown in Table 15; this is done in prevision of the quantification that will be performed in Section 6.4.8. Comparing the correlation classes to those given in Table 14 shows which events are determined based on the same state of knowledge.

The sequence of events that leads to an improper laser peening end state on Figure 11 is labeled “IPLP.”

There is no need to perform a Monte Carlo sampling to obtain the characteristics of the distribution pertaining to improper laser peening. This is because the sequence of events is the product of lognormal distributions and therefore is also a lognormal distribution. Application of Equations 37 and 38 yields a median of 1.0×10^{-8} per waste package and an error factor of 18.

The mean is calculated with Equation 36 and is 4.7×10^{-8} per waste package. Based on Equations 40 and 41, the 5th and the 95th percentiles are obtained by calculating the following equations:

$$5^{th} \text{ percentile} = \frac{m_{50}}{EF} \quad (\text{Eq. 42})$$

$$95^{th} \text{ percentile} = m_{50} \times EF \quad (\text{Eq. 43})$$

Equations 42 and 43 yield 5.6×10^{-10} and 1.8×10^{-7} for the 5th and 95th percentiles, respectively.

In the discussion that follows, which will be used in Section 6.4.8, it is shown that the probability of having a waste package subjected to improper laser peening is independent of the fact that another waste package has already been subjected to improper laser peening. In other words, the fact that a waste package is affected by an improper laser peening does not increase the probability that the subsequent waste package to be processed is also subjected to improper laser peening.

Table 15. Description of Events for Improper Laser Peening of the Waste Package Outer Lid Weld

Event Name	Event Description (Failure-Oriented)	Mean Probability	Correlation Class
INIT	Placeholder initiating event	1 ^a	N/A
LS_PRCSS	Process malfunction occurs during the laser peening	5.46×10^{-3}	HTPC
LS_ANN	Operator fails to respond to alarm (annunciator) triggered by process malfunction	2.66×10^{-4}	HTAN
LS_ACR	Checker fails to detect that operator did not respond to alarm triggered by process malfunction	3.23×10^{-2}	HTAC

NOTE: ^aThis is a placeholder with a value of unity. It has no uncertainty.

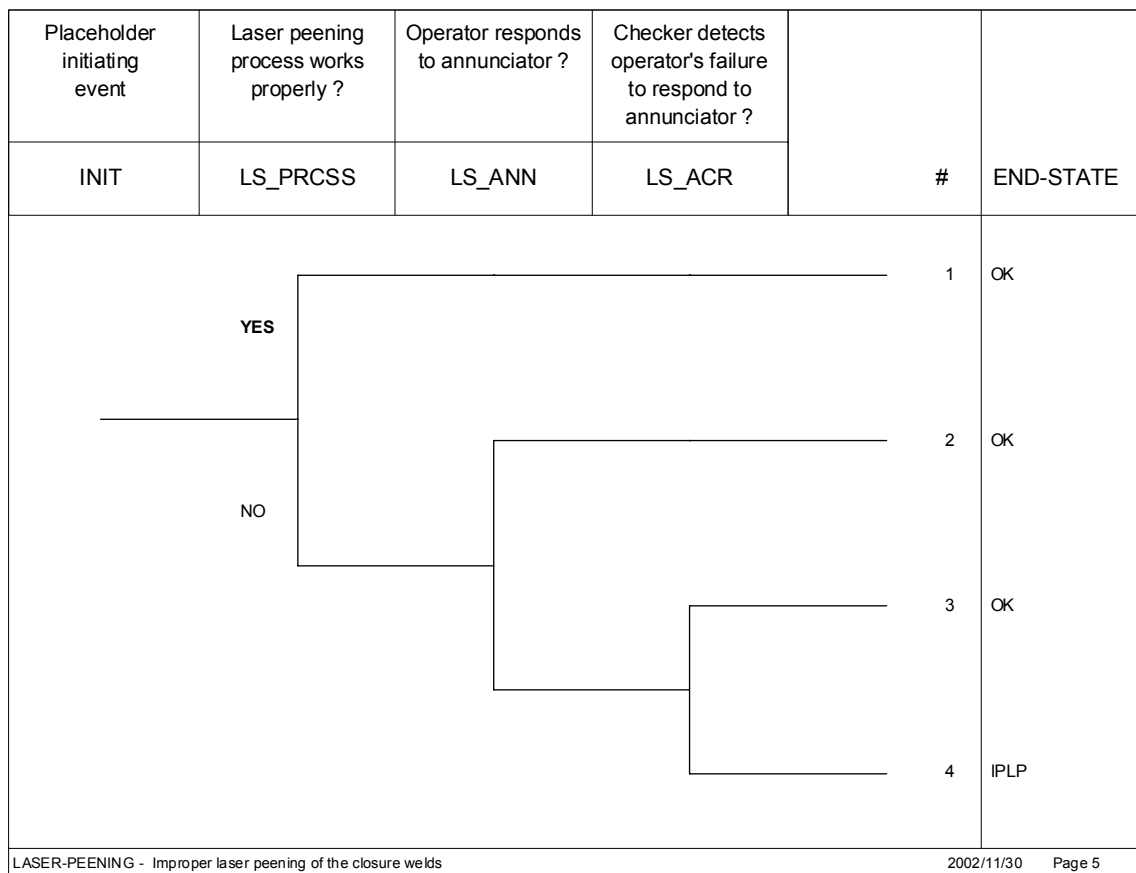


Figure 11. Event Tree for Improper Laser Peening of the Outer Lid Weld of the Waste Package

The rationale for this is similar to that given in Section 6.2.4 for improper heat treatment. Improper laser peening of a waste package will be initiated by a significant process malfunction. This will in turn trigger an alarm. Improper laser peening will ensue if both the operator and the checker fail to respond to the alarm. There is no reason other than coincidence for the subsequent waste package to receive an improper laser peening, unless the operator and the checker consider that the alarm triggered by the process malfunction is a false indication. This situation can be discarded from further consideration because it is incompatible with the highly controlled operating conditions under which laser peening of the waste package closure weld will be performed. Indeed, the operator and the checker would have to justify why they considered the alarm to be a false indication, and subsequent verifications would prove them wrong. The fact that the corresponding waste packages were subjected to an improper laser peening would thus be detected.

Therefore, based on the previous information, occurrences of waste package improper laser peening events can be considered independent from each other.

As a side remark, it is worth noting that the probability of having an undetected improper heat treatment (analyzed in Section 6.2.4) is much greater than the probability of having an undetected improper laser peening. This difference is due to the fact that, because there are different types of waste packages, several heat treatment programs (each applying only to a

certain type of waste packages) were assumed (Assumption 5.4.1). This results in the possibility that the operator might perform an error of commission in selecting the heat treatment program corresponding to a given type of waste package (an error of decision was judged implausible, see Section 6.2.4). In comparison, the laser peening process applies to the outer lid welds only, and these welds are essentially the same for all types of waste packages. More precisely, as far as the outer lid welds are concerned, only their diameters differ according to the type of waste package considered, and this difference will readily be accounted for in order to enable the laser peening process to even begin. In other words, it is not credible that the laser peening apparatus can be set to an incorrect position, corresponding to the diameter of a different type of waste package, without that being detected. Thus, there is no opportunity for having an improper selection of a laser peening program, as there is for the heat treatment process. This dissimilarity explains the difference in the resulting probabilities. As for the other principal cause for having an undetected improper heat treatment or laser peening, namely an undetected significant process malfunction, its probability of occurrence was evaluated in the same way for both heat treatment and laser peening, using a deliberately undetailed but conservative approach. Consequently, the undetected significant process malfunction does not contribute to the difference in probabilities between improper heat treatment and improper laser peening.

6.2.6 Contamination

In order to evaluate the probability that a waste package has its surface contaminated by some corrosion-enhancing material, and that this contamination remains undetected, it is necessary to know the manipulations the waste package is going to be subjected to from its fabrication to its emplacement in the repository. Only preliminary information is available at this time. Therefore, it is necessary to make a set of assumptions on the scenario that could lead to the contamination of the waste package. These are given in Section 5.6.

Two types of contamination are possible on the surface of the waste package, as explained below.

The first type is a contamination that leaves visible marks on the surface of the waste package (such as dirt, oil, etc.). Should such contamination occur before reception at the repository surface facility, it is expected that during the initial waste package inspection the contamination will be detected (Assumption 5.6.1). Should contamination occur in the surface facilities, it is expected to happen prior to the final inspection of the waste package (Assumption 5.6.2).

The second type is a contamination that does not leave visible marks on the surface of the waste package. The most likely source for such a contamination is an improper cleaning of the waste package. Assumption 5.6.3 summarizes the conditions required for this contamination scenario.

The elementary probabilities of the events involved in the waste package contamination by improper cleaning are as follows:

- The probability that the maintenance policies governing the stockage of the cleaning agents utilized for the waste package (use of a separate stockage area) are not observed has a median of 0.01 and an error factor of 5. This is based on Item 1 of Table 4.

- Should all the cleaning agents be stocked in the same area, the probability that the technician in charge of the cleaning selects an improper cleaning agent is 0.003 (median) with an error factor of 3. This is based on Item 6 of Table 4.
- During the QA check of the cleaning process, the failure of the checker to detect that the technician in charge of the waste package cleaning chose an incorrect cleaning agent is approximated by an HEP of 0.1 (median) with an error factor of 5. This is based on Item 8 of Table 4, which gives a probability value for a comparable event, namely the failure of an operator to select a control in a set of similar-appearing controls identified by labels only.

Notice that because this type of contamination is not visible to the naked eye, it cannot be spotted during the inspection performed in the surface facilities of the repository.

The elementary probabilities of the events involved in the waste package contamination inside the surface facilities of the repository, leaving visible traces on the metal, are as follows:

- The probability of occurrence for the contamination has a median of 0.01 and an error factor of 5. This is based on the fact that for a contamination of the waste package to occur, the policy governing the manipulation of the waste package has to be improperly carried out. The probability value is based on Item 1 of Table 4.
- The probability that the operator fails to detect visible traces of contamination during the final inspection of the waste package, performed remotely by camera, is estimated at 0.002 (median) with an error factor of 3. This is based on Item 5 of Table 4, which gives a probability value for a comparable event, namely the failure of an operator to check-read a display with difficult-to-see limit marks.

The previous information is used to develop an event tree for the contamination of the waste package. The software code SAPHIRE is used to perform this task, and the resulting event tree is shown on Figure 12. The electronic files of the SAPHIRE project are contained in Attachment II. Table 16 shows the events, along with their mean probability.

The probability of contaminating the waste package during at least one of its eight cleanings identified in Assumption 5.6.3 is quantified using a simple fault tree, called ICLNG (given in Attachment II). To quantify this probability, the fault tree combines the basic events required to have an improper cleaning, using logic gates (OR and AND). For an improper cleaning to occur, three basic events are required (therefore, they are connected with an AND gate). The first is common to all of the eight improper cleanings. It corresponds to the failure to observe the maintenance policies governing the stockage of the cleaning agents. The two other basic events represent the failure of the cleaning itself, which requires both the failure of the operator to select the correct cleaning agent, and the failure of the subsequent QA check of the process. Because the eight cleanings are considered to be independent from each other, they are connected through an OR gate in the fault tree. The mean probability is calculated using a Monte Carlo sampling with 90,000 realizations. The seed value (randomly chosen) is 22,877. Before performing the calculation, nominally identical basic events are correlated together, since their distribution is determined with the same state of knowledge (see Section 6.2.4 for more information on

correlation of nominally identical events). This applies to the eight basic events representing the improper selection of the cleaning agent on the one hand and the eight basic events representing the failure of the QA check on the other hand. The mean probability of fault tree ICLNG is shown on Table 16. It is given for information only because the real inputs that serve for the quantification of the event tree are the basic events on which the fault tree is developed.

The sequences of events that lead to waste package contamination end states on Figure 12 are labeled “CONT.”

Table 16. Description of Events for Contamination of the Waste Package

Event Name	Event Description (Failure-Oriented)	Mean Probability
INIT	Placeholder initiating event	1 ^a
ICLNG	Contamination of the waste package occurs during its cleaning	7.2×10^{-5} ^b
CONT	Visible contamination in the surface facilities of the repository	1.61×10^{-2}
CAM_DET	Operator fails to detect visible traces of waste package contamination during final inspection performed via remote camera	2.50×10^{-3}

NOTES: ^a This is a placeholder with a value of unity. It has no uncertainty.

^b Probability value is based on quantification of associated fault tree (given in Attachment II). Only two significant figures are shown.

A Monte Carlo sampling was performed with 90,000 realizations on the resultant events. Monte Carlo sampling is performed to propagate the variability of the events to obtain the characteristics of the resulting distribution. The seed value for the sampling (randomly chosen) is 59,027. The sample size is chosen large enough to get a good approximation on the main characteristics of the distribution.

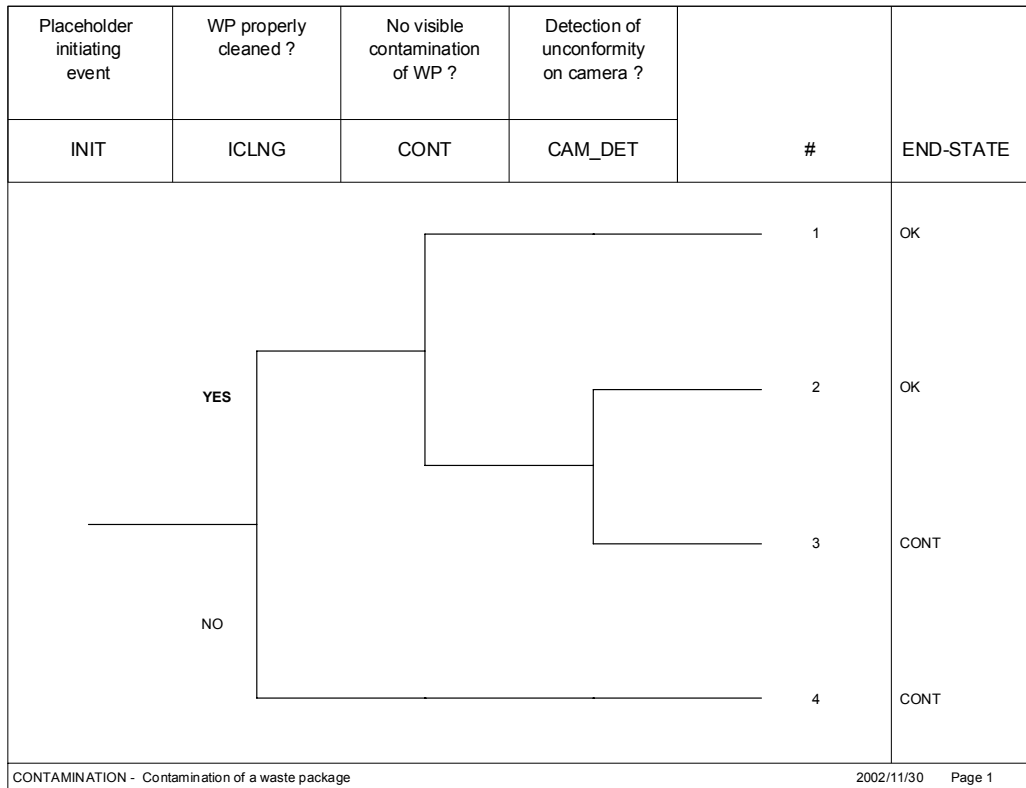


Figure 12. Event Tree for Contamination of the Waste Package

Notice that except for the basic events of the fault tree ICLNG mentioned previously, none of the other events need to be correlated together, because each of them represents a different type of failure.

The resulting mean, median, 5th percentile, and 95th percentile are 1.1×10^{-4} , 5.9×10^{-5} , 1.1×10^{-5} , and 3.6×10^{-4} per waste package, respectively.

6.2.7 Improper Handling

This section estimates the probability that a waste package is subjected to handling damage, without being detected, prior to its emplacement in the repository. Handling damage is defined as any visible gouging or denting of the waste package surface that may jeopardize the performance of the Alloy 22 barrier.

The evaluation of the probability of waste package damage by mishandling requires a set of assumptions in order to identify the main features that could lead to such an event. These are Assumptions 5.7.1 to 5.7.3.

The elementary probabilities of the events involved in waste package mishandling are as follows:

- The probability of damaging a waste package by mishandling is approximated by a lognormal distribution with a median of 4.8×10^{-5} per waste package handling and an

error factor of 10. Also, there are four potential occasions during which the waste package may be mishandled. This is based on Assumption 5.7.4.

- The probability that the operator fails to detect visible traces of damage during the final inspection of the waste package, performed remotely by camera, is estimated at 0.002 (median) with an error factor of 3. This is based on Item 5 of Table 4, which gives a probability value for a comparable event, namely the failure of an operator to check-read a display with difficult-to-see limit marks.

The previous information is used to develop an event tree for the damage of the waste package by mishandling. The software code SAPHIRE is used to perform this task, and the resulting event tree is shown on Figure 13. The electronic files of the SAPHIRE project are contained in Attachment II. Table 17 shows the events, along with their mean probability.

Notice that the probability of damaging the waste package by mishandling during at least one of the four potential occasions identified in Assumption 5.7.2 is quantified using a simple fault tree called MISH (given in Attachment II). The four basic events (each of them representing a potential occasion for mishandling) are connected through an OR logic gate. The mean probability is calculated using a Monte Carlo sampling with 90,000 realizations. The seed value (randomly chosen) is 49,107. It should be noted that the four basic events are correlated together, since their distribution is based on the same state of knowledge (see Section 6.2.4 for more information on correlation of nominally identical events). The mean probability of the fault tree MISH is shown on Table 17. It is given for information only because the real inputs that serve for the quantification of the event tree are the basic events on which the fault tree is developed.

The sequence of events that leads to waste package contamination end state on Figure 13 is labeled “MISH.”

Table 17. Description of Events for Damage of the Waste Package by Mishandling

Event Name	Event Description (Failure-Oriented)	Mean Probability
INIT	Placeholder initiating event	1 ^a
MISH	Damage to the waste package occurs by mishandling	1.9×10^{-4} ^b
CAM_DET	Operator fails to detect visible traces of waste package contamination during final inspection performed via remote camera	2.50×10^{-3}

NOTES: ^a This is a placeholder with a value of unity. It has no uncertainty.

^b Probability value is based on quantification of associated fault tree (given in Attachment II). Only two significant figures are shown.

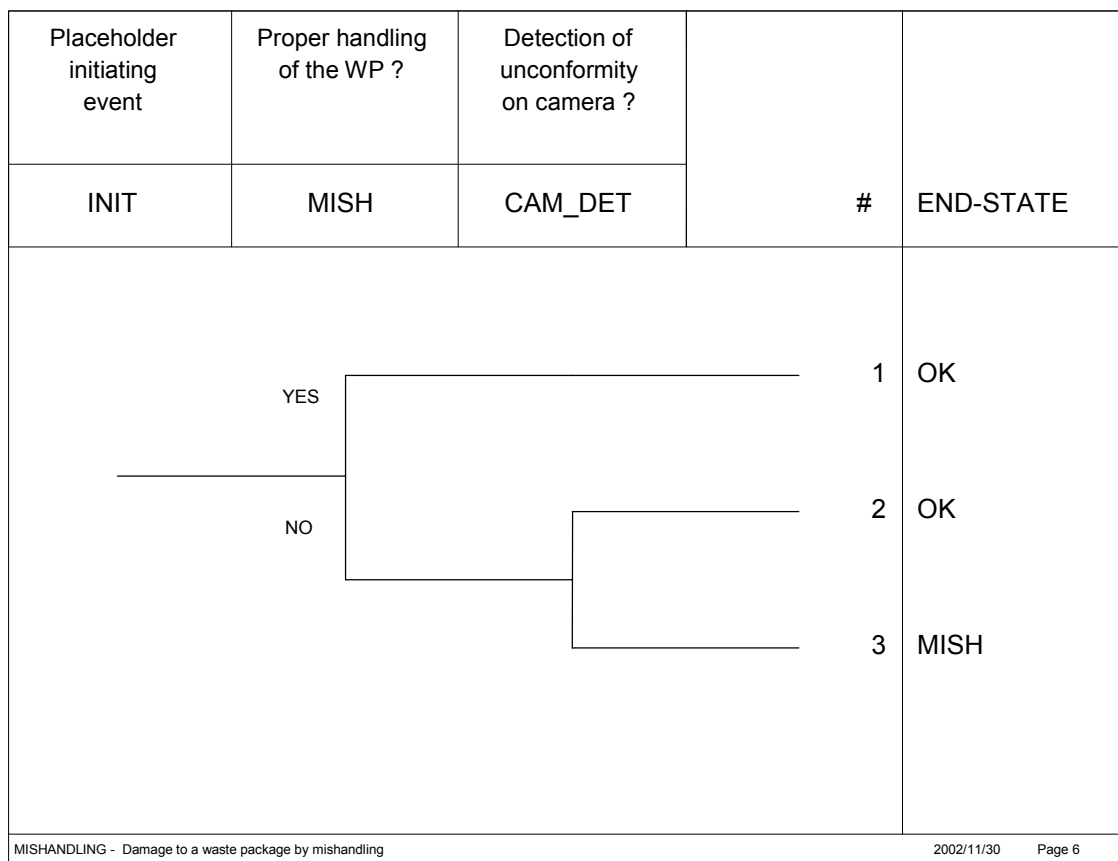


Figure 13. Event Tree for Damage to the Waste Package by Mishandling

A Monte Carlo sampling was performed with 90,000 realizations on the resultant events. Monte Carlo sampling is performed to propagate the variability of the events to obtain the characteristics of the resulting distribution. The seed value for the sampling (randomly chosen) is 59,027. The sample size is chosen large enough to get a good approximation on the main characteristics of the distribution.

Notice that except for the basic events of the fault tree MISH mentioned previously, none of the other events need to be correlated together because each of them represents a different type of failure.

The resulting mean, median, 5th percentile, and 95th percentile are 4.8×10^{-7} , 1.4×10^{-7} , 1.1×10^{-8} , and 1.8×10^{-6} per waste package, respectively.

In the discussion that follows, which will be used in Section 6.4.8, it is shown that the probability that a waste package is damaged by mishandling is independent of the fact that another waste package has already been damaged by mishandling. In other words, the fact that a waste package is damaged when handled does not increase the probability that the subsequent waste package to be processed will also be damaged through handling.

The rationale for this is based on the fact that the dominant cause for a damage to the waste package by mishandling is human error (see Assumption 5.7.4). The only reason, other than

coincidence, for two consecutive waste packages to be mishandled is that the operator makes the same mistake in handling the waste package. This situation is incompatible with the highly controlled operating conditions under which handling of the waste package will be performed. Indeed, handling operations will be governed by strict procedures and controls, developed to eliminate potentials for recurring handling errors. Such handling errors would denote a major flaw in handling operations that is not expected to pass the tight controls and reviews these handling operations will be subjected to. Furthermore, such a flaw would likely affect several waste packages in a row, and it is not credible that recurring damages to waste packages would go unnoticed.

Therefore, based on the previous information, occurrences of waste package damage by mishandling can be considered independent from each other.

6.2.8 Administrative Error Leading to Unanticipated Conditions

Administrative error leading to an unanticipated operating environment must be more specifically defined for a waste package so it can be evaluated. The types of administrative errors that could lead to unanticipated operating conditions are those that could affect the waste package surface temperature and humidity history and thus impact corrosion rates, result in placement in prohibited areas, or allow water to contact the waste package at times earlier than expected.

The temperature at the surface of the waste package is mainly governed by the temperature in the drift where the waste package is located rather than the heat output within the waste package. The reason for this is that the waste package is a metallic container with a rather large heat transfer area (see the dimensions of a typical waste package in Section 4.1.1). Therefore, the increase in heat output generated by a thermally overloaded waste package (which can be expected not to exceed a few kilowatts) would be quickly dissipated into the drift and is not expected to alter the waste package surface temperature to an extent significant enough to jeopardize its postclosure performance. The peak waste package temperature would envelope any variations in the waste package surface temperature due to thermal loading variations. Therefore this event will not be considered further.

Early water contact or early exposure to rockfall could result if human error during placement of the drip shield results in a gap between drip shield segments or if the drip shield fails early due to fabrication defects; this is investigated in Section 6.3.

6.3 MECHANISMS FOR EARLY DRIP SHIELD FAILURE

The approach followed to investigate the mechanisms that may lead to the early failure of the drip shield is based on what has been done for the waste package. Of the 12 types of defects that are identified in Section 6.2, four are not applicable (as discussed in Section 6.2), and only the following eight are considered applicable to the drip shield:

- Weld flaws
- Base metal flaws
- Improper weld material
- Improper base material

- Improper heat treatment
- Contaminants
- Handling or installation damage
- Administrative or operational error.

These defects are evaluated in the following subsections.

6.3.1 Weld Flaws

No detailed information on the density and size distribution of the flaws to be expected in titanium welds was found in the literature. That is why it is necessary to make an assumption on these distributions. Based on Assumption 5.8.1, the flaw density and size distributions in titanium welds are taken to be the same as those of Alloy 22 weld flaws. Also, based on Assumption 5.8.2, the welds of the drip shield will be UT inspected.

The previous assumptions make it possible to use the work performed in Section 6.2.1 to determine the characteristics of the flaws in titanium welds. Because there is no information yet on the precise geometry of the titanium welds, only preliminary estimates are made and a simplified approach is followed.

The flaw density and size distribution of the titanium weld flaws are taken to be the same as those of the 25-mm thick outer lid weld of the waste package. The reason for this choice is that this weld geometry has been the most extensively studied in this analysis. This information is used in Section 6.2.2 to evaluate the volumetric flaw density in base metal. After applying a correction factor of one-eighth, the volumetric flaw density in inspected base metal is approximately 21 flaws per cubic meter of metal. Removing this correction factor yields the volumetric density of flaws in the welds, which is therefore $21 \times 8 = 168$ flaws per cubic meter of weld.

Using the fact that there is approximately 110 kg of titanium welds in the drip shield (see Section 4.1.1) and that the density of titanium is about 4.51 g/cm^3 (see Section 4.1.1), the volume occupied by the welds is estimated at $2.44 \times 10^{-2} \text{ m}^3$. This yields an average of $168 \times 2.44 \times 10^{-2} = 4.1$ weld flaws in the drip shield.

Also, based on Table 13, the mean size of the flaws that remain in the welds after UT inspection is 1.3 mm. The 5th and the 95th percentiles are 0.099 and 2.8 mm, respectively. Notice that these values are governed by the UT PND curve rather than the geometry of the welds (see Section 6.2.1.3 for more information).

6.3.2 Base Metal Flaws

There are mainly two types of imperfections that might affect the base metal of the titanium drip shield: low-density and high-density inclusions (Graham 2002).

Low-density inclusions, also called hard-alpha defects, have been extensively studied, and information on their density and size distribution is presented in Section 4.1.4. Based on Assumption 5.9.1, this information is deemed adequate for characterizing the hard-alpha defects expected in the drip shield base metal.

High-density inclusions are typically tungsten carbide coming from tool bit or machining. Based on Assumption 5.9.2, the frequency of occurrence for these inclusions is taken to be the same as the frequency of occurrence of hard-alpha defects. Also, because these inclusions are usually quite small, on the order of 1 mm or less in spherical equivalent size (Graham 2002), it is conservative to consider that they have the same size distribution as the hard-alpha defects, which in comparison can reach several inches in length.

Table 8 gives a set of data points for the hard-alpha inclusion anomaly distribution curve to be used in this analysis. This anomaly distribution curve gives the expected number of hard-alpha defects per million pounds of titanium as a function of their size or, in terms of probability, the probability of having an inclusion of a given size or larger per million pounds of titanium, which is called the exceedance probability (FAA 2001, p. A3-1). To obtain the exceedance probability pertaining to a given size, the anomaly distribution curve is linearly interpolated on a log-log scale. It should also be noted that the hard-alpha defects are supposed to be spherically shaped and uniformly distributed throughout the part (see Section 4.1.4 for more information on characteristics of anomaly distribution curves).

Based on this information a Mathcad calculation, given in Attachment I, is performed to express the anomaly distribution curve in terms of the expected number of high-density and low-density inclusions in the drip shield as a function of the diameter of the defect in mm. The corresponding curve is shown on Figure 14. The total mass of the drip shield, 5000 kg, based on Table 3, is used to perform this calculation.

Table 18 shows the results for inclusions of size 0.5 mm and 1 mm. A Poisson distribution is used to make the calculation. The parameter of the Poisson distribution is the expected number of flaws of 0.5 mm or 1 mm expected in the drip shield (see Attachment I for details of the calculation).

Table 18. Probability of Having 0.5-mm or 1-mm Inclusions in the Drip Shield

Number of Flaws	0.5-mm Inclusion			1-mm Inclusion		
	0	1	2 or more	0	1	2 or more
Probability per drip shield	0.95	5.3×10^{-2}	1.5×10^{-3}	0.99	1.0×10^{-2}	5.4×10^{-5}

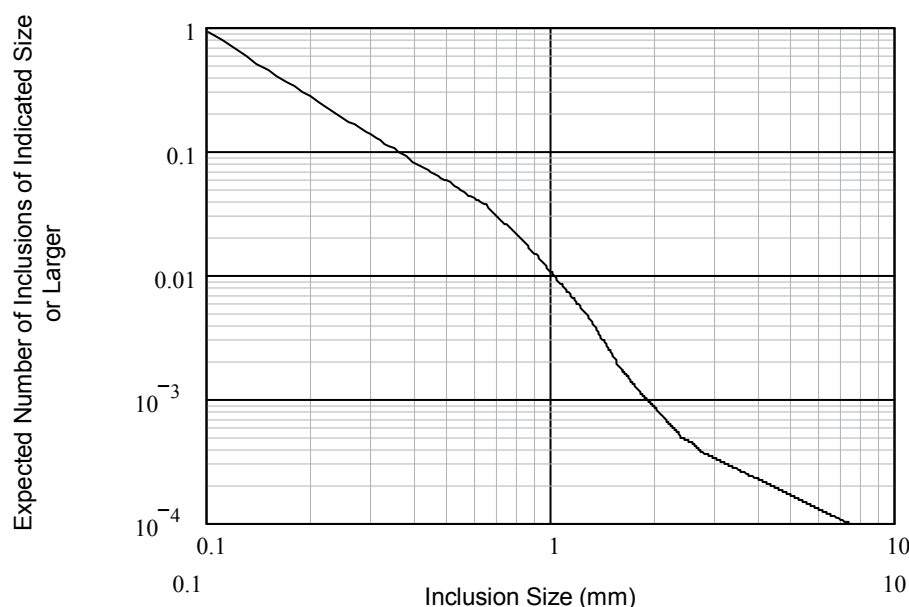


Figure 14. Anomaly Distribution Curve for Inclusions in the Drip Shield

A basic comparison of the frequency of occurrence of inclusions in base metal titanium with the frequency of occurrence of flaws due to improper repairs of the base metal is performed as follows.

The same approach as that of Section 6.2.2 is followed. In that section, it was assumed that the allowable surface of base metal Alloy 22 that could be repaired was 100 cm^2 . Keeping this surface and considering that the thickness of the titanium plates to be used in the drip shield is 15 mm (see Section 4.1.1), a work volume of $V_{bm} = 0.1 \times 0.1 \times 0.015 = 1.5 \times 10^{-4} \text{ m}^3$ is found. Then, using the same parameters F_{bm} and λ_{bm} as in Section 6.2.2, the mean number of flaws resulting from improper base metal repair is evaluated at: $F_{bm} \times \lambda_{bm} \times V_{bm} = 6.4 \times 10^{-6}$. A comparison to Figure 14 shows that the frequency of occurrence for this type of flaw is negligible compared to that of inclusions.

6.3.3 Improper Weld Material or Base Metal

The probability that improper weld material or base metal is used for the drip shield. The probability that this mistake goes unnoticed is evaluated in the same way as the probability of using improper weld material or base metal for the Alloy 22 barrier of the waste package analyzed in Section 6.2.3. Therefore, the assumptions used in that section also apply here.

The results are the same as those found in Section 6.2.3 (i.e., the median, the mean, and the error factor are 3.5×10^{-8} per drip shield, 5.0×10^{-8} per drip shield, and 4.0, respectively).

6.3.4 Improper Heat Treatment

The probability of an improper heat treatment of the drip shield that would go unnoticed is evaluated in the same way as the probability of improper heat treatment of the waste package analyzed in Section 6.2.4. Therefore, the assumptions used in that section also apply here.

The evaluation is performed by developing the same event tree as that which was used for the improper heat treatment of the waste package. The only difference is that only one heat treatment is performed for the drip shield and not two as for the waste package (one for the shell, one for the top lid). The event tree that is used for the evaluation can be found in the SAPHIRE files of Attachment II. It is not given here because it is the same as that shown on Figure 9.

A Monte Carlo sampling was performed with 90,000 realizations on the resultant events. Monte Carlo sampling is performed to propagate the variability of the events to obtain the characteristics of the resulting distribution. The seed value for the sampling (randomly chosen) is 59,027. The sample size is chosen large enough to get a good approximation on the main characteristics of the distribution.

Nominally identical events are correlated together prior to the uncertainty analysis.

The resulting mean, median, 5th percentile, and 95th percentile are 1.3×10^{-5} , 1.5×10^{-6} , 6.1×10^{-8} , and 5.3×10^{-5} per drip shield, respectively.

6.3.5 Contamination

The probability of a drip shield surface contamination that would remain unnoticed is evaluated in the same manner as the probability of contaminating the waste package analyzed in Section 6.2.6. The assumptions are very similar to what was done for the waste package and are given in Section 5.10. Notice that the inspection of the drip shield just before it leaves for the underground repository does not need to be performed remotely since the drip shield is not radioactive. Nevertheless, for the sake of simplicity and because it is conservative, the same HEP as for the remote inspection of the waste package is used.

The probabilities of the events leading to contamination of the drip shield are the same as those used for evaluating the probability of contaminating the waste package. The quantification is the same. As a consequence, the resulting probability is also the same. The mean, median, 5th percentile, and 95th percentile are 1.1×10^{-4} , 5.9×10^{-5} , 1.1×10^{-5} , and 3.6×10^{-4} per drip shield, respectively.

6.3.6 Improper Handling

The probability of a drip shield damage that would remain unnoticed is evaluated in the same way as the probability of damaging the waste package analyzed in Section 6.2.7. The assumptions are very similar to what was done for the waste package and are given in Section 5.11. Notice that the inspection of the drip shield just before it leaves for the underground repository does not need to be performed remotely, since the drip shield is not radioactive. Nevertheless, for the sake of simplicity and because it is conservative the same HEP as for the remote inspection of the waste package is used.

The probabilities of the events leading to damage of the drip shield by mishandling are the same as those used for evaluating the probability of damaging the waste package. As a consequence, the resulting probability is the same. The mean, median, 5th percentile, and 95th percentile are 4.8×10^{-7} , 1.4×10^{-7} , 1.1×10^{-8} , and 1.8×10^{-6} per drip shield, respectively.

6.3.7 Drip Shield Emplacement Error

This section estimates the probability that a drip shield is improperly emplaced in the repository, leaving a gap between adjacent drip shields. Note that such a gap would be small. Most likely it would not exceed the length of the connecting plates because otherwise it would leave a readily visible opening between the drip shields and it is not credible that such a gap would go unnoticed.

The evaluation requires making an assumption on the drip shield emplacement procedure given in Assumption 5.12.1.

The elementary probabilities of the events involved in drip shield emplacement error are as follows:

- The probability that the operator fails to properly interlock the drip shield to be emplaced with the adjacent drip shield is approximated by a lognormal distribution with a median of 0.003 and an error factor of 3. This is based on Item 7 of Table 4, which gives a probability value for a comparable event, namely the failure to correctly mate a connector.
- The probability that the verification that adjacent drip shields are correctly interlocked, performed remotely by camera, fails to detect a gap between the drip shields, is estimated at 0.002 (median) with an error factor of 3. This is based on Item 5 of Table 4, which gives a probability value for a comparable event, namely the failure of an operator to check-read a display with difficult-to-see limit marks.

The previous information is used to develop an event tree for drip shield emplacement error. The software code SAPHIRE is used to perform this task, and the resulting event tree is shown on Figure 15. The electronic files of the SAPHIRE project are contained in Attachment II. Table 19 shows the events along with their mean probability. Note that the means are calculated based on the median and the error factor using Equation 36.

Table 19. Description of Events for Drip Shield Emplacement Error

Event Name	Event Description (Failure-Oriented)	Mean Probability
INIT	Placeholder initiating event	1 ^a
DS_INTRLCK	Failure to properly interlock adjacent drip shields	3.75×10^{-3}
CAM_DET	Operator fails to detect gap between two improperly interlocked drip shields	2.50×10^{-3}

NOTE: ^a This is a placeholder with a value of unity. It has no uncertainty.

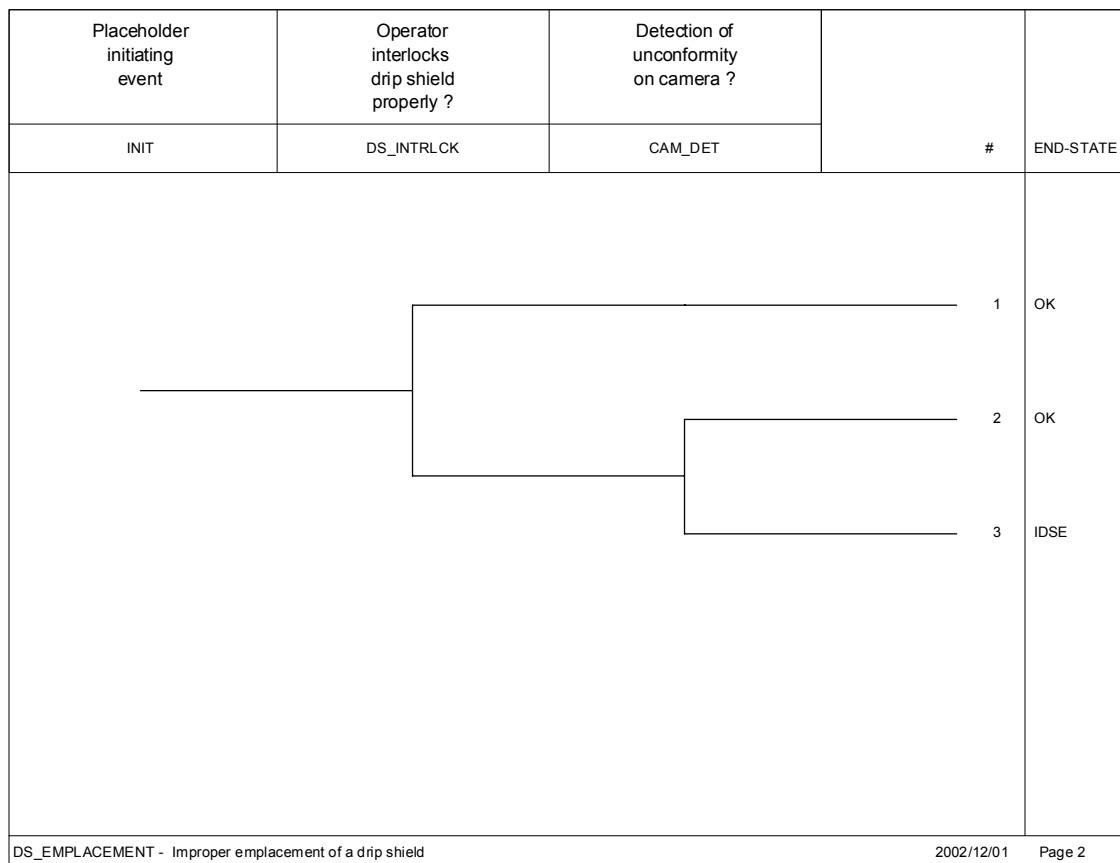


Figure 15. Event Tree for Drip Shield Emplacement Error

The sequence of events that leads to an emplacement error end state on Figure 15 is labeled “IDSE.”

There is no need to perform a Monte Carlo sampling to obtain the characteristics of the distribution pertaining to drip shield emplacement error. This is because the sequence of events is the product of lognormal distribution and therefore is also a lognormal distribution. Application of Equations 37 and 38 yields a median of 6.0×10^{-6} per drip shield and an error factor of 4.7. The mean is calculated with Equation 36 and is 9.3×10^{-6} per drip shield. The 5th (respectively 95th) percentile is obtained by dividing (respectively multiplying) the median by the error factor and is therefore 1.3×10^{-6} (respectively 2.8×10^{-5}) per drip shield.

6.4 CONSEQUENCES OF THE OCCURRENCE OF DEFECTS ON WASTE PACKAGE OR DRIP SHIELD

The investigations described in Sections 6.2 and 6.3 have identified several types of defects that are applicable to the waste package or the drip shield and which also have a probability greater than the threshold given in Section 4.2. These types of defects are weld flaws, base metal flaws, improper weld material, improper heat treatment, improper laser peening, contamination, improper handling, and administrative error leading to unanticipated conditions (reduced down to drip shield emplacement error).

The purpose of this section is to identify the consequences of the occurrence of such defects. Some defect types have negligible consequences while some other defect types may lead to stress corrosion cracking, localized corrosion, formation of grain-boundary precipitates, etc. It is beyond the scope of this analysis to investigate the impacts of these latter phenomena on waste package or drip shield performance. This will be carried out elsewhere.

6.4.1 Consequences of Weld Flaws or Base Metal Flaws

Any outer-surface-breaking flaws in combination with the presence of an aggressive environment and sufficiently high residual stresses from the weld could potentially lead to stress corrosion cracking.

Another possible consequence of surface breaking flaws of any size is their growth by other corrosion processes.

6.4.2 Consequences of Improper Weld Material or Base Metal

In the case of the improper weld material used in the reactor vessel weld discussed in Section 6.2.3, the substituted material had a composition that was only slightly different from the specified material, and further impact on performance was to be minimal. However, Section 6.1.1 indicates that there have been pressure-vessel failures associated with the use of incorrect weld material, although it is not stated whether the specified material was incorrect or the material used was not that which was specified. Due to the strict controls that will govern the fabrication of the waste package and the drip shield, it is expected that the material composition of improper weld material or base metal would only differ slightly from the material composition of Alloy 22 or Titanium Grade 7.

In view of the high corrosion resistance of the materials the consequences of the use of such improper material is expected to be insignificant.

6.4.3 Consequences of Improper Heat Treatment

While the likelihood of improper heat treatment is small, the consequences of improper heat treatment can be significant. Improper rate of cooling of alloys such as Alloy 22 may result in the precipitation of carbides and intermetallic compounds along the grain boundaries. This in turn enhances the susceptibility of the material to localized corrosion. Formation of grain-boundary precipitates also enhances the susceptibility of the material to stress corrosion cracking. As a result of these competing effects, identification of a single and specific mechanism of degradation is not possible. These effects are applicable to the waste package Alloy 22 outer barrier and outer barrier lids (i.e., the outer lid and the middle lid).

Concerning the drip shield, improper heat treatment could lead to susceptibility to stress corrosion cracking.

6.4.4 Consequences of Improper Laser Peening

Consequences of improper laser peening for stress mitigation may lead to the introduction of unacceptable amounts of cold work in the material and increased susceptibility to stress corrosion cracking.

6.4.5 Consequences of Contamination

The consequence of a contamination of the surface of the waste package or the drip shield is not expected to be significant from the corrosion standpoint. The waste package outer barrier is made of highly corrosion-resistant material over a wide range of chemical conditions. This is supported by the results from the ongoing long-term corrosion tests in environments with 1,000 times the concentrations of various adverse chemical species that may be expected in the repository. The test environments include significantly high chloride concentrations (approximately 7,000 ppm) and acidic conditions (pH of 2.7) compared to the potential contamination and do not exhibit increased corrosion rates (BSC 2003h, Section 6.9.1).

The same conclusion is reached with Titanium Grade 7 of the drip shield. Tests on Titanium Grade 16 (an analog of Grade 7) performed in the same environments as those mentioned previously, have not shown increased corrosion rates (BSC 2003g, Table 6 and Section 8).

6.4.6 Consequences of Damage by Mishandling

Gouges on the waste package outer surface may provide sites for stress corrosion cracks of Alloy 22 if the resulting stress profiles are conducive to the initiation and propagation of stress corrosion cracking.

Concerning the drip shield, damage by mishandling could also cause increased susceptibility to stress corrosion cracking.

6.4.7 Consequences of Drip Shield Emplacement Error

As noted in Section 6.3.7, the gap between two adjacent drip shields improperly interlocked is expected to be small. It is not credible that the inspection performed on camera would not detect an incorrect emplacement leaving a gap exceeding the length of the connecting plates of the drip shields. That is why dripping water from the drift is not expected to fall directly onto the underlying waste package but will most likely hit the connecting plate first, which will divert it from the waste package surface.

6.4.8 Summary and Discussion

In light of the high corrosion resistance of Alloy 22 and Titanium Grade 7 under expected repository conditions, two types of defects can be discarded from further consideration. These are improper weld material or base metal and surface contamination (see Sections 6.4.2 and 6.4.5).

Another type of defect that is not expected to affect the performance of the waste package is the drip shield emplacement error. As mentioned in Section 6.4.7, this defect is credible only for

small gaps, which will not allow for water dripping onto the waste package. Therefore, this type of defect is discarded from further consideration.

Some other types of defects appear to be similar. This is the case of waste package weld flaws and base metal flaws. The frequency of occurrence of base metal flaws is much lower than that of the weld flaws. Based on the results of Section 6.2.2, the probability of having at least one flaw is 1.0×10^{-5} per waste package in the base metal. In comparison, this probability is $1 - 0.80 = 0.20$ for the outer lid weld and $1 - 0.77 = 0.23$ for the middle lid weld, after UT inspection (see Table 13). Also, the discussion in Section 6.2.1.3 shows that the probability of occurrence for flaws in the seam welds of the waste package given in Table 13 is very conservative. Therefore, these flaws appear to be negligible compared to the flaws in the closure welds of the waste package (namely, the outer lid weld and the middle lid weld). As a consequence, the base metal flaws and the seam weld flaws of the waste package can be discarded from further consideration. Only the flaws in the closure welds are recommended to be investigated in further analyses.

Improper heat treatment, improper laser peening, or mishandling of the waste package might have adverse consequences on waste package performance, as noted in Sections 6.4.3, 6.4.4, and 6.4.6. A potential consequence common to the three types of defect is increased susceptibility to stress corrosion cracking. An evaluation is performed in SAPHIRE to quantify the probability that a waste package is affected by at least one of the previous defect types. To do this, duplicates of the event trees shown on Figures 9, 10, 11, and 13 are created in SAPHIRE, and the end state of the sequences of events resulting in a defective waste package are labeled “DMWP.” Also, nominally identical events are correlated together (see Section 6.2.4 for more information on correlation of nominally identical events). Note that these events are those which have the same correlation class in Tables 14 and 15. The electronic files of the SAPHIRE files are contained in Attachment II.

A Monte Carlo sampling was performed with 90,000 realizations on the resultant events. Monte Carlo sampling is performed to propagate the variability of the events to obtain the characteristics of the resulting distribution. The seed value for the sampling (randomly chosen) is 59,027. The sample size is chosen large enough to get a good approximation on the main characteristics of the distribution.

The resulting mean, median, 5th percentile, and 95th percentile are 2.8×10^{-5} , 3.7×10^{-6} , 2.9×10^{-7} , and 1.1×10^{-4} per waste package, respectively. The maximum value yielded by the Monte Carlo sampling is 7.44213×10^{-3} .

To make these results more tractable, they are fit to a lognormal distribution. This fit is supported by the fact that the basic events involved in the sequences leading to a defective waste package are lognormal, and that the sum and product of lognormal distributions is approximately lognormal (Swain and Guttman 1983, pp. A-4 to A-6). In order to keep the most significant and conservative characteristics of the uncertainty analysis performed previously, a lognormal distribution that approximates the mean and the 95th percentile calculated by Monte Carlo sampling is determined.

To do this, the following approach is used. Equations 36 and 43 are utilized to determine the characteristics of the lognormal distribution. They form a system of equations in which m , m_{95} , and EF (the mean, the 95th percentile, and the error factor of the lognormal distribution, respectively) are variables. Since m and m_{95} are already known from the Monte Carlo sampling, it is possible to combine Equations 36 and 43 together, in order to form a new equation in which EF is the only variable. This equation is as follows:

$$m_{95} - m \cdot EF \cdot \exp\left[-\frac{1}{2} \cdot \left(\frac{\ln(EF)}{1.645}\right)^2\right] = 0 \quad (\text{Eq. 44})$$

Calculations performed using Mathcad (see Attachment I) show that Equation 44 has no exact solution. Nevertheless, the function on the left side of the equation is shown to reach a minimum for a value of EF approximately equal to 15. This value is chosen for the fitting lognormal distribution.

Therefore, the probability of a defective waste package due to improper heat treatment, improper laser peening, or mishandling is evaluated by a lognormal distribution with a mean of 2.8×10^{-5} per waste package and an error factor of 15. Notice that this distribution has a median of 7.2×10^{-6} , a 5th percentile of 4.8×10^{-7} , and a 95th percentile of 1.1×10^{-4} per waste package, respectively. When comparing to the results of the Monte Carlo sampling, these results appear to be conservative.

The fact that the lognormal distribution is defined for all positive numbers leads to excessively conservative probability estimates when the upper percentiles of the distribution are calculated. That is why the lognormal distribution has been truncated. In other words, it is considered that the probability of having a defective waste package due to improper heat treatment, improper laser peening, or mishandling, will not exceed a certain maximum value. This value is selected as the maximum value of the Monte Carlo simulations, and is equal to 7.44213×10^{-3} . This corresponds to the 99.999th percentile of the lognormal distribution. Thus, only a tiny portion of the original lognormal distribution is eliminated. This ensures that the resulting truncated distribution will provide adequate estimates of the probability of having a defective waste package and will prevent unrealistic upper percentiles from being considered.

Based on the discussions in Sections 6.2.4, 6.2.5, and 6.2.7, occurrences of improper waste package heat treatment, laser peening, or damage by mishandling can be considered as independent from each other. In other words, the global probability calculated previously is given for each waste package individually and the fact that one waste package is affected by one of the defect types mentioned previously will not increase the probability that another waste package is affected by the same type of defect.

As a consequence, the probability on the number of waste packages that are affected by improper heat treatment, improper laser peening, or damage by mishandling, and subsequently emplaced in the repository, can be evaluated using a Poisson distribution. The parameter of the Poisson distribution is calculated as the product of the probability of having a waste package affected with improper heat treatment, improper laser peening, or damage by mishandling (estimated

previously and fitted to a lognormal distribution) and the number of waste packages to be emplaced in the repository.

It is important to note that the main contributor to the probability distribution obtained previously is the improper heat treatment of the waste package. Additionally, any consequences of improper laser peening or damage by mishandling are considered subsumed by the consequences of improper heat treatment. Although the welding and laser peening of the weld of the outer lid will negate any adverse fabrication heat treatment effects, the region in which these effects is negated is considered small. Therefore, it is conservative to subsume the effects of improper laser peening into the consequences of an improper heat treatment. Damage by mishandling can occur at any point on the surface of the waste package and it is therefore appropriate to subsume its consequences into those of an improper heat treatment.

As previously mentioned in Section 6.4.3, improper heat treatment may enhance susceptibility to stress corrosion cracking, but might also lead to the formation of grain-boundary precipitates. In fact, identification of a single and specific mechanism of degradation is not possible. Therefore, the following recommendations are made for evaluating the consequences of improper heat treatment of the Alloy 22 waste package outer barrier components.

- A failure of the waste package outer barrier shell and outer barrier lids should be assumed.
- The affected waste packages should be assumed to fail immediately upon initiation of degradation processes.
- The entire waste package outer barrier surface area should be considered affected by improper heat treatment.
- The materials of the entire affected area should be assumed lost upon failure of the waste packages because the affected area will be subjected to stress corrosion cracking and highly enhanced localized and general corrosion.

These recommendations are conservative but appropriate for their intended purpose and represent the worst case degradation rate.

It should be noted that a grouping of defect types similar to what was done previously for the waste package could be also done for the drip shield. For example, improper heat treatment and damage by mishandling have both in common to potentially result in increased susceptibility to stress corrosion cracking. The situation is also the same for weld flaws and base metal flaws, which are very similar types of defects. However, in this analysis, more emphasis is put on the defect types of the waste package than on the defect types of the drip shield. That is why groupings of the defect types that might affect the drip shield have not been performed nor has a fitting of the probabilities of occurrence of such defects to a distribution.

6.5 FEATURES, EVENTS, AND PROCESSES INCLUDED IN MODEL

The development of a comprehensive list of FEPs potentially relevant to postclosure performance of a repository at Yucca Mountain is an ongoing, iterative process based on site-

specific information, design, and regulations. The approach for developing an initial list was documented in *The Development of Information Catalogued in REV00 of the YMP FEP Database* (Freeze et al. 2001). To support the TSPA-LA model, the FEP list (DTN: MO0407SEPFEPLA.000) was re-evaluated in accordance with *The Enhanced Plan for Features, Events, and Processes (FEPs) at Yucca Mountain* (BSC 2002, Section 3.2). Table 20 provides a list of FEPs that are included in the TSPA-LA models described in this calculation, and provides specific references to sections within this document. Table 21 provides a list of the FEPs that have been excluded. The summary of the disposition and the details of the exclusion of these FEPs are documented in *FEPs Screening of Processes and Issues in Drip Shield and Waste Package Degradation* (BSC 2004b).

Table 20. Features, Events, and Processes Included (Screened In) in TSPA-LA and Addressed in this Report

FEP No.	FEP Name	Sections Where Disposition is Described
2.1.03.08.0A	Early Failure of Waste Package	Section 6.2

Table 21. Features, Events, and Processes Excluded (Screened Out) in this Report

FEP No.	FEP Name	Sections Where Disposition is Described
2.1.03.08.0B	Early Failure of Drip Shield	Section 6.3
1.1.08.00.0A	Inadequate Quality Control and Deviations from Design	Section 6.4

7. CONCLUSIONS

The first part of this analysis (Section 6.1) performed a review of available literature on defect-related early failures of welded metallic components. Types of components examined included boilers and pressure vessels, nuclear fuel rods, underground storage tanks, radioactive-cesium capsules, and dry-storage casks for spent nuclear fuel. The fractions of the total populations that failed due to defect-related causes during the intended lifetime of the components were generally in the range of 10^{-3} to 10^{-6} per container. In most cases, defects that led to failure of the component required an additional stimulus to cause failure (i.e., the component was not failed when it was placed into service). In fact, there were several examples that indicated that even commercial standards of quality control could reduce the rate of initially failed components well below 10^{-4} per container.

Twelve generic types of defects that could cause early failures in the components examined were identified. These are weld flaws, base metal flaws, improper weld material, improper base metal, improper heat treatment, improper weld flux material, poor weld joint design, contaminants, mislocated welds, missing welds, handling or installation damage, and an administrative error resulting in an unanticipated environment. However, the duration of time required for a defect of a given type and severity to lead to failure is highly dependent on the service conditions to which the component is subjected. As a result, there is insufficient information available in the literature to defensibly relate the cumulative effect of the environment, or stresses to which the examined components were subjected, to the waste package or drip shield. In addition, factors such as the differing degrees of inspection and the

extent to which different materials are affected by a given type of defect make direct extrapolations of defect-related failure rates indefensible. Accordingly, the information on the fraction of components that experienced defect-related failure during the components intended lifetime were not directly applied to waste packages or drip shields. However, information on the frequency of occurrence of particular types of defects was used in the estimate of waste package-defect occurrence rate in some cases.

The second part of the analysis (Section 6.2) focused on estimating the probability that specific defect types will occur on the outer barrier of the waste package despite a set of quality controls designed to prevent their occurrence. This was done for eight of the 12 generic defect types identified in the literature review. The remaining four defect types (improper weld flux, missing welds, mislocated welds, and poor joint design) were judged to be inapplicable to waste packages (see Section 6.2 for details) or estimated to have a sufficiently low probability such that they could be considered incredible. Note that a defect type specific to the outer lid weld of the waste package was also analyzed, namely, improper laser peening of the weld. Also, only one type of administrative error leading to unanticipated conditions was shown to require further consideration, namely, the emplacement error of the drip shield, treated in Section 6.3.

The third part of the analysis (Section 6.3) focused on the defects that could affect the drip shield, based on the investigations of Sections 6.1 and 6.2. The defects analyzed were weld flaws, base metal flaws, improper weld material, improper base metal, improper heat treatment, contamination, damage by mishandling, and an emplacement error.

The fourth part of the analysis (Section 6.4) investigated the consequences of the defect types analyzed in Sections 6.2 and 6.3. Some defect types have been identified to have negligible consequences on the performance of the waste package or the drip shield (i.e., improper weld and base metal materials, contamination, and drip shield emplacement error). The other defect types have been identified to potentially increase susceptibility to stress corrosion cracking, localized corrosion, etc.

For the waste package, these latter defect types are as follows:

- Flaws in the closure welds of the waste package, namely the outer lid weld and the middle lid weld.
- Improper heat treatment, improper laser peening, and mishandling of the waste package. These types of defects were grouped together because they all share the same consequence of increasing the susceptibility of the waste package to stress corrosion cracking. It should be noted that among these three types of defects, the improper heat treatment is, by far, the dominant one in terms of probability. Also, since an improperly heat-treated waste package might be susceptible to increased aging and phase instability, it is not possible to identify a single and specific mechanism of degradation. That is why recommendations are made for evaluating the consequences of improper heat treatment of the Alloy 22 waste package outer barrier (see Section 6.4.8).

For the drip shield, the defect types that might increase susceptibility to stress corrosion cracking or localized corrosion are as follows:

- Weld flaws
- Base metal flaws
- Improper heat treatment
- Damage by mishandling.

Table 22 summarizes the main results pertaining to the defect types to consider in assessing waste package and drip shield performance. Note that these results are suitable for their intended use and that they are reasonable compared to the inputs.

As a final note, it is important to remember that a waste package or drip shield with one of the types of defects shown in Table 22 is not due to fail at emplacement. Failure of the waste package (drip shield) will only occur after degradation processes take place, which may happen hundreds of years after emplacement. Also, even if a waste package were to be affected by an early failure, its radionuclide inventory may not necessarily be available for transport. This is because most through-wall penetrations, especially cracks from stress corrosion cracking, are usually of limited length and thickness.

Table 22. Defect Types to Consider in Assessing Waste Package and Drip Shield Performance

Waste Package Defect Type	Evaluation of Probability per Waste Package	Comment
Weld flaws	See Table 11 to Table 13	Consider only closure welds
Improper heat treatment grouped with improper laser peening and waste package damaged by mishandling	Lognormal distribution: Median = 7.2×10^{-6} per waste package Mean = 2.8×10^{-5} per waste package Error factor = 15 Upper truncation value = 7.44213×10^{-3} per waste package	See recommendations in Section 6.4.8. Use a Poisson distribution for the probability on the number of waste packages affected (parameter of the Poisson distribution is the product of probability on the left and number of waste packages in the repository)
Drip Shield Defect Type	Main Characteristics	Comment
Weld flaws	Mean number of flaws: 4.1 per drip shield Mean size of flaw: 1.3 mm	See Section 6.3.1
Base metal flaws	See Table 18	See Section 6.3.2
Improper heat treatment	Mean probability: 1.3×10^{-5} per drip shield	See Section 6.3.4
Damage by mishandling	Mean probability: 4.8×10^{-7} per drip shield	See Section 6.3.6

This analysis contains two attachments:

- ATTACHMENT I contains a paper copy of the Mathcad calculations performed in this analysis.
- ATTACHMENT II is a CD-ROM containing the files developed for the Mathcad calculations of ATTACHMENT I and the SAPHIRE evaluations.

Table 23. CD-ROM Directory Listing

File Name	Date	Time	Size (bytes)
Early Failure Mathcad File.mcd	09/02/2003	04:38p	213,444
Early Failure SAPHIRE.zip	02/24/2003	09:07a	73,985

8. INPUTS AND REFERENCES

8.1 DOCUMENTS CITED

ANS (American Nuclear Society) 1999. "World List of Nuclear Power Plants." *Nuclear News*, 42, (3), 52-56. La Grange Park, Illinois: American Nuclear Society. TIC: 244680.

ASM International 1990a. *Properties and Selection: Nonferrous Alloys and Special-Purpose Materials*. Volume 2 of *ASM Handbook*. Formerly 10th Edition, Metals Handbook. 5th Printing 1998. Materials Park, Ohio: ASM International. TIC: 241059.

ASM International 1990b. *Properties and Selection: Irons, Steels, and High-Performance Alloys*. Volume 1 of *Metals Handbook*. 10th Edition. Materials Park, Ohio: ASM International. TIC: 245666.

ASM International 1993. *Welding, Brazing, and Soldering*. Volume 6 of *ASM Handbook*. Materials Park, Ohio: ASM International. TIC: 10199.

ASM International 2001. "2002 Thermal Source Book with Buyer's Guide." *Heat Treating Progress*, 1, (7), 89-107. Materials Park, Ohio: ASM International. TIC: 253418.

Apostolakis, G. and Kaplan, S. 1981. "Pitfalls in Risk Calculations." *Reliability Engineering*, 2, 135-145. Barking, England: Applied Science Publishers. TIC: 253648.

Babcock & Wilcox 1970a. *Analysis and Resolution of Dye-Penetrant Indications in AISI-304 Alloy Cladding of Reactor Coolant System Elbows*. BAW-1364. Barberton, Ohio: Babcock & Wilcox. TIC: 245526.

Babcock & Wilcox 1970b. *Analysis and Resolution of Dye-Penetrant Indications in Submerged Arc Weld Cladding of Reactor Coolant System Straight Piping*. BAW-1363. Barberton, Ohio: Babcock & Wilcox. TIC: 245525.

Babcock & Wilcox 1979. *Records Investigation Report Related to Off-Chemistry Welds in Material Surveillance Specimens and Response to IE Bulletins 78-12 and 78-12A - Supplement*. Mt. Vernon, Indiana: Babcock & Wilcox. TIC: 244621.

BSC 2001a. *Repository Design, Waste Package, Project 21-PWR Waste Package with Absorber Plates, Sheet 1 of 3, Sheet 2 of 3, and Sheet 3 of 3*. DWG-UDC-ME-000001 REV A. Las Vegas, Nevada: Bechtel SAIC Company. ACC: MOL.20020102.0174.

BSC 2001b. *Waste Package Misload Probability*. CAL-WHS-MD-000001 REV 00. Las Vegas, Nevada: Bechtel SAIC Company. ACC: MOL.20011212.0186.

BSC 2002. *The Enhanced Plan for Features, Events, and Processes (FEPs) at Yucca Mountain*. TDR-WIS-PA-000005 REV 00. Las Vegas, Nevada: Bechtel SAIC Company. ACC: MOL.20020417.0385.

BSC 2003a. *Repository Design Project, RDP/PA IED Typical Waste Package Components Assembly (2)*. 800-IED-WIS0-00202-000-00A. Las Vegas, Nevada: Bechtel SAIC Company. ACC: ENG.20030702.0002.

BSC 2003b. *Repository Design Project, Repository/PA IED Interlocking Drip Shield and Emplacement Pallet*. 800-IED-WIS0-00401-000-00A. Las Vegas, Nevada: Bechtel SAIC Company. ACC: ENG.20030730.0004.

BSC 2003c. *Design and Engineering, D&E/PA/C IED Typical Waste Package Components Assembly 1 of 9*. 800-IED-WIS0-00201-000-00C. Las Vegas, Nevada: Bechtel SAIC Company. ACC: ENG.20030917.0002.

BSC 2003d. *Repository Design Project, RDP/PA IED Typical Waste Package Component Assembly (6)*. 800-IED-WIS0-00206-000-00A. Las Vegas, Nevada: Bechtel SAIC Company. ACC: ENG.20030707.0002.

BSC 2003e. *Stress Corrosion Cracking of the Drip Shield, the Waste Package Outer Barrier, and the Stainless Steel Structural Material*. ANL-EBS-MD-000005 REV 01 ICN 00. Las Vegas, Nevada: Bechtel SAIC Company. ACC: DOC.20030717.0001.

BSC 2003f. *21-PWR UCF Prototype Fabrication Specification*. 000-3SS-DSU0-00300-000-00A. Las Vegas, Nevada: Bechtel SAIC Company. ACC: ENG.20030804.0001.

BSC 2003g. *General Corrosion and Localized Corrosion of the Drip Shield*. ANL-EBS-MD-000004 REV 01. Las Vegas, Nevada: Bechtel SAIC Company. ACC: DOC.20030626.0001.

BSC 2003h. *General Corrosion and Localized Corrosion of Waste Package Outer Barrier*. ANL-EBS-MD-000003 REV 01. Las Vegas, Nevada: Bechtel SAIC Company. ACC: DOC.20030916.0010.

BSC 2004a. *Technical Work Plan for: Regulatory Integration Modeling and Analysis of the Waste Form and Waste Package*. TWP-WIS-MD-000009 REV 00. Las Vegas, Nevada: Bechtel SAIC Company. ACC: DOC.20040616.0006.

BSC 2004b. *FEPs Screening of Processes and Issues in Drip Shield and Waste Package Degradation*. ANL-EBS-PA-000002 REV 03. Las Vegas, Nevada: Bechtel SAIC Company.

Bush, S.H. 1983. *Reliability of Nondestructive Examination*. NUREG/CR-3110. Volume 3. Washington, D.C.: U.S. Nuclear Regulatory Commission. TIC: 218323.

CRWMS M&O 2000. *Analysis of Mechanisms for Early Waste Package Failure*. ANL-EBS-MD-000023 REV 02. Las Vegas, Nevada: CRWMS M&O. ACC: MOL.20001011.0196.

D'Agostino, R.B. and Stephens, M.A., eds. 1986. *Goodness-Of-Fit Techniques*. Statistics, Textbooks and Monographs Volume 68. New York, New York: Marcel Dekker. TIC: 253256.

DOE (U.S. Department of Energy) 2004. *Quality Assurance Requirements and Description*. DOE/RW-0333P, Rev. 16. Washington, D.C.: U.S. Department of Energy, Office of Civilian Radioactive Waste Management. ACC: DOC.20040823.0004.

Doubt, G. 1984. *Assessing Reliability and Useful Life of Containers for Disposal of Irradiated Fuel Waste*. AECL-8328. Chalk River, Ontario, Canada: Atomic Energy of Canada Limited. TIC: 227332.

Eide, S.A. and Calley, M.B. 1993. "Generic Component Failure Data Base." *PSA '93, Proceedings of the International Topical Meeting on Probabilistic Safety Assessment, Clearwater Beach, Florida, January 26-29, 1993*. 2, 1175-1182. La Grange Park, Illinois: American Nuclear Society. TIC: 247455.

EPA (U.S. Environmental Protection Agency) 1987a. *Causes of Release from UST Systems*. EPA 510-R-92-702. Washington, D.C.: Environmental Protection Agency. TIC: 244679.

EPA 1987b. *Causes of Release from UST Systems: Attachments*. EPA 510-R-92-703. Washington, D.C.: Environmental Protection Agency. TIC: 244678.

EPRI (Electric Power Research Institute) 1997. *The Technical Basis for the Classification of Failed Fuel in the Back-End of the Fuel Cycle*. EPRI TR-108237. Palo Alto, California: Electric Power Research Institute. TIC: 236839.

FAA (Federal Aviation Administration) 2001. *Damage Tolerance for High Energy Turbine Engine Rotors*. Advisory Circular AC 33.14-1. Washington, D.C.: U.S. Department of Transportation, Federal Aviation Administration. TIC: 253277.

Framatome Cogema Fuels. 1996. *Fuel Integrity*. Proprietary 12-1244558-00. Lynchburg, Virginia: Framatome Cogema Fuels. ACC: MOL.19990930.0110.

Freeze, G.A.; Brodsky, N.S.; and Swift, P.N. 2001. *The Development of Information Catalogued in REV00 of the YMP FEP Database*. TDR-WIS-MD-000003 REV 00 ICN 01. Las Vegas, Nevada: Bechtel SAIC Company. ACC: MOL.20010301.0237.

Graham, R. 2002. "Re: Information Request on Commercially Pure Titanium." E-mail from R. Graham (Wah Chang) to P. Macheret, January 18, 2002. ACC: MOL.20021217.0020.

Grainawi, L. 1999. "Manufacturing Defects." Memo from L. Grainawi (Steel Tank Institute) to J. Massari (Framatome Technologies), April 20, 1999. TIC: 244544.

Heasler, P.G. and Doctor, S.R. 1996. *Piping Inspection Round Robin*. NUREG/CR-5068. Washington, D.C.: U.S. Nuclear Regulatory Commission. TIC: 244618.

Hua, F.; Sarver, J.; Jevic, J.; and Gordon, G. 2002. "General Corrosion Studies of Candidate Container Materials in Environments Relevant to Nuclear Waste Repository." *Corrosion/2002, 57th Annual Conference & Exposition, April 7-11, 2002, Denver, Colorado*. Paper No. 02530. Houston, Texas: NACE International. TIC: 252067.

Hodges, M.W. 1998. "Confirmatory Action Letter 97-7-001, Technical Evaluation, Docket No: 72-1007." Washington, D.C.: U.S. Nuclear Regulatory Commission. Accessed November 2, 1999. TIC: 244630. <http://www.nrc.gov/OPA/reports/sn072298.htm>

Ikeda, B.M. and Shoesmith, D.W. 1997. *Industrial Experience with Titanium*. AECL-11750. Pinawa, Manitoba, Canada: Whiteshell Laboratories. TIC: 235003.

Khaleel, M.A.; Chapman, O.J.V.; Harris, D.O.; and Simonen, F.A. 1999. "Flaw Size Distribution and Flaw Existence Frequencies in Nuclear Piping." *Probabilistic and Environmental Aspects of Fracture and Fatigue: The 1999 ASME Pressure Vessels and Piping Conference*. PVP-386. Pages 127-144. New York, New York: American Society of Mechanical Engineers. TIC: 245621.

Martz, H.F. and Waller, R.A. 1991. *Bayesian Reliability Analysis*. Malabar, Florida: Krieger Publishing Company. TIC: 252996.

Modarres, M. 1993. *What Every Engineer Should Know About Reliability and Risk Analysis*. New York, New York: Marcel Dekker. TIC: 238168.

NBBPVI (National Board of Boiler and Pressure Vessel Inspectors) 1999. "Incident Reports." Columbus, Ohio: National Board of Boiler and Pressure Vessel Inspectors. Accessed September 29, 1999. TIC: 245629. <http://www.nationalboard.com/incidents.html>

NRC (U.S. Nuclear Regulatory Commission) 1975. *Reactor Safety Study: An Assessment of Accident Risks in U.S. Commercial Nuclear Power Plants*. WASH-1400. Washington, D.C.: U.S. Nuclear Regulatory Commission. TIC: 236923.

NRC 1978. *Atypical Weld Material in Reactor Pressure Vessel Welds*. IE Bulletin No. 78-12. Washington, D.C.: U.S. Nuclear Regulatory Commission, Office of Inspection and Enforcement. ACC: MOL.20030922.0136.

NRC 1983. *PRA Procedures Guide, A Guide to the Performance of Probabilistic Risk Assessments for Nuclear Power Plants*. NUREG/CR-2300. Two volumes. Washington, D.C.: U.S. Nuclear Regulatory Commission. TIC: 205084.

NRC 2000. *Technical Basis and Implementation Guidelines for a Technique for Human Event Analysis (ATHEANA)*. NUREG-1624, Rev. 1. Washington, D.C.: U.S. Nuclear Regulatory Commission. TIC: 252116.

NRC 2003: *Yucca Mountain Review Plan, Final Report*, NUREG-1804, Rev. 2. Washington, D.C.: U.S. Nuclear Regulatory Commission, Office of Nuclear Material Safety and Safeguards. TIC: 254568.

Plinski, M.J. 2001. *Waste Package Operations Fabrication Process Report*. TDR-EBS-ND-000003 REV 02. Las Vegas, Nevada: Bechtel SAIC Company. ACC: MOL.20011003.0025.

Potts, G.A. and Proebstle, R.A. 1994. "Recent GE BWR Fuel Experience." *Proceedings of the 1994 International Topical Meeting on Light Water Reactor Fuel Performance, West Palm Beach, Florida, April 17-21, 1994*. Pages 87-95. La Grange Park, Illinois: American Nuclear Society. TIC: 243043.

Sano, Y.; Kimura, M.; Sato, K.; Obata, M.; Sudo, A.; Hamamoto, Y.; Shima, S.; Ichikawa, Y.; Yamazaki, H.; Naruse, M.; Hida, S.; Watanabe, T.; and Oono, Y. 2000. "Development and Application of Laser Peening System to Prevent Stress Corrosion Cracking of Reactor Core Shroud." *Proceedings of the 8th International Conference on Nuclear Engineering, ICONE-8, Baltimore, Maryland, April 2-6 2000*. New York, New York: American Society of Mechanical Engineers. TIC: 251262.

Schuster, G.J.; Doctor, S.R.; and Heasler, P.G. 1998. *Density and Distribution of Flaw Indications in PVRUF*. Volume 1 of *Characterization of Flaws in U.S. Reactor Pressure Vessels*. NUREG/CR-6471. Washington, D.C.: U.S. Nuclear Regulatory Commission. TIC: 253278.

Schuster, G.J.; Doctor, S.R.; Pardini, A.F.; and Crawford, S.L. 2000. *Validation of Flaw Density and Distribution in the Weld Metal of the PVRUF Vessel*. Volume 2 of *Characterization of Flaws in U.S. Reactor Pressure Vessels*. NUREG/CR-6471. Washington, D.C.: U.S. Nuclear Regulatory Commission. TIC: 253278.

Shamblen, C.E. and Woodfield, A.P. 2002. "Progress in Titanium-Alloy Hearth Melting." *Industrial Heating*. Pittsburgh, Pennsylvania: Business News Publishing. Accessed November 8, 2002. TIC: 253543.
<http://www.industrialheating.com/CDA/ArticleArchiveSearch/1,2822,,00.html>

Shcherbinskii, V.G. and Myakishev, V.M. 1970. "Statistical Distribution of Welding Defects with Respect to Azimuth." *Translated from Defektoskopiya, No. 4*, 143-144. New York, New York: Plenum Publishing. TIC: 247890.

Simonen, F.A. and Chapman, O.J.V. 1999. "Measured Versus Predicted Distributions of Flaws in Piping Welds." *Probabilistic and Environmental Aspects of Fracture and Fatigue, 1999 ASME Pressure Vessels and Piping Conference, Boston, Massachusetts, August 1-5, 1999*. Rahman, S., ed. PVP-Vol. 386. Pages 101-113. New York, New York: American Society of Mechanical Engineers. TIC: 245621.

S.M. Stoller and Company 1976. *Nuclear Power Experience*. Pages 5, 44. Boulder, Colorado: S.M. Stoller and Company. TIC: 245630.

Smith, T.A. and Warwick, W.A. 1978. "Survey of Defects in Pressure Vessels Built to High Standards of Construction." *The Annual Winter Meeting of the American Society of Mechanical Engineers, San Francisco, California, December 10-15, 1978*. PVP-PB-032. Pages 21-53. New York, New York: American Society of Mechanical Engineers. TIC: 244550.

Swain, A.D. and Guttman, H.E. 1983. *Handbook of Human Reliability Analysis with Emphasis on Nuclear Power Plant Applications Final Report*. NUREG/CR-1278. Washington, D.C.: U.S. Nuclear Regulatory Commission. TIC: 246563.

Tschoepe, E., III; Lyle, F.F., Jr.; Dancer, D.M.; Interrante, C.G.; and Nair, P.K. 1994. *Field Engineering Experience with Structural Materials*. San Antonio, Texas: Center for Nuclear Waste Regulatory Analyses. TIC: 244536.

Yang, R.L. 1997. "Meeting the Challenge of Managing Nuclear Fuel in a Competitive Environment." *Proceedings of the 1997 International Topical Meeting on LWR Fuel Performance, Portland, Oregon, March 2-6, 1997*. Pages 3-10. La Grange Park, Illinois: American Nuclear Society. TIC: 232556.

8.2 CODES, STANDARDS, REGULATIONS, AND PROCEDURES

10 CFR 63. Energy: Disposal of High-Level Radioactive Wastes in a Geologic Repository at Yucca Mountain, Nevada. Readily available.

14 CFR 33. Aeronautics and Space: Airworthiness Standards: Aircraft Engines. Readily available.

AP-3.12Q, Rev. 2, ICN 2. *Design Calculations and Analyses*. Washington, D.C.: U.S. Department of Energy, Office of Civilian Radioactive Waste Management. ACC: DOC.20030827.0013.

AP-SI.1Q, Rev. 5, ICN 2. *Software Management*. Washington, D.C.: U.S. Department of Energy, Office of Civilian Radioactive Waste Management. ACC: DOC.20030902.0003.

AP-SV.1Q, Rev. 1, ICN 1. *Control of the Electronic Management of Information*. Washington, D.C.: U.S. Department of Energy, Office of Civilian Radioactive Waste Management. ACC: DOC.20030902.0011.

8.3 SOURCE DATA, LISTED BY DATA TRACKING NUMBER

MO030214WPWF01.000. *Waste Package Weld Flaw Data*. Submittal date: 02/14/2003.

8.4 SOFTWARE CODES

Software Code: SAPHIRE. V7.18. PC - Windows 2000/NT 4.0. 10325-7.18-00.

ATTACHMENT I
MATHCAD SPREADSHEETS

NOTE: all calculations performed with Default values of Mathcad Built-in variables (in Math Options menu).

Calculation of the weld flaw size distribution in the Y direction

Inputs: See Section 4.1.3.2

Location of the onset of the flaw in the Y direction, converted to mm: vector YO_i , i between 0 and 6.

$$YO_0 := 25.4 \frac{3}{8} \qquad YO_4 := 25.4 \frac{11}{16}$$

$$YO_1 := 25.4 \frac{3}{8}$$

$$YO_2 := 25.4 \frac{11}{16} \qquad YO_5 := 25.4 \frac{3}{8}$$

$$YO_3 := 25.4 \frac{7}{16} \qquad YO_6 := 25.4 \frac{3}{16}$$

Location of the end of the flaw in the Y direction, converted to mm: vector YE_i , i between 0 and 6.

$$YE_0 := 25.4 \frac{7}{16} \qquad YE_4 := 25.4 \frac{13}{16}$$

$$YE_1 := 25.4 \frac{7}{16}$$

$$YE_2 := 25.4 \frac{13}{16} \qquad YE_5 := 25.4 \frac{9}{16}$$

$$YE_3 := 25.4 \frac{9}{16} \qquad YE_6 := 25.4 \frac{3}{4}$$

$$YO = \begin{pmatrix} 9.525 \\ 9.525 \\ 17.4625 \\ 11.1125 \\ 17.4625 \\ 9.525 \\ 4.7625 \end{pmatrix} \qquad YE = \begin{pmatrix} 11.1125 \\ 11.1125 \\ 20.6375 \\ 14.2875 \\ 20.6375 \\ 14.2875 \\ 19.05 \end{pmatrix}$$

The size of the flaws in the Y direction, given in Vector Y_f , is calculated from YO and YE as:

$$Y_f := YE - YO \quad Y_f = \begin{pmatrix} 1.5875 \\ 1.5875 \\ 3.175 \\ 3.175 \\ 3.175 \\ 4.7625 \\ 14.2875 \end{pmatrix}$$

The sum of the flaw sizes in the Y direction, s_t , is therefore: $s_t := \sum_{i=0}^6 Y_{f_i}$

$$s_t = 31.75 \quad \text{mm}$$

Number of flaws detected through UT inspections: $n_f := 7$

PDF for flaw size parameter:

Call λ_s the flaw size parameter in the Y direction. The posterior PDF for λ_s is given by Equation 2 of Section 6.2.1.1.1.

$$p_{\lambda_s}(x) := \frac{s_t^{n_f}}{\Gamma(n_f)} \cdot x^{n_f-1} \cdot \exp(-x s_t)$$

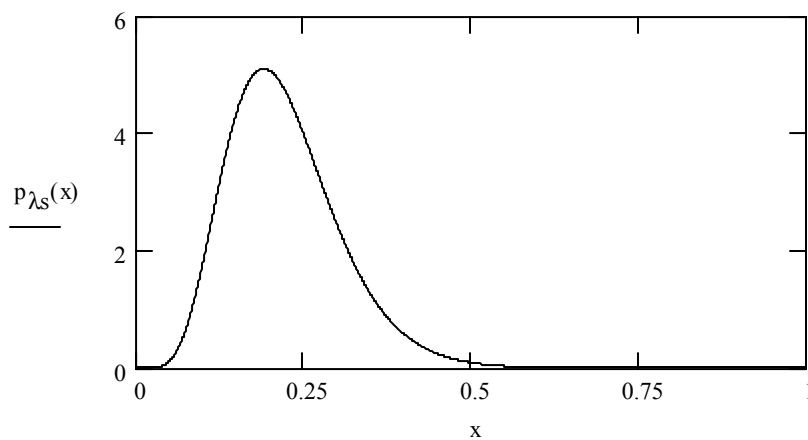


Figure I.1 Weld Flaw size PDF

The mean (λ_{sm}), the 5th ($\lambda_{s0.05}$), and the 95th ($\lambda_{s0.95}$) percentiles are calculated based on Equations 3, 4, and 5 of Section 6.2.1.1.1 as:

$$\lambda_{sm} := \frac{n_f}{s_t} \quad \lambda_{sm} = 0.2205 \quad \text{per mm}$$

$$\lambda_{s0.05} := \frac{qchisq(0.05, 2 \cdot n_f)}{2 \cdot s_t} \quad \lambda_{s0.05} = 0.1035 \quad \text{per mm}$$

$$\lambda_{s0.95} := \frac{qchisq(0.95, 2 \cdot n_f)}{2 \cdot s_t} \quad \lambda_{s0.95} = 0.373 \quad \text{per mm}$$

Flaw size distribution in the Y direction, accounting for weld thickness:

A generalized cumulative flaw size distribution, accounting for the thickness t (in mm) of the weld, is defined in Equation 6 of Section 6.2.1.1.1 as:

$$P_{sg}(s, \lambda_s, t) := \frac{pexp(s, \lambda_s)}{pexp(t, \lambda_s)}$$

PDF for the flaw size distribution before UT inspection and repair (see Equation 8 of Section 6.2.1.1.1)

$$p_{sg}(s, \lambda_s, t) := \frac{dexp(s, \lambda_s)}{pexp(t, \lambda_s)}$$

Comparison with alternative flaw size distribution:

Define alternative flaw size distribution as:

$$P_{alt}(s, \lambda_{alt}, t) := pexp\left(\frac{s}{t}, \lambda_{alt}(t)\right)$$

Here $\lambda_{alt}(t)$ is a function of t and has no dimension. To compare with P_{sg} above, consider only the mean values of λ_s and λ_{alt} . Equation 3 of Section 6.2.1.1.1 is applied to the total size of the flaws, normalized to the weld thickness t . This yields:

$$\lambda_{alt}(t) := \frac{\frac{n_f}{s_t}}{t}$$

Because $\lambda_{sm} := \frac{n_f}{s_t}$ we have: $\lambda_{alt}(t) := \lambda_{sm} \cdot t$

Therefore, for the mean value of the flaw size parameter: $P_{alt}(s, \lambda_{alt}, t) := pexp(s, \lambda_{sm})$

Comparing $P_{sg}(s, \lambda_{sm}, t)$ to $P_{alt}(s, \lambda_{alt}, t)$ shows immediately that $P_{alt}(s, \lambda_{alt}, t) < P_{sg}(s, \lambda_{sm}, t)$. Thus it is more conservative to use P_{sg} .

Verification of goodness-of-fit with chi-square test (see Equation 7 of Section 6.2.1.1.1):

Number of cells considered: $M := 3$ thickness $t_w := 25 \text{ mm}$

The cells are chosen to be approximately equiprobable (using a trial and error approach).

cell range	observed frequencies (from Y_f)	expected frequencies
$c_{1b} := 0 \quad c_{1e} := 1.8$	$N_1 := 2$	$e_1 := n_f \left(P_{sg}(c_{1e}, \lambda_{sm}, t_w) + -P_{sg}(c_{1b}, \lambda_{sm}, t_w) \right)$
$c_{2b} := 1.8 \quad c_{2e} := 4.9$	$N_2 := 4$	$e_2 := n_f \left(P_{sg}(c_{2e}, \lambda_{sm}, t_w) + -P_{sg}(c_{2b}, \lambda_{sm}, t_w) \right)$
$c_{3b} := 4.9 \quad c_{3e} := 25$	$N_3 := 1$	$e_3 := n_f \left(P_{sg}(c_{3e}, \lambda_{sm}, t_w) + -P_{sg}(c_{3b}, \lambda_{sm}, t_w) \right)$
$e_1 = 2.3023 \quad e_2 = 2.3401 \quad e_3 = 2.3577$		

Pearson statistic: $X_2 := \sum_{i=1}^3 \frac{(N_i - e_i)^2}{e_i} \quad X_2 = 1.999$

Comparison to: $qchisq(0.95, 1) = 3.8415$ shows that the fit is appropriate to the significance level considered.

Flaw size distribution:

the PDF for the distribution is given in Equation 9 of Section 6.2.1.1.1.

$$p_{msg}(s, t) := \int_0^{\infty} p_{sg}(s, \lambda_s, t) \cdot p_{\lambda_s}(\lambda_s) d\lambda_s$$

the CDF is given by Equation 10 of Section 6.2.1.1.1. $P_{msg}(s, t) := \int_0^s p_{msg}(u, t) du$

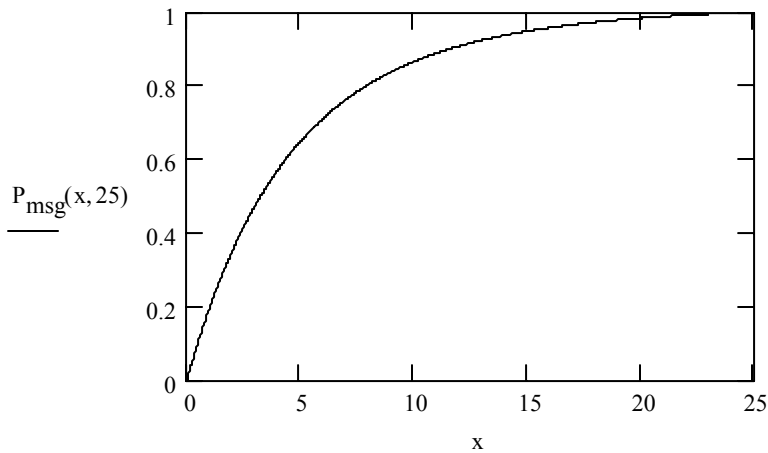


Figure I.2 Weld Flaw Size CDF

mean: $\int_0^{25} p_{msg}(u, 25) \cdot u du = 4.8225$ 5th percentile: $\text{root}(P_{msg}(s, 25) - 0.05, s, 0.1, 3) = 0.231$
 95th percentile: $\text{root}(P_{msg}(s, 25) - 0.95, s, 3, 20) = 15.1691$

The mean (λ_{dm}), the 5th ($\lambda_{d0.05}$), and the 95th ($\lambda_{d0.95}$) percentiles are calculated based on Equations 14, 15, and 16 of Section 6.2.1.1.2 as:

$$\lambda_{dm} := \frac{2n_f + 1}{2 \cdot L_t} \quad \lambda_{dm} = 0.0966 \quad \text{flaws per meter of weld}$$

$$\lambda_{d0.05} := \frac{\text{qchisq}(0.05, 2 \cdot n_f + 1)}{2 \cdot L_t} \quad \lambda_{d0.05} = 0.0468 \quad \text{flaws per meter of weld}$$

$$\lambda_{d0.95} := \frac{\text{qchisq}(0.95, 2 \cdot n_f + 1)}{2 \cdot L_t} \quad \lambda_{d0.95} = 0.1611 \quad \text{flaws per meter of weld}$$

The CDF for the flaw density parameter is given in Equation 13.

$$P_{\lambda_d}(x) := \int_0^x p_{\lambda_d}(u) du$$

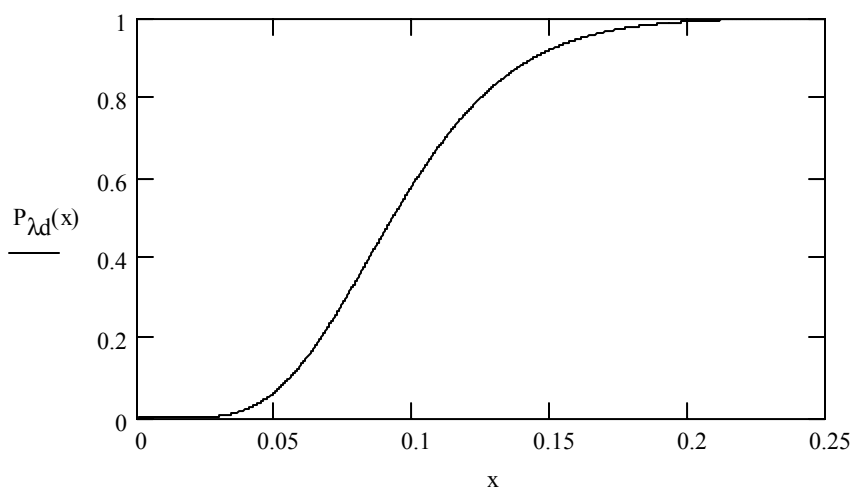


Figure I.4 Weld Flaw Density Parameter CDF

Probability on the number of flaws (0,1,2 or more) with the mean flaw density parameter is:

$$\text{dpois}(0, \lambda_{dm} \cdot L_{wp}) = 0.6258$$

$$\text{dpois}(1, \lambda_{dm} \cdot L_{wp}) = 0.2933$$

$$1 - \text{ppois}(1, \lambda_{dm} \cdot L_{wp}) = 0.0809$$

Verification of goodness-of-fit with chi-square test (see Equation 7 of Section 6.2.1.1.1 and information in Section 6.2.1.1.2):

Number of cells considered: $M := 4$ Length of weld in a specimen ring (m): $L_{wp} = 4.85$
 Number of observations $n := 16$

cell	observed frequencies	expected frequencies
0 flaw	$N_1 := 12$	$e_1 := n \cdot \text{dpois}(0, \lambda_{dm} \cdot L_{wp})$
1 flaw	$N_2 := 2$	$e_2 := n \cdot \text{dpois}(1, \lambda_{dm} \cdot L_{wp})$
2 flaws	$N_3 := 1$	$e_3 := n \cdot \text{dpois}(2, \lambda_{dm} \cdot L_{wp})$
3 or more flaws	$N_4 := 1$	$e_4 := n \cdot (1 - \text{ppois}(2, \lambda_{dm} \cdot L_{wp}))$
$e_1 = 10.0125$ $e_2 = 4.6934$ $e_3 = 1.1$		$e_4 = 0.1941$

Pearson statistic:
$$X_2 := \sum_{i=1}^4 \frac{(N_i - e_i)^2}{e_i}$$
 $X_2 = 5.2962$

Comparison to: $qchisq(0.95, 2) = 5.9915$ shows that the fit is appropriate to the significance level considered.

Calculation of the flaw depth distribution

Inputs: the onset of the 8 UT indications in the Y direction, in mm.

$$YO = \begin{pmatrix} 9.525 \\ 9.525 \\ 17.4625 \\ 11.1125 \\ 17.4625 \\ 9.525 \\ 4.7625 \end{pmatrix}$$

Verification of goodness-of-fit with uniform distribution using chi-square test (see Equation 7 of Section 6.2.1.1.1):

Number of cells considered: $M := 3$

The cells are chosen to be equiprobable.

$$\frac{25}{3} = 8.3333$$

cell range	observed frequencies	expected frequencies
$c_{1b} := 0$ $c_{1e} := 8.33$	$N_1 := 1$	$e_1 := n_f \frac{1}{3}$
$c_{2b} := 8.33$ $c_{2e} := 16.67$	$N_2 := 4$	$e_2 := n_f \frac{1}{3}$
$c_{3b} := 16.67$ $c_{3e} := 25$	$N_3 := 2$	$e_3 := n_f \frac{1}{3}$

Pearson statistic: $X_2 := \sum_{i=1}^3 \frac{(N_i - e_i)^2}{e_i}$ $X_2 = 2$

Comparison to: $qchisq(0.95, 2) = 5.9915$ shows that the fit is appropriate to the significance level considered.

Orientation of the flaws:

inputs: See Section 4.1.3.2

Length of the flaws in the X direction, converted in mm: vector X_i , i between 0 and 6.

$$X_0 := 25.4 \left(54 + \frac{5}{8} + -54 + \frac{-1}{2} \right) \quad X_4 := 25.4 \left(21 + \frac{1}{4} + -20 + \frac{-7}{8} \right)$$

$$X_1 := 25.4 \left(56 + \frac{3}{8} + -55 + \frac{-3}{4} \right)$$

$$X_2 := 25.4 \left(19 + \frac{7}{8} + -19 + \frac{-1}{8} \right) \quad X_5 := 25.4 \left(3 + \frac{5}{8} + -3 + \frac{-1}{8} \right)$$

$$X_3 := 25.4 \left(48 + \frac{5}{8} + -47 + \frac{-1}{4} \right) \quad X_6 := 25.4 \left(4 + \frac{11}{16} + -4 + \frac{-5}{16} \right)$$

Location of the flaw in the Z direction, converted in mm: vector Z_i , i between 0 and 6.

$$Z_0 := 25.4 \left(\frac{9}{16} + \frac{-1}{2} \right) \quad Z_4 := 25.4 \left(\frac{5}{8} + \frac{-9}{16} \right)$$

$$Z_1 := 25.4 \left(\frac{9}{16} + \frac{-1}{2} \right)$$

$$Z_2 := 25.4 \left(\frac{5}{8} + \frac{-9}{16} \right) \quad Z_5 := 25.4 \left(\frac{11}{16} + \frac{-9}{16} \right)$$

$$Z_3 := 25.4 \left(\frac{9}{16} + \frac{-1}{2} \right) \quad Z_6 := 0$$

$$X = \begin{pmatrix} 3.175 \\ 15.875 \\ 19.05 \\ 34.925 \\ 9.525 \\ 12.7 \\ 9.525 \end{pmatrix} \quad Z = \begin{pmatrix} 1.5875 \\ 1.5875 \\ 1.5875 \\ 1.5875 \\ 1.5875 \\ 3.175 \\ 0 \end{pmatrix}$$

Characterization of the angle distribution:

The angle (converted from radians to degrees) between the flaw and the direction of the weld is given for each flaw by the vector θ

$$i := 0..6$$

$$\theta_i := \frac{360}{2\pi} \cdot \text{atan} \left(\frac{Z_i}{X_i} \right)$$

$$\theta = \begin{pmatrix} 26.5651 \\ 5.7106 \\ 4.7636 \\ 2.6026 \\ 9.4623 \\ 14.0362 \\ 0 \end{pmatrix} \quad \theta := \text{sort}(\theta) \quad \theta = \begin{pmatrix} 0 \\ 2.6026 \\ 4.7636 \\ 5.7106 \\ 9.4623 \\ 14.0362 \\ 26.5651 \end{pmatrix}$$

The PDF of θ is given in Equation 17 of Section 6.2.1.1.4 as:

$$p_{\theta}(\theta, \sigma) := 2 \cdot \text{dnorm}(\theta, 0, \sigma)$$

The CDF is:

$$P_{\theta}(\theta, \sigma) := 2 \cdot \text{pnorm}(\theta, 0, \sigma) - 1$$

Determine the PDF for σ .

The likelihood function related to the observed angles is:

$$L_{\theta}(\sigma) := \prod_{i=0}^6 p_{\theta}(\theta_i, \sigma)$$

Application of Bayes' theorem (Equation 19 of Section 6.2.1.1.4) yields the posterior PDF for σ :

$$p_{\sigma}(\sigma) := \frac{\frac{L_{\theta}(\sigma)}{\sigma}}{\int_0^{\infty} \frac{L_{\theta}(u)}{u} du}$$

The mean value for σ is: $\sigma_m := \int_0^{\infty} x p_{\sigma}(x) dx$ $\sigma_m = 13.9054$

The 5th percentile is: $\sigma_{0.05} := \text{root} \left(\int_0^a p_{\sigma}(x) dx - 0.05, a, 2, 20 \right)$ $\sigma_{0.05} = 8.6518$

The 95th percentile is: $\sigma_{0.95} := \text{root} \left(\int_0^a p_{\sigma}(x) dx - 0.95, a, 10, 60 \right)$ $\sigma_{0.95} = 21.5941$

Maximum likelihood estimator for σ : use formula given in Martz and Waller 1991, p. 225:

$$\sigma_{mle} := \sqrt{\frac{\sum_{i=0}^6 (\theta_i)^2}{n_f}}$$

$\sigma_{mle} = 12.2727$

Verification of goodness-of-fit with chi-square test (see Equation 7 of Section 6.2.1.1.1):

Number of cells considered: $M := 3$

The cells are chosen to be approximately equiprobable.

cell range	observed frequencies	expected frequencies
$c_{1b} := 0 \quad c_{1e} := 5.6$	$N_1 := 3$	$e_1 := n_f (P_{\theta}(c_{1e}, \sigma_m) - P_{\theta}(c_{1b}, \sigma_m))$
$c_{2b} := 5.6 \quad c_{2e} := 12.7$	$N_2 := 2$	$e_2 := n_f (P_{\theta}(c_{2e}, \sigma_m) - P_{\theta}(c_{2b}, \sigma_m))$
$c_{3b} := 12.7$	$N_3 := 2$	$e_3 := n_f (1 - P_{\theta}(c_{3b}, \sigma_m))$
$e_1 = 2.1899 \quad e_2 = 2.2825 \quad e_3 = 2.5275$		

Pearson statistic: $X_2 := \sum_{i=1}^3 \frac{(N_i - e_i)^2}{e_i}$ $X_2 = 0.4447$

Comparison to: $qchisq(0.95, 1) = 3.8415$ shows that the fit is appropriate to the significance level considered.

**Expected fraction of flaws with an angle θ greater than 45 degrees
(Equation 20 of 6.2.1.1.4):**

$$F_{\theta} := \int_0^{\infty} (1 - P_{\theta}(45, u)) \cdot p_{\sigma}(u) du$$

$F_{\theta} = 8.0502 \times 10^{-3}$ This corresponds to around 0.8% of the flaws.

Characterization of UT inspection on WP closure weld:

flaw size s in mm

UT reliability curve given in Equation 21:

$\varepsilon := 0.005$ $v := 3$ $s_{01} := 5$ mm alternative value of s_0 is: $s_{02} := 2.5$ mm

$$P_{ND1}(s, \varepsilon, s_0, v) := \varepsilon + 0.5 \cdot (1 - \varepsilon) \cdot \operatorname{erfc}\left(v \cdot \ln\left(\frac{s}{s_0}\right)\right)$$

UT reliability curve given in Equation 22:

$\beta_1 := -2.67$ $\beta_2 := 1.6709$ per mm

$$P_{ND2}(s, \beta_1, \beta_2) := 1 - \frac{1}{1 + \exp(-\beta_1 + -\beta_2 \cdot s)}$$

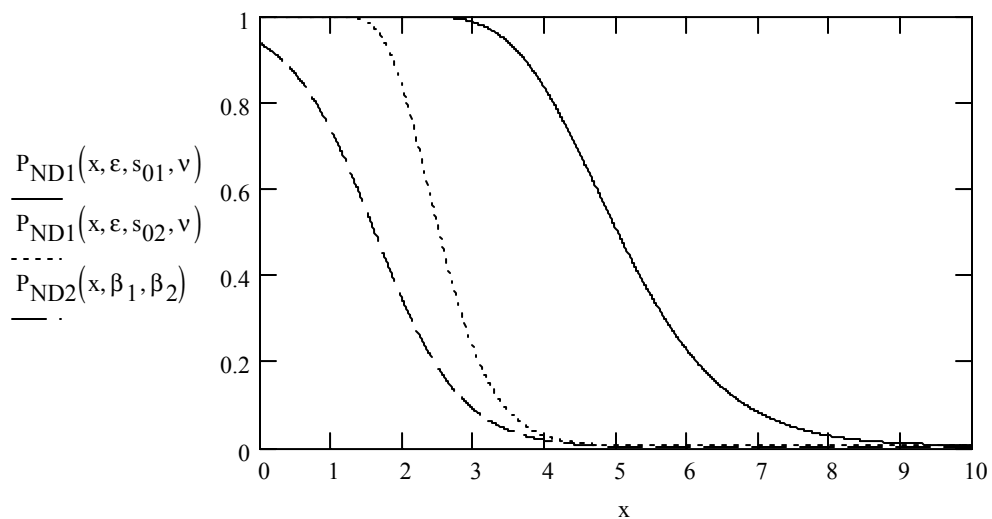


Figure I.5 UT Weld Flaw Detection Reliability Curve

In the following, the UT PND curve considered is that given by $P_{ND1}(s, \varepsilon, s_0, v)$, with $s_0 := 2.5$ mm

$$1 - P_{ND1}(2.5, \varepsilon, 2.5, v) = 0.4975$$

Flaw size distribution after UT inspection and repair:

Fraction of flaws that remain in the weld after UT inspection and repair (Equation 23):

$$F_{ND}(t, \lambda_s, \epsilon, s_0, v) := \int_0^t p_{sg}(s, \lambda_s, t) \cdot P_{ND1}(s, \epsilon, s_0, v) ds$$

PDF for the flaw size after UT inspection and weld repair (Equation 25), accounting for all possible values of λ_s , weighted by their probability:

$$p_{msgut}(s, t, \epsilon, s_0, v) := \int_0^\infty \frac{p_{sg}(s, \lambda_s, t) \cdot P_{ND1}(s, \epsilon, s_0, v)}{F_{ND}(t, \lambda_s, \epsilon, s_0, v)} \cdot p_{\lambda_s}(\lambda_s) d\lambda_s$$

Corresponding CDF (Equation 26):

$$P_{msgut}(s, t, \epsilon, s_0, v) := \int_0^s p_{msgut}(u, t, \epsilon, s_0, v) du$$

Graphical representation for outer closure weld of WP (t=25mm):

$$t := 25 \quad \epsilon = 5 \times 10^{-3} \quad s_0 = 2.5 \quad v = 3$$

The CDF is calculated for 100 points between 0 and the 99.6th percentile

$$s_{0.996} := \text{root}(P_{msgut}(s, t, \epsilon, s_0, v) - 0.996, s, 3, 10)$$

$$s_{0.996} = 6.1177$$

$$n_s := 100 \quad i := 1..n_s$$

$$S_{i,0} := \frac{i \cdot s_{0.996}}{n_s}$$

$$S_{i,1} := P_{\text{msgut}}(S_{i,0}, t, \epsilon, s_0, v)$$

Also we have: $S_{0,0} := 0$ $S_{0,1} := 0$

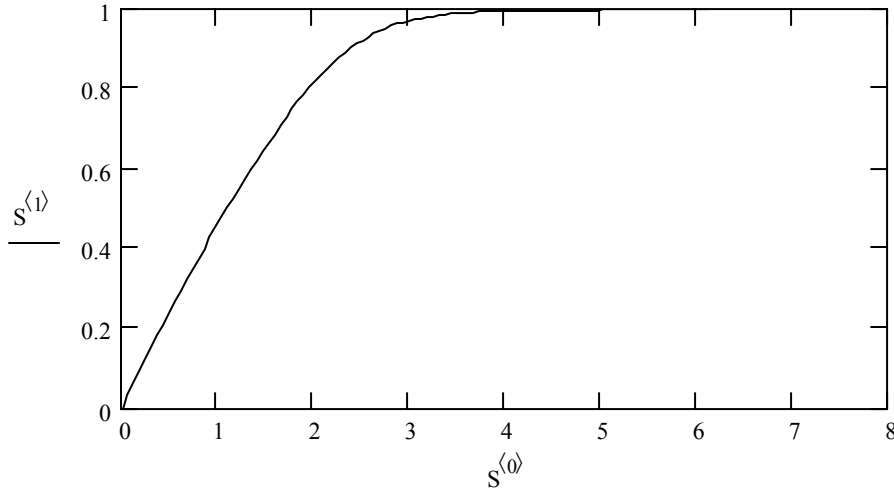


Figure I.6 Weld Flaw Size CDF After UT Inspection & Weld Flaw Repair

The mean flaw size is calculated using the formula given in Equation 27.

$$s_{\text{mgut}}(t, \epsilon, s_0, v) := \int_0^t P_{\text{msgut}}(u, t, \epsilon, s_0, v) \cdot u \, du$$

$$s_{\text{mgut}}(t, \epsilon, s_0, v) = 1.2527 \quad \text{mm}$$

5th percentile: $\text{root}(P_{\text{msgut}}(s, t, \epsilon, s_0, v) - 0.05, s, 0.01, 1) = 0.09853$

95th percentile: $\text{root}(P_{\text{msgut}}(s, t, \epsilon, s_0, v) - 0.95, s, 1, 5) = 2.7585$

Flaw density parameter after UT inspection and weld repair:

The flaw density parameter after UT inspection and weld repair λ_{dut} is given in Equation 28.

$$\lambda_{\text{dut}}(\lambda_d, \lambda_s, t, \varepsilon, s_0, v) := \lambda_d \cdot F_{\text{ND}}(t, \lambda_s, \varepsilon, s_0, v)$$

It is a function of 2 independent random variables: λ_d and λ_s . The CDF is calculated using latin hypercube sampling.

size of the sampling: $n_s := 2000$

$i := 1..n_s$

$RD_{i-1,0} := i$

$RD_{i-1,1} := \text{rnd}(1.0)$

$RD_{i-1,2} := \text{rnd}(1.0)$

$RK1 := \text{csort}(RD, 1)$

$RK2 := \text{csort}(RD, 2)$

RK1 and RK2 are two matrixes whose first column contain a permutation on the integers on the interval $[1, n_s]$.

Define two sets of random values. Each random value is selected within one of the equiprobable n_s intervals that partition $[0, 1]$. 2 sets are created, one for each random variable.

$$X^{\langle 0 \rangle} := \frac{RK1^{\langle 0 \rangle} - 1 + \text{runif}(n_s, 0, 1)}{n_s}$$

$$X^{\langle 1 \rangle} := \frac{RK2^{\langle 0 \rangle} - 1 + \text{runif}(n_s, 0, 1)}{n_s}$$

Calculate a set of sample values for each of the random variables:

$a := 0.1$

$$q_{\lambda_s}(y) := \text{root} \left(\int_0^a p_{\lambda_s}(u) du - y, a, 0, 1 \right)$$

$$q_{\lambda_d}(y) := \text{root} \left(\int_0^a p_{\lambda_d}(u) du - y, a, 0, 1 \right)$$

$i := 0..n_s - 1$

$$Y_{i,0} := q_{\lambda_s}(X_{i,0})$$

$$Y_{i,1} := q_{\lambda_d}(X_{i,1})$$

Calculate a set of sample values for λ_{dut} defined in Equation 28:

$$t = 25 \quad \varepsilon = 5 \times 10^{-3} \quad s_0 = 2.5 \quad v = 3$$

$$Z_{i,0} := \lambda_{\text{dut}}(Y_{i,1}, Y_{i,0}, t, \varepsilon, s_0, v)$$

Sort the sample values and rank them on [0,1]

$$Z := \text{sort}(Z)$$

$$Z_{i,1} := \frac{i+1}{n_s}$$

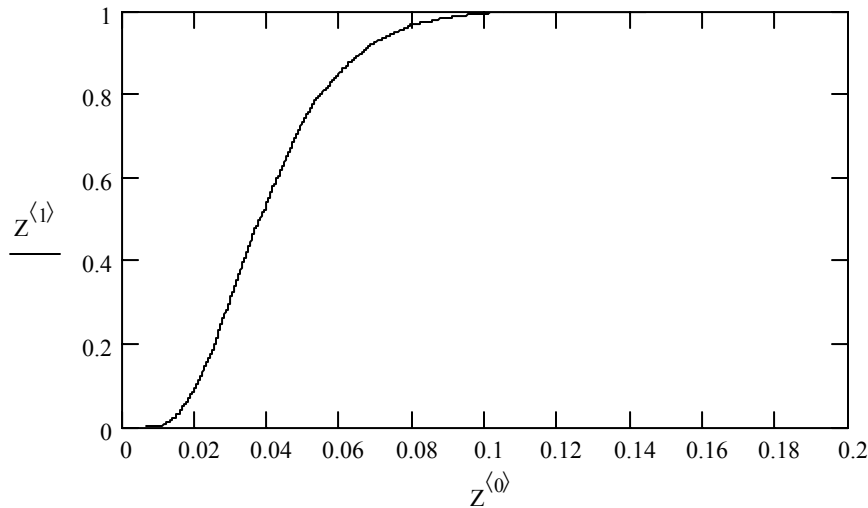


Figure I.7 Weld Flaw Density CDF After UT Inspection and Weld Flaw Repair

Estimated mean of λ_{dut} , based on sample values (see Equation 29):

$$\lambda_{\text{dmut}} := \sum_{i=0}^{n_s-1} \frac{Z_{i,0}}{n_s} \quad \lambda_{\text{dmut}} = 0.0407 \quad \text{flaw per meter of weld} \quad \lambda_{\text{dmut}25} := \lambda_{\text{dmut}}$$

5th percentile: $\text{interp}(Z^{(1)}, Z^{(0)}, 0.05) = 0.0166$ flaws / m

95th percentile: $\text{interp}(Z^{(1)}, Z^{(0)}, 0.95) = 0.0756$ flaws / m

5th percentile and 95th percentiles calculated by linear interpolation on sample values.

Probability on the number of flaws (0,1, 2 or more) with the mean flaw density parameter is:

$$\text{dpois}(0, \lambda_{\text{dmut}} \cdot L_{\text{wp}}) = 0.8207$$

$$\text{dpois}(1, \lambda_{\text{dmut}} \cdot L_{\text{wp}}) = 0.1622$$

$$1 - \text{ppois}(1, \lambda_{\text{dmut}} \cdot L_{\text{wp}}) = 0.0171$$

Calculation sheet for characterizing flaws in the other welds of the WP:

$$\varepsilon = 5 \times 10^{-3} \quad s_0 = 2.5 \text{ mm} \quad v = 3$$

flat closure lid weld: diameter: $D_{\text{flat}} := 1.527 \text{ m}$ length of weld: $L_{\text{flat}} := \pi D_{\text{flat}}$
(see Table 2 for input values) $L_{\text{flat}} = 4.7972 \text{ m}$
rounded up to: $L_{\text{flat}} := 4.80 \text{ m}$

lid thickness: $t_{\text{flat}} := 10 \text{ mm}$

after UT, the CDF on the flaw size accounting for uncertainties on λ_s is given by: $P_{\text{msgut}}(s, t_{\text{flat}}, \varepsilon, s_0, v)$

mean flaw size: $s_{\text{mgut}}(t_{\text{flat}}, \varepsilon, s_0, v) := \int_0^{t_{\text{flat}}} P_{\text{msgut}}(u, t_{\text{flat}}, \varepsilon, s_0, v) \cdot u \, du$

$$s_{\text{mgut}}(t_{\text{flat}}, \varepsilon, s_0, v) = 1.2252 \text{ mm}$$

5th percentile: $\text{root}(P_{\text{msgut}}(s, t_{\text{flat}}, \varepsilon, s_0, v) - 0.05, s, 0.01, 1) = 0.09835$

95th percentile: $\text{root}(P_{\text{msgut}}(s, t_{\text{flat}}, \varepsilon, s_0, v) - 0.95, s, 1, 5) = 2.7389$

Before UT, the mean, the 5th and the 95th percentiles were:

mean: $\int_0^{10} P_{\text{msg}}(u, 10) \cdot u \, du = 3.3395$ 5th percentile: $\text{root}(P_{\text{msg}}(s, t_{\text{flat}}) - 0.05, s, 0.1, 3) = 0.204$
95th percentile: $\text{root}(P_{\text{msg}}(s, t_{\text{flat}}) - 0.95, s, 3, 20) = 8.5759$

the main features of the flaw density parameter after UT are determined by latin hypercube sampling:

$$n_s = 2 \times 10^3 \text{ samples}$$

$$Z := 0 \text{ (initialization of vector)}$$

$$Z_{i,0} := \lambda_{\text{dut}}(Y_{i,1}, Y_{i,0}, t_{\text{flat}}, \varepsilon, s_0, v)$$

Sort the sample value and rank them on [0,1]

$$Z := \text{sort}(Z) \quad Z_{i,1} := \frac{i+1}{n_s}$$

Estimated mean of λ_{dmut} , based on sample values (see Equation 29):

$$\lambda_{\text{dmut}} := \sum_{i=0}^{n_s-1} \frac{Z_{i,0}}{n_s} \quad \lambda_{\text{dmut}} = 0.0463 \text{ flaw per meter of weld}$$

5th percentile: $\text{linterp}(Z^{\langle 1 \rangle}, Z^{\langle 0 \rangle}, 0.05) = 0.0211 \text{ flaw / m}$

95th percentile: $\text{linterp}(Z^{\langle 1 \rangle}, Z^{\langle 0 \rangle}, 0.95) = 0.0809 \text{ flaw / m}$

Probability on the number of flaws (0,1, and 2 or more) with the mean flaw density parameter is:

before UT:

$$\text{dpois}(0, \lambda_{\text{dm}} \cdot L_{\text{flat}}) = 0.6288$$

$$\text{dpois}(1, \lambda_{\text{dm}} \cdot L_{\text{flat}}) = 0.2917$$

$$1 - \text{ppois}(1, \lambda_{\text{dm}} \cdot L_{\text{flat}}) = 0.0795$$

after UT:

$$\text{dpois}(0, \lambda_{\text{dmut}} \cdot L_{\text{flat}}) = 0.8006$$

$$\text{dpois}(1, \lambda_{\text{dmut}} \cdot L_{\text{flat}}) = 0.178$$

$$1 - \text{ppois}(1, \lambda_{\text{dmut}} \cdot L_{\text{flat}}) = 0.0213$$

Seam welds of the WP:

$$\varepsilon = 5 \times 10^{-3} \quad s_0 = 2.5 \text{ mm} \quad v = 3$$

Length of weld in the bottom lid weld taken to be the same as for the outer closure lid weld:

$$L_{\text{wp}} = 4.85 \text{ m}$$

Length of the weld seaming the two half-cylinder:

Diameter taken at $D_{\text{seam}} := 1.544 \text{ m}$ (average of inner and outer diameter of WP, see Table 2)

Length of one longitudinal seam taken at: $L_{\text{long}} := 5.165 \text{ m}$

So the total length of weld is:

$$L_{\text{seam}} := L_{\text{wp}} + \pi D_{\text{seam}} + L_{\text{long}} \quad L_{\text{seam}} = 14.8656 \text{ m}$$

rounded to: $L_{\text{seam}} := 15 \text{ m}$

Thickness of the weld is conservatively taken at: $t_{\text{seam}} := 20 \text{ mm}$

after UT, the CDF on the flaw size is given by: $P_{\text{msgut}}(s, t_{\text{seam}}, \varepsilon, s_0, v)$

the main features of the flaw size after UT are:

$$\text{mean flaw size: } s_{\text{mgut}}(t_{\text{seam}}, \epsilon, s_0, v) := \int_0^{t_{\text{seam}}} p_{\text{msgut}}(u, t_{\text{seam}}, \epsilon, s_0, v) \cdot u \, du$$

$$s_{\text{mgut}}(t_{\text{seam}}, \epsilon, s_0, v) = 1.247 \quad \text{mm}$$

$$\text{5th percentile: } \text{root}(P_{\text{msgut}}(s, t_{\text{seam}}, \epsilon, s_0, v) - 0.05, s, 0.01, 1) = 0.09851$$

$$\text{95th percentile: } \text{root}(P_{\text{msgut}}(s, t_{\text{seam}}, \epsilon, s_0, v) - 0.95, s, 1, 5) = 2.7558$$

Before UT, the mean, the 5th and the 95th were:

$$\begin{aligned} \text{mean: } \int_0^{20} p_{\text{msg}}(u, 20) \cdot u \, du &= 4.5543 & \text{5th percentile: } \text{root}(P_{\text{msg}}(s, t_{\text{seam}}) - 0.05, s, 0.1, 3) &= 0.2283 \\ & & \text{95th percentile: } \text{root}(P_{\text{msg}}(s, t_{\text{seam}}) - 0.95, s, 3, 20) &= 13.8487 \end{aligned}$$

the main features of the flaw density parameter after UT are determined by latin hypercube sampling on:

$$n_s = 2 \times 10^3 \quad \text{samples}$$

$$Z := 0 \quad (\text{initialization of vector})$$

$$Z_{i,0} := \lambda_{\text{dut}}(Y_{i,1}, Y_{i,0}, t_{\text{seam}}, \epsilon, s_0, v)$$

Sort the sample value and rank them on [0,1]

$$Z := \text{sort}(Z) \quad Z_{i,1} := \frac{i+1}{n_s}$$

Estimated mean of λ_{dut} , based on sample values (see Equation 29):

$$\lambda_{\text{dmu}} := \sum_{i=0}^{n_s-1} \frac{Z_{i,0}}{n_s} \quad \lambda_{\text{dmu}} = 0.0413 \quad \text{flaw per meter of weld}$$

$$\text{5th percentile: } \text{linterp}(Z^{\langle 1 \rangle}, Z^{\langle 0 \rangle}, 0.05) = 0.0173 \quad \text{flaw / m}$$

$$\text{95th percentile: } \text{linterp}(Z^{\langle 1 \rangle}, Z^{\langle 0 \rangle}, 0.95) = 0.0759 \quad \text{flaw / m}$$

Probability on the number of flaws (0,1, and 2 or more) with the mean flaw density parameter is:

before UT:

$$\text{dpois}\left(0, \lambda_{\text{dm}} \cdot L_{\text{seam}}\right) = 0.2346$$

$$\text{dpois}\left(1, \lambda_{\text{dm}} \cdot L_{\text{seam}}\right) = 0.3402$$

$$1 - \text{ppois}\left(1, \lambda_{\text{dm}} \cdot L_{\text{seam}}\right) = 0.4252$$

after UT:

$$\text{dpois}\left(0, \lambda_{\text{dmut}} \cdot L_{\text{seam}}\right) = 0.5385$$

$$\text{dpois}\left(1, \lambda_{\text{dmut}} \cdot L_{\text{seam}}\right) = 0.3333$$

$$1 - \text{ppois}\left(1, \lambda_{\text{dmut}} \cdot L_{\text{seam}}\right) = 0.1282$$

Comparison with results from Khaleel et al. (1999)

Flaw size for 25-mm thick weld:

$$s_{50k} := 25.4 \left[0.1169 + -0.0445 \frac{25}{25.4} + 0.00797 \left(\frac{25}{25.4} \right)^2 \right]$$

$$s_{50k} = 2.0529 \quad \text{mm}$$

$$\sigma_k := 0.09733 + 0.345 \frac{25}{25.4} + -0.07268 \left(\frac{25}{25.4} \right)^2$$

$$\sigma_k = 0.3665$$

mean size of the flaw (See Equation 34 of Section 6.2.1.1.3):

$$s_{mk} := s_{50k} \cdot \exp\left(0.5 \cdot \sigma_k^2\right)$$

$$s_{mk} = 2.1955 \quad \text{mm}$$

$$\text{5th percentile:} \quad \text{qlnorm}\left(0.05, \ln(s_{50k}), \sigma_k\right) = 1.1235 \quad \text{mm}$$

$$\text{95th percentile:} \quad \text{qlnorm}\left(0.95, \ln(s_{50k}), \sigma_k\right) = 3.7511 \quad \text{mm}$$

Apply a UT inspection of the same type that the one used in the analysis (i.e., using P_{ND1}):

Fraction of remaining flaws:

$$F_k := \int_0^{25} \text{dlnorm}\left(u, \ln(s_{50k}), \sigma_k\right) \cdot P_{\text{ND1}}\left(u, \varepsilon, s_0, v\right) du \quad F_k = 0.6761$$

PDF for the size of the remaining flaws:

$$p_{\text{skut}}(s) := \frac{\text{dlnorm}(s, \ln(s_{50k}), \sigma_k) \cdot P_{\text{NDI}}(s, \varepsilon, s_0, v)}{F_k}$$

CDF for the size of the remaining flaws:

$$P_{\text{skut}}(s) := \int_0^s p_{\text{skut}}(u) \, du$$

mean size of the flaws remaining in the weld:

$$s_{\text{mkut}} := \int_0^{25} p_{\text{skut}}(u) \cdot u \, du \quad s_{\text{mkut}} = 1.8168 \quad \text{mm}$$

5th percentile: $\text{root}(P_{\text{skut}}(s) - 0.05, s, 1, 5) = 1.0507$

95th percentile: $\text{root}(P_{\text{skut}}(s) - 0.95, s, 1, 5) = 2.7312$

Flaw density for non-inspected welds:

$$\lambda_{\text{dk}} := 0.0448 \frac{1000}{25.4} \quad \lambda_{\text{dk}} = 1.7638 \quad \text{flaws per meter of weld (no inspection)}$$

$$\frac{\lambda_{\text{dk}}}{\lambda_{\text{dm}}} = 18.2492$$

surface of triangle delimited by $B_3A_1B_1$ is: $S_2 := \frac{L_1 \cdot L_2}{2}$ $S_2 = 4.513 \times 10^{-3}$ inch²

surface of triangle delimited by $B_2A_2B_4$ is: $S_3 := \frac{L_1 \cdot L_3}{2}$ $S_3 = 9.0508 \times 10^{-3}$ inch²

surface of triangle delimited by $C_5B_3C_3$ and triangle delimited by $C_4B_4C_6$:

distance $B_3C_3 = \text{distance } B_4C_4 = BC = L_4$ $L_4 := 0.43$ inch

angle $C_5B_3C_3$ is: $\alpha_3 := \frac{25 \cdot 2\pi}{360}$ $\alpha_3 = 0.4363$ radians

angle $C_4B_4C_6$ is: $\alpha_4 := \frac{29 \cdot 2\pi}{360}$ $\alpha_4 = 0.5061$ radians

length C_5C_3 is: $L_5 := L_4 \cdot \tan(\alpha_3)$ $L_5 = 0.2005$ inch

length C_4C_6 is: $L_6 := L_4 \cdot \tan(\alpha_4)$ $L_6 = 0.2384$ inch

surface of triangle delimited by $B_3A_1B_1$ is: $S_4 := \frac{L_4 \cdot L_5}{2}$ $S_4 = 0.0431$ inch²

surface of triangle delimited by $B_2A_2B_4$ is: $S_5 := \frac{L_4 \cdot L_6}{2}$ $S_5 = 0.0512$ inch²

surface of rectangle delimited by $A_1B_1B_2A_2$ and rectangle delimited by $C_4B_4B_3C_3$:

rectangle delimited by $A_1B_1B_2A_2$ is: $S_6 := 2 \cdot r_0 \cdot L_1$ $S_6 = 0.1038$ inch²

rectangle delimited by $C_4B_4B_3C_3$ is: $S_7 := (2r_0 + L_2 + L_3) \cdot L_4$ $S_7 = 0.1356$ inch²

Calculation of the cross-area:

total surface is: $S := S_1 + S_2 + S_3 + S_4 + S_5 + S_6 + S_7$ $S = 0.3718$ inch²

$$\begin{aligned} \text{in metric system: } S &:= S \cdot 0.0254^2 \\ S &= 2.3988 \times 10^{-4} \text{ m}^2 \end{aligned}$$

Estimation of the total volume of weld in the 16 specimen rings (in mm³):

$$16 \cdot \pi \cdot D_{wp} \cdot S \cdot 1000^3 = 18610540.3277924$$

Volumetric weld flaw density of flaws after UT inspection and repair:

$$\lambda_{bm} := \frac{\lambda_{dmut25}}{8 \cdot S} \quad \lambda_{bm} = 21.2339 \text{ flaws /m}^3$$

Probability on the number of flaws in the Alloy 22 barrier of a WP: See Equation 39 of Section 6.2.2.

$$\text{Volume of base metal affected: } V_{rbm} := 0.1 \cdot 0.1 \cdot 0.02 \quad V_{rbm} = 2 \times 10^{-4} \text{ m}^3$$

$$P_{nbm}(n, \lambda_{bm}, V_{wp}) := 1 - F_{bm} + F_{bm} \cdot \text{ppois}(n, \lambda_{bm} \cdot V_{wp})$$

$$\lambda_{bm} \cdot V_{rbm} = 4.2468 \times 10^{-3}$$

$$F_{bm} = 2.017 \times 10^{-3} \quad F_{bm} \lambda_{bm} \cdot V_{rbm} = 8.5659 \times 10^{-6}$$

Probability of having at least one flaw on a randomly selected WP:

$$1 - P_{nbm}(0, \lambda_{bm}, V_{rbm}) = 8.5477 \times 10^{-6} \quad (\text{rigorous evaluation})$$

$$F_{bm} \lambda_{bm} \cdot V_{rbm} = 8.5659 \times 10^{-6} \quad (\text{simpler evaluation})$$

Characterization of anomaly distribution curve in base-metal titanium used for the drip shield:

Express the Anomaly distribution curve in units of the metric system:

See Section 4.1.4

defect inspection area in square mils put in Column 0 of Matrix E

Exceedance probability per million pounds of titanium put in Column 1 of Matrix E

$$E := \begin{pmatrix} 100 & 6.6 \\ 200 & 3.6 \\ 300 & 2.6 \\ 400 & 2.0 \\ 500 & 1.7 \\ 600 & 1.3 \\ 700 & 1.1 \\ 800 & 0.90 \\ 900 & 0.75 \\ 1000 & 0.65 \\ 2000 & 0.21 \\ 3000 & 0.084 \\ 4000 & 0.051 \\ 5000 & 0.037 \\ 6000 & 0.028 \\ 7000 & 0.022 \\ 8000 & 0.020 \\ 9000 & 0.017 \\ 10000 & 0.016 \\ 20000 & 0.010 \end{pmatrix}$$

Anomalies are spherically shaped so their diameter in mm is: $M^{(0)} := 0.02542 \cdot \sqrt{\frac{E^{(0)}}{\pi}}$

The number of defect per million pound of titanium is converted to the number of defect per millior kg of titanium. Also, the number if multiplied by 2 to account for both low- and high-density inclusions.

$$M^{\langle 1 \rangle} := \frac{2 \cdot E^{\langle 1 \rangle}}{0.45359237}$$

In the metric system, the set of data points for the anomaly distribution curve is:

	0	1
0	0.2866	29.101
1	0.4053	15.8733
2	0.4964	11.464
3	0.5732	8.8185
4	0.6409	7.4957
5	0.702	5.732
6	0.7583	4.8502
7	0.8107	3.9683
8	0.8598	3.3069
9	0.9063	2.866
10	1.2818	0.9259
11	1.5698	0.3704
12	1.8127	0.2249
13	2.0266	0.1631
14	2.2201	0.1235
15	2.3979	0.097
16	2.5635	0.0882
17	2.719	0.075
18	2.8661	0.0705
19	4.0533	0.0441

M =

Column 0: diameter of the defect in mm
Column 1: expected number of defects per million kg of titanium

A linear interpolation on a log-log scale is done to these data to get the anomaly exceedance curve for any defect size.

$$d(x) := 10^{\text{interp}\left(\log\left(M^{\langle 0 \rangle}\right), \log\left(M^{\langle 1 \rangle}\right), \log(x)\right)}$$

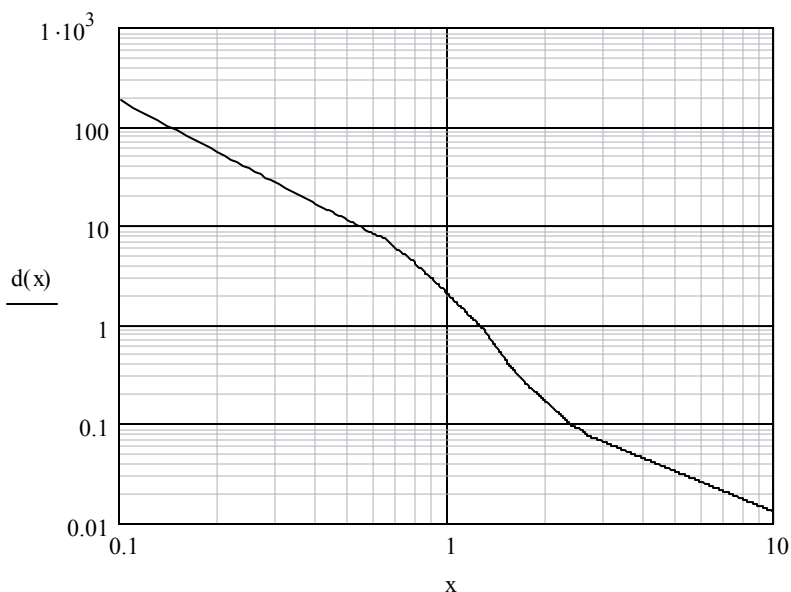


Figure I. 8 Titanium Weld Anomaly Distribution Curve

The density of inclusions in the DS is obtained by multiplying the function above by the mass of the DS, expressed in million kg.

$m_{ds} := 0.005$ million kg of titanium (see table 3 of Section 4.1.1)

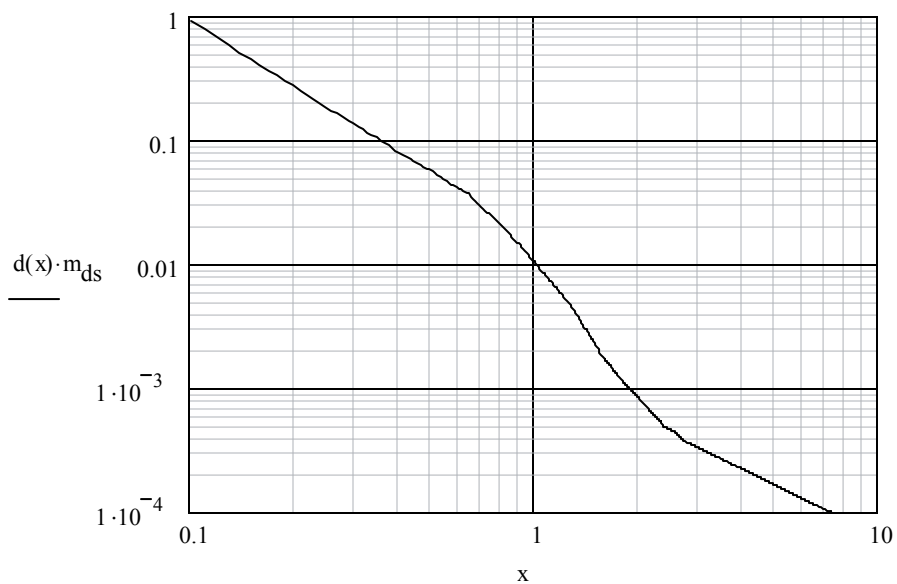


Figure I. 9 Titanium Mass Weld Anomaly Distribution Curve

Probability on the number of flaws in the DS:

	.5 mm	1 mm
0 flaw	$\text{dpois}(0, d(.5) \cdot m_{\text{ds}}) = 0.945$	$\text{dpois}(0, d(1) \cdot m_{\text{ds}}) = 0.9897$
1 flaw	$\text{dpois}(1, d(.5) \cdot m_{\text{ds}}) = 5.3462 \times 10^{-2}$	$\text{dpois}(1, d(1) \cdot m_{\text{ds}}) = 1.0292 \times 10^{-2}$
2 or more flaws	$1 - \text{ppois}(1, d(0.5) \cdot m_{\text{ds}}) = 1.5412 \times 10^{-3}$	$1 - \text{ppois}(1, d(1) \cdot m_{\text{ds}}) = 5.3699 \times 10^{-5}$

Fitting of distribution related to defective WP due to improper heat treatment, improper laser peening, or damage by mishandling to lognormal distribution

mean of distribution: $m := 2.8 \cdot 10^{-5}$

95th percentile: $m_{95} := 1.1 \cdot 10^{-4}$

Lognormal fitting performed by keeping the mean value and calculating the error factor that approximates the 95th percentile above.

Call $f(x)$ the function defined by:

$$f(x) := m_{95} - m \cdot x \cdot \exp \left[-0.5 \cdot \left(\frac{\ln(x)}{1.645} \right)^2 \right]$$

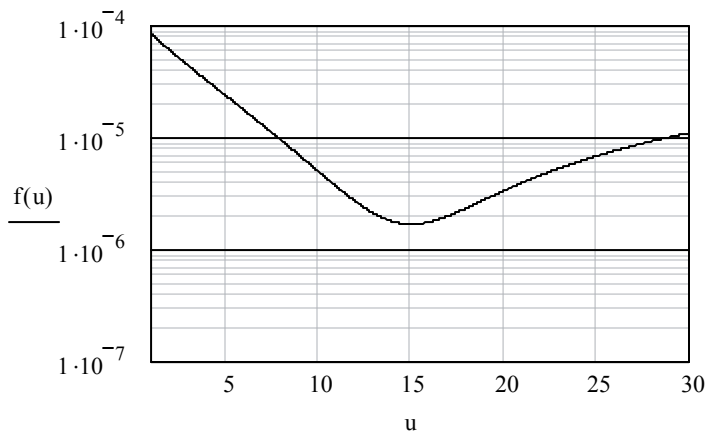


Figure I.10 Minimum Error Factor Determination Curve

$x := 5$

Minimize(f, x) = 14.9697

Take EF := 15

the median of the lognormal distribution is: $ml := m \cdot \exp \left[-0.5 \cdot \left(\frac{\ln(EF)}{1.645} \right)^2 \right]$

$$ml = 7.2222 \times 10^{-6}$$

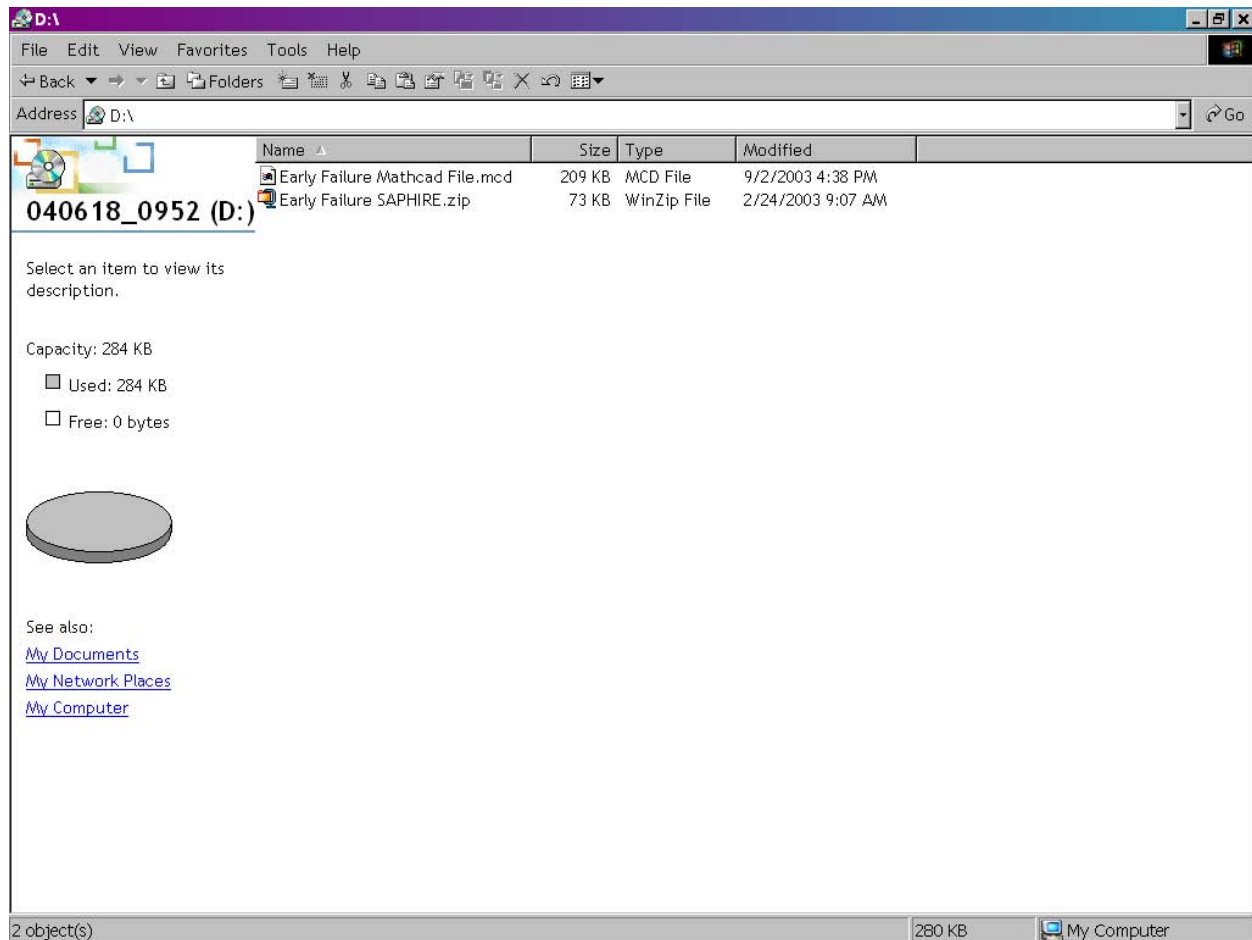
95th percentile is: $ml \cdot EF = 1.0833 \times 10^{-4}$ 5th percentile: $\frac{ml}{EF} = 4.8148 \times 10^{-7}$

percentile of the lognormal distribution at the upper value yielded by Sapphire results:

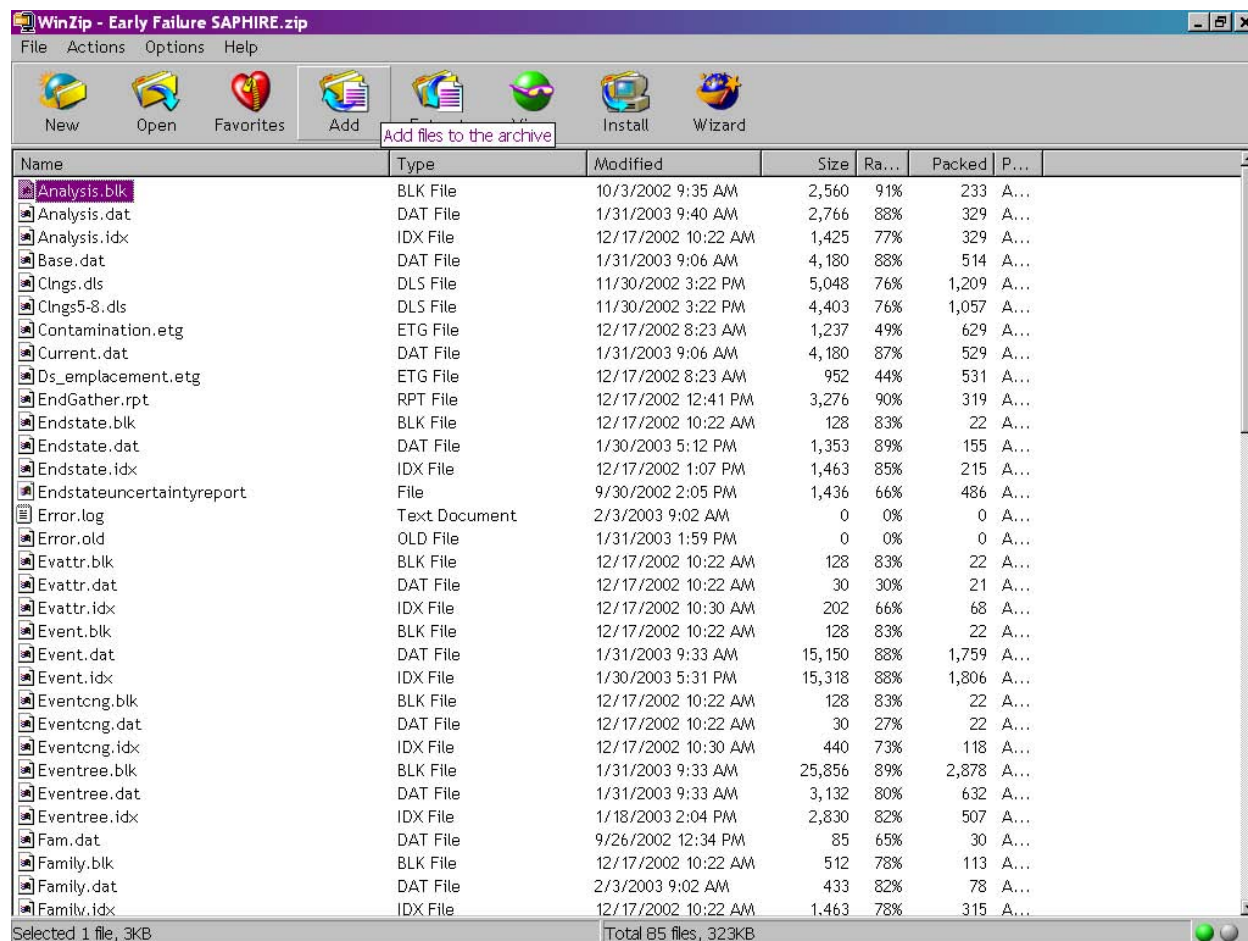
$$\text{plnorm} \left(7.44213 \cdot 10^{-3}, \ln(7.2 \cdot 10^{-6}), \frac{\ln(15)}{1.645} \right) = 0.99999$$

INTENTIONALLY LEFT BLANK

ATTACHMENT II: LISTING OF FILES ON CD-ROM



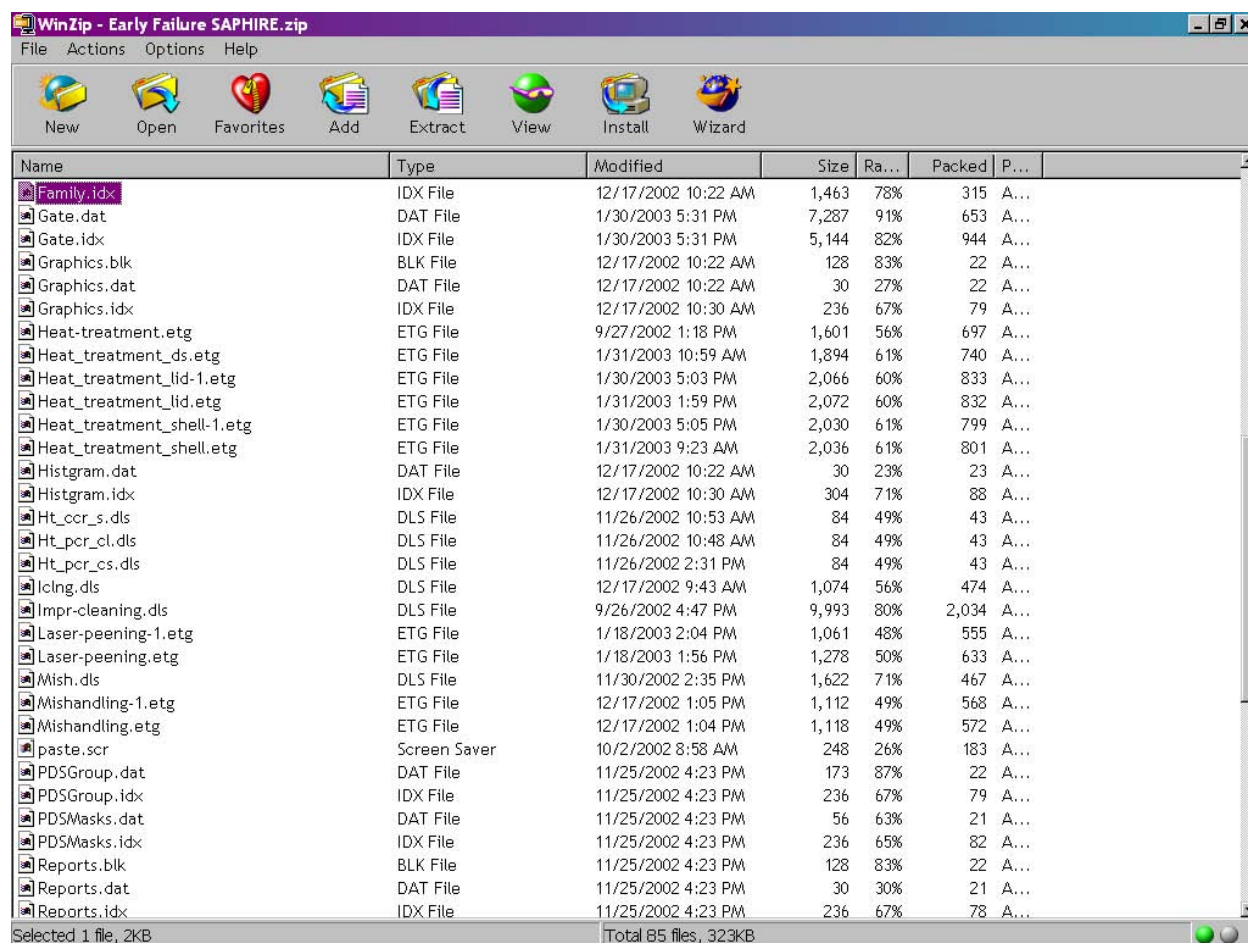
Listing of Files Contained In Compressed Folder “Early Failure SAPHIRE.zip” (Part 1 of 3)



The screenshot shows the WinZip application window titled "WinZip - Early Failure SAPHIRE.zip". The window has a menu bar with "File", "Actions", "Options", and "Help". Below the menu bar is a toolbar with icons for "New", "Open", "Favorites", "Add", "Add files to the archive", "Install", and "Wizard". The main area displays a list of files and folders with columns for Name, Type, Modified, Size, Ra..., Packed, and P... The list includes files like Analysis.blk, Analysis.dat, Analysis.idx, Base.dat, Clngs.dls, Clngs5-8.dls, Contamination.etg, Current.dat, Ds_emplacement.etg, EndGather.rpt, Endstate.blk, Endstate.dat, Endstate.idx, Endstateuncertaintyreport, Error.log, Error.old, Evattr.blk, Evattr.dat, Evattr.idx, Event.blk, Event.dat, Event.idx, Eventcng.blk, Eventcng.dat, Eventcng.idx, Eventtree.blk, Eventtree.dat, Eventtree.idx, Fam.dat, Family.blk, Family.dat, and Familv.idx. The status bar at the bottom indicates "Selected 1 file, 3KB" and "Total 85 files, 323KB".

Name	Type	Modified	Size	Ra...	Packed	P...
Analysis.blk	BLK File	10/3/2002 9:35 AM	2,560	91%	233	A...
Analysis.dat	DAT File	1/31/2003 9:40 AM	2,766	88%	329	A...
Analysis.idx	IDX File	12/17/2002 10:22 AM	1,425	77%	329	A...
Base.dat	DAT File	1/31/2003 9:06 AM	4,180	88%	514	A...
Clngs.dls	DLS File	11/30/2002 3:22 PM	5,048	76%	1,209	A...
Clngs5-8.dls	DLS File	11/30/2002 3:22 PM	4,403	76%	1,057	A...
Contamination.etg	ETG File	12/17/2002 8:23 AM	1,237	49%	629	A...
Current.dat	DAT File	1/31/2003 9:06 AM	4,180	87%	529	A...
Ds_emplacement.etg	ETG File	12/17/2002 8:23 AM	952	44%	531	A...
EndGather.rpt	RPT File	12/17/2002 12:41 PM	3,276	90%	319	A...
Endstate.blk	BLK File	12/17/2002 10:22 AM	128	83%	22	A...
Endstate.dat	DAT File	1/30/2003 5:12 PM	1,353	89%	155	A...
Endstate.idx	IDX File	12/17/2002 1:07 PM	1,463	85%	215	A...
Endstateuncertaintyreport	File	9/30/2002 2:05 PM	1,436	66%	486	A...
Error.log	Text Document	2/3/2003 9:02 AM	0	0%	0	A...
Error.old	OLD File	1/31/2003 1:59 PM	0	0%	0	A...
Evattr.blk	BLK File	12/17/2002 10:22 AM	128	83%	22	A...
Evattr.dat	DAT File	12/17/2002 10:22 AM	30	30%	21	A...
Evattr.idx	IDX File	12/17/2002 10:30 AM	202	66%	68	A...
Event.blk	BLK File	12/17/2002 10:22 AM	128	83%	22	A...
Event.dat	DAT File	1/31/2003 9:33 AM	15,150	88%	1,759	A...
Event.idx	IDX File	1/30/2003 5:31 PM	15,318	88%	1,806	A...
Eventcng.blk	BLK File	12/17/2002 10:22 AM	128	83%	22	A...
Eventcng.dat	DAT File	12/17/2002 10:22 AM	30	27%	22	A...
Eventcng.idx	IDX File	12/17/2002 10:30 AM	440	73%	118	A...
Eventtree.blk	BLK File	1/31/2003 9:33 AM	25,856	89%	2,878	A...
Eventtree.dat	DAT File	1/31/2003 9:33 AM	3,132	80%	632	A...
Eventtree.idx	IDX File	1/18/2003 2:04 PM	2,830	82%	507	A...
Fam.dat	DAT File	9/26/2002 12:34 PM	85	65%	30	A...
Family.blk	BLK File	12/17/2002 10:22 AM	512	78%	113	A...
Family.dat	DAT File	2/3/2003 9:02 AM	433	82%	78	A...
Familv.idx	IDX File	12/17/2002 10:22 AM	1,463	78%	315	A...

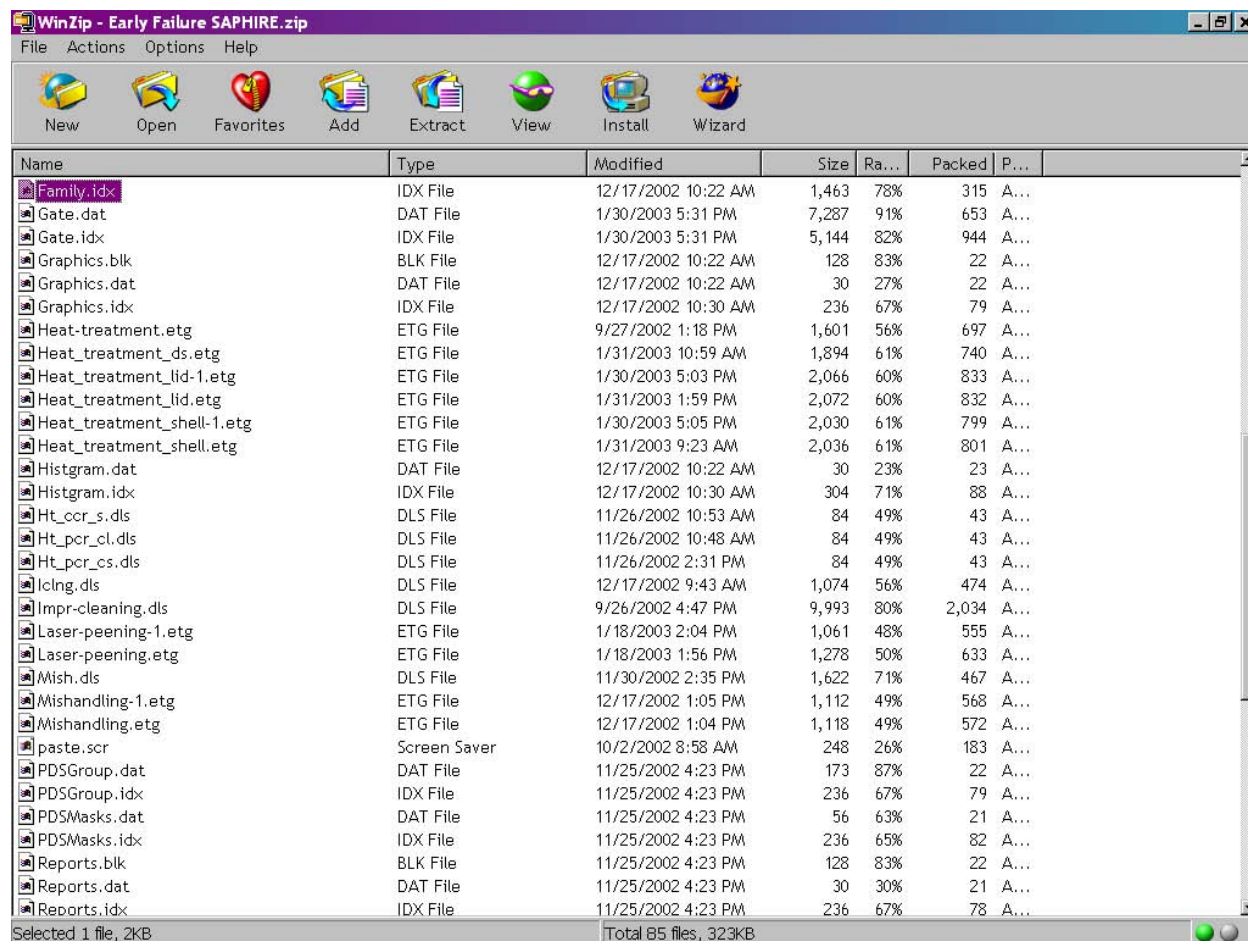
Listing of Files Contained In Compressed Folder “Early Failure SAPHIRE.zip” (Part 2 of 3)



The screenshot shows the WinZip application window titled "WinZip - Early Failure SAPHIRE.zip". The menu bar includes "File", "Actions", "Options", and "Help". The toolbar contains icons for "New", "Open", "Favorites", "Add", "Extract", "View", "Install", and "Wizard". The main window displays a list of files and folders with the following columns: Name, Type, Modified, Size, Ra..., Packed, and P... The status bar at the bottom indicates "Selected 1 file, 2KB" and "Total 85 files, 323KB".

Name	Type	Modified	Size	Ra...	Packed	P...
Family.idx	IDX File	12/17/2002 10:22 AM	1,463	78%	315	A...
Gate.dat	DAT File	1/30/2003 5:31 PM	7,287	91%	653	A...
Gate.idx	IDX File	1/30/2003 5:31 PM	5,144	82%	944	A...
Graphics.blk	BLK File	12/17/2002 10:22 AM	128	83%	22	A...
Graphics.dat	DAT File	12/17/2002 10:22 AM	30	27%	22	A...
Graphics.idx	IDX File	12/17/2002 10:30 AM	236	67%	79	A...
Heat-treatment.etg	ETG File	9/27/2002 1:18 PM	1,601	56%	697	A...
Heat_treatment_ds.etg	ETG File	1/31/2003 10:59 AM	1,894	61%	740	A...
Heat_treatment_lid-1.etg	ETG File	1/30/2003 5:03 PM	2,066	60%	833	A...
Heat_treatment_lid.etg	ETG File	1/31/2003 1:59 PM	2,072	60%	832	A...
Heat_treatment_shell-1.etg	ETG File	1/30/2003 5:05 PM	2,030	61%	799	A...
Heat_treatment_shell.etg	ETG File	1/31/2003 9:23 AM	2,036	61%	801	A...
Histogram.dat	DAT File	12/17/2002 10:22 AM	30	23%	23	A...
Histogram.idx	IDX File	12/17/2002 10:30 AM	304	71%	88	A...
Ht_ccr_s.dls	DLS File	11/26/2002 10:53 AM	84	49%	43	A...
Ht_pcr_cl.dls	DLS File	11/26/2002 10:48 AM	84	49%	43	A...
Ht_pcr_cs.dls	DLS File	11/26/2002 2:31 PM	84	49%	43	A...
Icing.dls	DLS File	12/17/2002 9:43 AM	1,074	56%	474	A...
Impr-cleaning.dls	DLS File	9/26/2002 4:47 PM	9,993	80%	2,034	A...
Laser-peening-1.etg	ETG File	1/18/2003 2:04 PM	1,061	48%	555	A...
Laser-peening.etg	ETG File	1/18/2003 1:56 PM	1,278	50%	633	A...
Mish.dls	DLS File	11/30/2002 2:35 PM	1,622	71%	467	A...
Mishandling-1.etg	ETG File	12/17/2002 1:05 PM	1,112	49%	568	A...
Mishandling.etg	ETG File	12/17/2002 1:04 PM	1,118	49%	572	A...
paste.scr	Screen Saver	10/2/2002 8:58 AM	248	26%	183	A...
PDSGroup.dat	DAT File	11/25/2002 4:23 PM	173	87%	22	A...
PDSGroup.idx	IDX File	11/25/2002 4:23 PM	236	67%	79	A...
PDSMasks.dat	DAT File	11/25/2002 4:23 PM	56	63%	21	A...
PDSMasks.idx	IDX File	11/25/2002 4:23 PM	236	65%	82	A...
Reports.blk	BLK File	11/25/2002 4:23 PM	128	83%	22	A...
Reports.dat	DAT File	11/25/2002 4:23 PM	30	30%	21	A...
Reports.idx	IDX File	11/25/2002 4:23 PM	236	67%	78	A...

Listing of Files Contained In Compressed Folder “Early Failure SAPHIRE.zip” (Part 3 of 3)



The screenshot shows the WinZip application window titled "WinZip - Early Failure SAPHIRE.zip". The menu bar includes "File", "Actions", "Options", and "Help". The toolbar contains icons for "New", "Open", "Favorites", "Add", "Extract", "View", "Install", and "Wizard". The main window displays a list of files and folders with the following columns: Name, Type, Modified, Size, Ra..., Packed, and P... The status bar at the bottom indicates "Selected 1 file, 2KB" and "Total 85 files, 323KB".

Name	Type	Modified	Size	Ra...	Packed	P...
Family.idx	IDX File	12/17/2002 10:22 AM	1,463	78%	315	A...
Gate.dat	DAT File	1/30/2003 5:31 PM	7,287	91%	653	A...
Gate.idx	IDX File	1/30/2003 5:31 PM	5,144	82%	944	A...
Graphics.blk	BLK File	12/17/2002 10:22 AM	128	83%	22	A...
Graphics.dat	DAT File	12/17/2002 10:22 AM	30	27%	22	A...
Graphics.idx	IDX File	12/17/2002 10:30 AM	236	67%	79	A...
Heat-treatment.etg	ETG File	9/27/2002 1:18 PM	1,601	56%	697	A...
Heat_treatment_ds.etg	ETG File	1/31/2003 10:59 AM	1,894	61%	740	A...
Heat_treatment_lid-1.etg	ETG File	1/30/2003 5:03 PM	2,066	60%	833	A...
Heat_treatment_lid.etg	ETG File	1/31/2003 1:59 PM	2,072	60%	832	A...
Heat_treatment_shell-1.etg	ETG File	1/30/2003 5:05 PM	2,030	61%	799	A...
Heat_treatment_shell.etg	ETG File	1/31/2003 9:23 AM	2,036	61%	801	A...
Histogram.dat	DAT File	12/17/2002 10:22 AM	30	23%	23	A...
Histogram.idx	IDX File	12/17/2002 10:30 AM	304	71%	88	A...
Ht_ccr_s.dls	DLS File	11/26/2002 10:53 AM	84	49%	43	A...
Ht_pcr_cl.dls	DLS File	11/26/2002 10:48 AM	84	49%	43	A...
Ht_pcr_cs.dls	DLS File	11/26/2002 2:31 PM	84	49%	43	A...
Icing.dls	DLS File	12/17/2002 9:43 AM	1,074	56%	474	A...
Impr-cleaning.dls	DLS File	9/26/2002 4:47 PM	9,993	80%	2,034	A...
Laser-peening-1.etg	ETG File	1/18/2003 2:04 PM	1,061	48%	555	A...
Laser-peening.etg	ETG File	1/18/2003 1:56 PM	1,278	50%	633	A...
Mish.dls	DLS File	11/30/2002 2:35 PM	1,622	71%	467	A...
Mishandling-1.etg	ETG File	12/17/2002 1:05 PM	1,112	49%	568	A...
Mishandling.etg	ETG File	12/17/2002 1:04 PM	1,118	49%	572	A...
paste.scr	Screen Saver	10/2/2002 8:58 AM	248	26%	183	A...
PDSGroup.dat	DAT File	11/25/2002 4:23 PM	173	87%	22	A...
PDSGroup.idx	IDX File	11/25/2002 4:23 PM	236	67%	79	A...
PDSMasks.dat	DAT File	11/25/2002 4:23 PM	56	63%	21	A...
PDSMasks.idx	IDX File	11/25/2002 4:23 PM	236	65%	82	A...
Reports.blk	BLK File	11/25/2002 4:23 PM	128	83%	22	A...
Reports.dat	DAT File	11/25/2002 4:23 PM	30	30%	21	A...
Reports.idx	IDX File	11/25/2002 4:23 PM	236	67%	78	A...